The *In Vivo* Effect of Osmolytes on Folate Metabolism

A Thesis Presented for the

Master of Science

Degree

The University of Tennessee, Knoxville

Timkhite-Kulu Berhane

Month, Date

Dedication

Acknowledgements

Abstract

Previous studies from the Howell lab have found that the addition of osmolytes weakens the binding of folate/dihydrofolate (DHF) *in vitro* to three different proteins capable of catalyzing the dihydrofolate reductase (DHFR) reaction: R67 DHFR [1], the chromosomal DHFR from *E. coli* [2] and FolM [3].These results supported preferential interaction of DHF with osmolytes compared to water. Thus, a working model where interaction of DHF- osmolytes shifts the binding away from the protein-ligand complex and towards the free species was proposed. Expanding upon these observations, osmotic stress is predicted to lower the catalytic efficiencies, through an increase in the K_m of enzymes involved in folate mediated one carbon metabolism. Folate enzymes catalyze the conversion of folates to different redox states. In this thesis, we explored the *in vivo* effects of increasing osmolytes on the activity of several essential folate pathway enzymes. Essential folate enzymes were selected and their genes were cloned into a tunable plasmid, pKTS, carrying the tetracycline promoter and a sequence encoding a protease degradation tag [4]. The pKTS clone was transformed into a knockout strain, followed by optimizing the *in vivo* protein production with tetracycline dependent cell growth. Then, the intracellular osmolality of the knockout *E. coli* was increased by growing on a minimal media with different sorbitol concentrations. Finally, the difference in osmolality between the control and test plates was used to assess the osmotic fitness of the host cell and the ability of the cloned gene to rescue the mutant cells to prototropy.

Our *in vivo* assays showed R67 DHFR and its quadruplicated synthetic gene, Quad4 [5], rescued *E. coli* DH5α from TMP pressure or *E. coli* LH-18 (*Dfol::kan*) from folate end product auxotrophy on minimal media. Growth of test cells on minimal media was blocked at a lower osmolality compared to growth of a positive control on supplemented media. These results demonstrate a proof of concept that our assay conditions evaluated the *in vivo* activity of R67 DHFR and Quad4 and found it to be sensitive to osmotic stress. .

The genes for two other folate pathway enzymes, methylene tetrahydrofolate reductase and serine hydroxymethyl transferase, were cloned into the pKTS vector. Their ability to respond to *in vivo* osmotic pressure can now be performed.

Finally, the ability of a strain carrying a mutant folylpolyglutamate synthase gene to withstand osmotic stress was explored. The results were limited by the strain's lower sensitivity to osmolality, thus further experiments will need to be performed.

.

Table of Contents

Dedication ii

Acknowledgements iii

Abstract iv

Table of Contents v

List of Tables ix

List of Figures x

List of Abbreviations xii

1 CHAPTER: INTRODUCTION 1

1.1 Osmolytes interaction with DHF/folate affect three DHFR enzymes activity 2

1.2 Osmoprotectants: natural organic solutes generated to rescue cells from osmotic stress. 5

1.3 Probing the activity of water up on R67 DHFR binding *in vivo* 7

1.4 Rationale for a genetic approach 8

1.5 Decreasing the [protein] and/or enzyme rate improve *in vivo* assay 10

1.6 *In vivo* osmootic stress study folate enzyme selection criteria 13

1.7 Selected folate cycle enzymes 17

1.7.1 Plasmid encoded R67 Dihydrofolate Reductase (R67 DHFR) 19

1.7.2 Folylpolyglutamate Synthase (FPGS) 21

1.7.3 5,10-Methylenetetrahydrofolate Reductase (MTHFR) 23

1.7.4 Serine Hydroxymethyl Transferase (SHMT) 24

1.7.5 Dihydropteroate Synthase (DHPS) 26

1.7.6 Thymidylate Synthase (TS) 27

2 CHAPTER: MATERIALS AND METHODS 29

2.1 Brief summary and step wise processes and rationales 29

2.2 Biological Materials 31

2.2.1 Bacterial strains 31

2.2.2 Plasmids 32
2.3 Cloning 38
2.3.1 Competent cell preparation 38
2.3.1.1 Chemically competent cell preparation. 38
2.3.1.2 Electrocompetent cell preparation 38
2.3.2 Introduction of NdeI and/or XhoI recognition sequences 39
2.3.2.1 Chemical Synthesis 39
2.3.2.2 PCR Method 40
2.3.3 TOPO TA cloning 41
2.3.4 Sample cleaning processes 42
2.3.5 Ligation and transformation 43
2.4 Tetracycline titration 44
2.5 Sorbitol titration 44
2.5.1 Quantifying osmolality of a media 45
2.6 Effects of osmolality on the function of plasmid encoded R67 DHFR and/or quad4 to rescue E. coli from TMP pressure 45
2.7 Effects of osmolality on the activity of folylpolyglutamate synthase (FPGS) ... 45
3 CHAPTER: RESULTS 47
3.1 Assessing the activity of R67 DHFR and/or Quad4 clones in the presence of increasing osmolality *in vivo* 47
3.1.1 Construction of R67 DHFR-pKTS and Quad4-pKTS 47
3.1.2 Tetracycline dependent *E. coli* DH5α and/or *E. coli* LH-18 (*ΔFolA::Kan*) growth on M9 and/or Bonner-Vogel minimal selective media 48
3.1.2.1 Tetracycline concentration required to produce sufficient R67 DHFR and/or Quad4 activity in vivo to confer TMP resistance to E. coli DH5α. 48
3.1.2.2 Tetracycline concentration required to induce sufficient R67 DHFR and/or Quad4 production to allow confluent growth of E. coli LH-18 (ΔFolA::Kan) on Bonner-Vogel minimal media 51

3.1.3 Effect of osmolality on the ability of the R67 DHFR and/or Quad4 to provide TMP resistance to *E.coli DH5α* 54

3.1.4 Effect of osmolality on the ability of R67 DHFR and/or Quad4-pKTS clones to rescue *E.coli* LH-18 to prototrophy 58

3.2 Can osmotic stress affect the *in vivo* activity of the *folC* gene product, FPGS?. 61

3.2.1 *E. coli*: SF2 *(F⁻ folC strA,)* a mutant strain with a lower activity of FPGS 61

3.2.2 Effect of osmolality on the function of *fol*C 62

3.2.2.1 Osmotic Stress effects on the growth of the SF2 strain on BV media supplemented with excess methionine and glycine/ml 62

3.2.2.2 Growth of the SF2 strain on BV media supplemented with a sub-optimal concentration of methionine 64

3.3 Cloning the Methylenetetrahydrofolate Reductase (MTHFR) gene (*metF)* into pKTS 65

3.3.1 Designing a primer, PCR amplification and cloning into the pCR 2.1 TOPO TA vector 66

3.3.2 Construction of the metF-pKTS plasmid 68

3.3.3 Assessing the growth pattern of *E. coli* JW3913-1 (Δ*metF::kan*) 70

3.3.4 Tetracycline concentration required to induce sufficient MTHFR production to rescue *E. coli* JW3913- (Δ*metF::kan*) 71

3.4 Initial experiments to explore the effect of *in vivo* osmotic stress on serine hydroxymethyl transferase activity 73

3.4.1.1 Designing a primer, PCR amplification and cloning into the pCR 2.1 TOPO TA vector 73

3.4.1.2 Construction of the glyA-pKTS plasmid 74

3.4.1.3 Assessing the growth pattern of E. coli JW2535-1 (ΔglyA::kan) 78

3.4.1.4 Identification of the tetracycline concentration required for sufficient in vivo SHMT production to rescue E. coli JW2535-1 (ΔglyA::kan) to prototrophy 79

3.5 Beginning steps to clone the dihydropteroate synthase gene into the pKTS plasmid 81

3.5.1 Assessing the quality of the *folP* clone and assessing the cloning sites in the gene 81

4 CHAPTER: DISCUSSION 83

4.1.1 R67 DHFR and/or Quad4 84

4.1.2 Folypolyglutamate Synthase (FPGS)..... 87

4.1.3 5,10-Methylenetetrahydrofolate Reductase (MTHFR)..... 89

4.1.4 Serine Hydroxymethyl Transferase (SHMT) 89

4.2 Conclusion 89

4.3 Future experiments..... 90

List of Tables

Table 1-1 Values of predicted μ_{23}/RT: interaction of folate species with betaine.....9

Table 1-2: Folate mediated one-carbon metabolism gene that are essential/letale for *E. coli*

Table 1-3: List of selected enzymes &~ distane between N/C terminus and the active site. 16

Table 2-1 List of *E. coli* strains, their genotypes, and sources 31

Table 2-2 List of folate enzyme clones.....33

Table 2-3 *E coli* one carbon metabolism genes DNA sequences and their corresponding protein products.....34

Table 2-4 List of PCR primer sequences used to introduce Nde1 and/or Xho1 restriction enzyme sites with their calculated T_M values.....41

Table 2-5 The folate end products added as supplement(s) to BV minimal media.....44

List of Figures

Figure 1-1 Folate contains pterin, pABA and glutamate moieties. 1

Figure 1-2 Models of preferential exclusion and B. preferential interaction.....2

Figure 1-3 Plot of ln K_a versus osmolality.....3

Figure 1-4 A plot of osmolality versus ln $k_{cat}/K_{m\ (DHF)}$ for R67 DHFR. 4

Figure 1-5 Model showing the preferential interaction of osmolytes with free DHF. 5

Figure 1-6 Chemical structures of selected naturally occurring osmolytes.....6

Figure 1-7 Effects of total enzyme activity on cell growth rate. 11

Figure 1-8 Map of the tunable vector pKTS.....12

Figure 1-9 pKTS : selection strategies for controlling intracellular [catalyst] 13

Figure 1-10 Simplified Model of Folate Cycle : Selected enzymes showed in arrows.....18

Figure 1-11 R67 Dihydrofolate reductase activity. 19

Figure 1-12 Structure of tetrameric R67 DHFR (1VIE).....20

Figure 1-13 Quadruplicated construct of R67 DHFR: Quad4.....20

Figure 1-14 Two reactions-one enzyme: bifunctional FPGS. 21

Figure 1-15 The structure of FPGS and the position of SF2 mutation.....22

Figure 1-16 Sequental catalytic mechanism of methylene-tetrahydrofolatereductase (MTHFR).

Figure 1-17 Crystal structure methylene-tetrahydrofolatereductase MTHFR.....24

Figure 1-18 Serine hydroxymethyltransferase catalyzes reversible reaction 25

Figure 1-19 Crystal structure Serine hydroxymethyltransferase (SHMT) 25

Figure 1-20 Dihydropteroate synthase (DHPS) attached pterin with pABA.....26

Figure 1-21 Crystal structure Dihydropteroate synthase (DHPS) 26

Figure 1-22 Thymidylate synthase (TS) plays a major role DNA synthesis. 27

Figure 1-23 Crystal structure thymidylate Synthase (TS) 28

Figure 2-1 Flow chart describing the general work flow.....30

Figure 3-1 Restriction enzyme digested R67 DHFR, pKTS. and pKTS DNA 48

Figure 3-2 Tetracycline dependent *E. coli* DH5α growth on M9 media. 50

Figure 3-3 Growth pattern of *E. coli* LH-18 in BV supplemented (A) and minimal (B) media.

Figure 3-4 Tetracycline dependent *E. coli* LH-18 growth on BV minimal media 53

Figure 3-5 Effect of osmolality on *E. coli* DH5α viability. 56

Figure 3-6 Effect of Osmolality on R67 DHFR and/or Quad4 to rescue DH5α from TMP^R .

Figure 3-7 Effect of osmolality on *E. coli* LH-18 viability. 59

Figure 3-8 Effect of osmolality on R67 DHFR and/or Quad4 activity on BV minimal plates.

Figure 3-9 The growth pattern of the *folC* mutant strain, SF2, and its parent strain MG1655.

Figure 3-10 The effect of increasing osmolality on the growth of *E. coli* SF2. 63

Figure 3-11 Assessing the effect of increasing osmolality on the ability of SF2 to grow in the presence of a sub-optimal methionine concentration. 65

Figure 3-12 PCR amplification of the *metF* gene.....67

Figure 3-13 NdeI and XhoI digested *metF*-pCR 2.1 and pKTS. 69

Figure 3-14 The growth pattern of the *metF* knockout strain *of E. coli* JW3913-1.....70

Figure 3-15 Tetracycline dependent *metF* production rescues JW3913-1 (Δ*metF*::kan) carrying the *metF*-pKTS plasmid.....72

Figure 3-16 *glyA* PCR product.....74

Figure 3-17 NdeI and XhoI digested *glyA*. 75

Figure 3-18 Partially digested *glyA*.plasmid.....77

Figure 3-19 The growth pattern of *E. coli* JW2535-1 (*ΔglyA::kan*).....78

Figure 3-20 Tetracycline dependent *glyA* production.....80

Figure 3-21 NdeI and XhoI digested *folP*.....82

List of Abbreviations

Δn_w	Number of water molecules
10-HCO-THF	10-Formyltetrahydrofolate/10-formyl-THF
1C	One-carbon
5,10-CH=THF	5,10-Methenyltetrahydrofolate
5,10-CH_2-THF/CH_2-THF	5,10-Methylenetetrahydrofolate
5,6,7,8-THF	5, 6,7,8-Tetrahydrofolate/Tetrahydrofolate
5-CH_3-THF/CH_3-THF	5-methyltetrahydrofolate
5-CHO-THF	5-Formyltetrahydrofolate/5-formyl-THF
6-HMDP	6-hydroxymethyl-7,8-dihydropterin diphosphate
7,8-DHF/DHF	7, 8-Dihydrofolate
Å	Angstrom (10^{-8} cm)
a_{H2O}	water activity
ATP	Adenosine triphosphate
BV	Bonner-Vogel minimal media
DHFR	Dihydrofolate Reductase
DHFS	Dihydrofolate synthase
DHNA	1,4-Dihydroxy-2-naphthoic acid
DHPPP	6-hydroxymethyl-7,8-dihydropterin pyrophosphate
DHPS	Dihydropteroate synthase
dTMP	Thymidine monophosphate
dUMP	Deoxyuridine monophosphate
EcDHFR	*E. coli* Dihydrofolate reductase
F^-	Does not carry F plasmid
F^+	Carries F plasmid for conjugation.
FAD	Flavin adenine dinucleotide
Fol	Folate
FPGS	Folylpolyglutamate synthase
GST tag	Glutatione-S-Transferase tag
H_2HMPt-P_2	(2-amino-4-hydroxy-7,8-dihydropteridin-6-yl)methyl trihydrogen diphosphate
H_2MPt-P_2	7,8-dihydropterin-methyl diphosphate
H_2PtPP	Dihydropteroate-6-pyrophosphate
HMDP	6-hydroxymethyl-7,8-dihydropterin
HPPK	6-hydroxymethyl-7,8-dihydropterin pyrophosphokinase
IPTG	Isopropyl β-D-1-thiogalactopyranoside
ITC	Isothermal Titration Calorimetry
k_a	association constant

k_{cat}	Catalytic rate constant
K_d	Dissociation constant (Binding)
K_i	Inhibition constant
K_m	Michaelis Menten constant
kV/cm	kilovolt/centimeter
MOE	Molecular Operating Environment Computer Program
MOPS	3-(N-Morpholino)propanesulfonic acid
MTHFR	Methylenetetrahydrofolate Reductase
$NADP^+$	Nicotinamide adenine dinucleotide phosphate (oxidized form)
NADPH	Nicotinamide adenine dinucleotide phosphate (reduced form)
ng	nanogram
Osm	Osmolality
pABA	p-aminobenzoate
PCR	polymerase chain reaction
PDB	Protein Data Bank
PEG	Poly Ethylene Gycol
PG5	Pteroylpenta- γ-L-glutamate
P_{tet}	Tetracycline promoter
R67 DHFR	R67 Dihydrofolate Reductase
racA	Reduced occurrence of unwanted recombination in cloned DNA
rpm	Revolutions/Minute
S.O.C.	Super Optimal Broth with glucose cell growth media
SHMT	Serine Hydroxymethyl Transferase
SsrA	Small stable RNA A
strA	Streptomycin resistance
TetR	Tetracycline repressor protein
Tn10	Transposon with Tetracycline resistance
TS	Thymidilate Synthase
wt	wild type
X-gal	5-bromo-4-chloro-3-indolyl-beta-D-galacto-pyranoside
YT	Yeast Extract Trypton

1 CHAPTER: INTRODUCTION

Folate is also known as vitamin B9 and its structure is composed of pterin, *p*-aminobenzoate (pABA), and glutamate moieties Figure 1-1 these molecules are essential for life. Human and higher animals cannot synthesize folate, thus they obtain folate from their diet. Plants and bacteria synthesize folate de novo. In all domains of life, folates are required for several cellular processes such as DNA, RNA, purine nucleotide, and amino acid synthesis. In the folate pathway, tetrahydrofolate (THF) is the active species as it can carry methyl or formyl groups on either its N5 and/or N10 position(s). These molecules are one carbon carriers that lead to synthesis of thymidylate, serine, methionine, etc.

Figure 1-1 (below) [6].

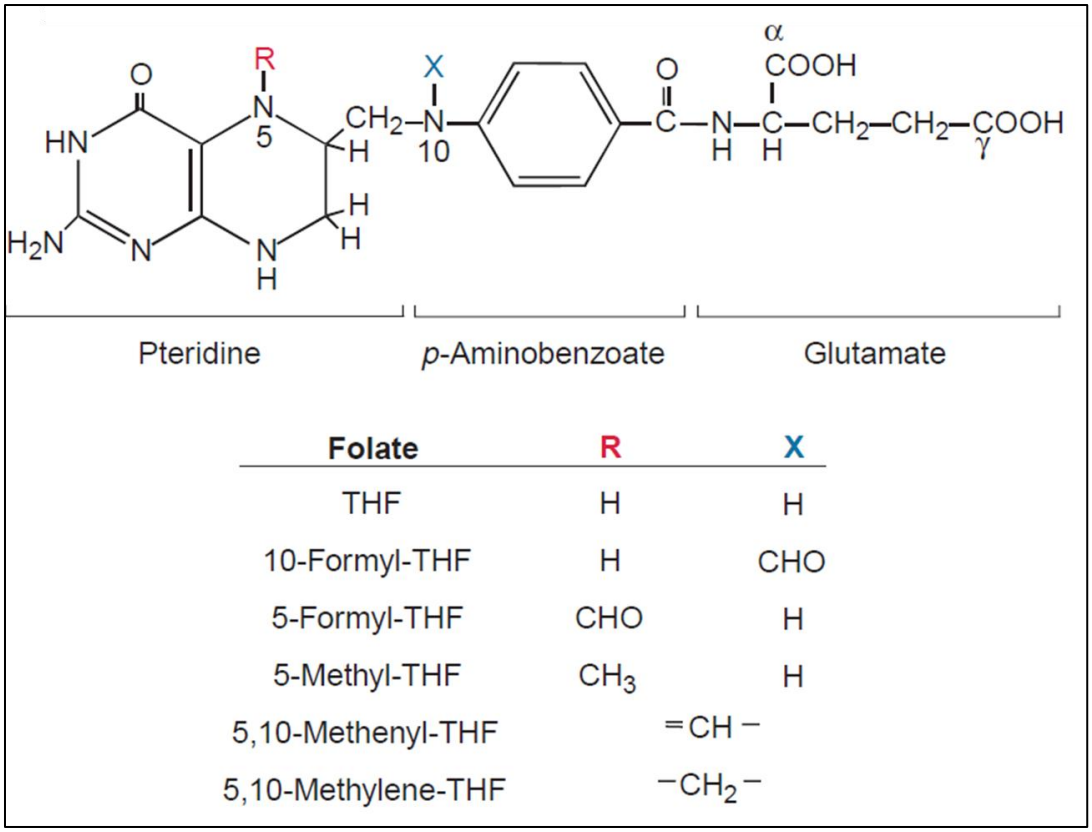

Figure 1-1 Folate contains pterin, pABA and glutamate moieties.
Tetrahydrofolate, shown above, plays a role in the folate pathway by adding carbons at the N5 (R) and/or N10 (X) position(s) [6]

1.1 Osmolytes interaction with DHF/folate affect three DHFR enzymes activity

The Howell lab has studied the structure-function relationship in dihydrofolate reductase (DHFR). Recent studies have focused on examining the role of water on folate/DHF and/or cofactor binding. One way of examining the activity of water in binding is to perturb the water molecules in the hydration shell of the interacting molecules (for example, protein plus ligand) by the gradual increase of osmolyte (co-solvent) concentration and monitoring the change in catalytic efficiency and/or binding. A typical result is tighter binding of a ligand to protein as fewer water molecules need to be removed and the desolvation penalty is decreased. Another case is provided if the affinity of the protein surface is greater for osmolytes compared to the water molecules, then the osmolytes compete with water and weakly interact with the protein surface. A cartoon representation of preferential interaction and preferential exclusion of osmolytes from a protein surface is presented in Figure 1-2 (below). If osmolytes are more difficult to remove than water, then the binding equilibrium will be shifted towards free state, which will weaken binding. Thus, Chopra et al. studied the role of water on binding in the primitive enzyme, R67 DHFR [1].

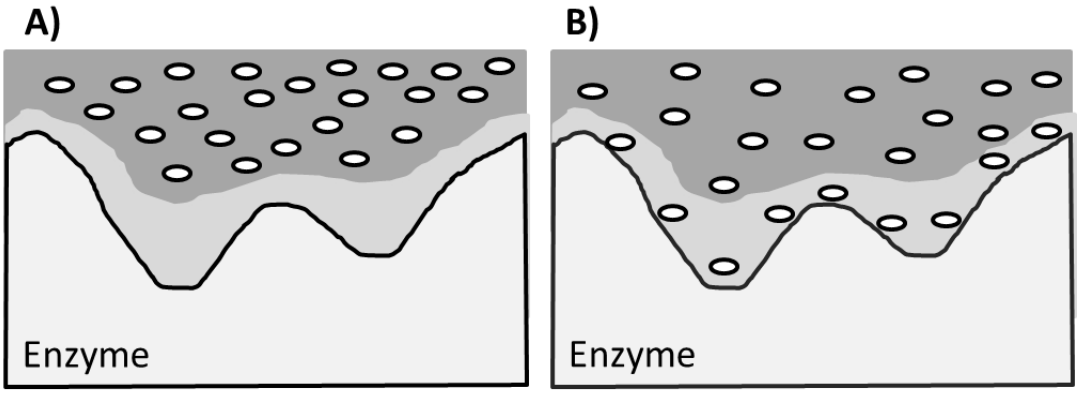

Figure 1-2 Models of preferential exclusion and B. preferential interaction
ation layer of the enzyme is shown in light grey, while the bulk solvent is dark grey. Osmolytes are represented by white ovals [7]

The binding of NADPH to apo R67 DHFR was investigated using isothermal titration calorimetry (ITC). Tighter binding was observed upon the addition of ethylene glycol, sucrose, Me_2SO, glycine betaine, or PEG400 as shown in

Figure 1-3 Plot of ln Ka versus osmolality (below/right) [1]. This result is the typical observation associated with osmotic stress studies as a lower water concentration leads to a decreased desolvation barrier associated with binding. All osmolytes tested have the same effect, consistent with exclusion of the osmolytes from the surfaces of NADPH and R67 DHFR [1].

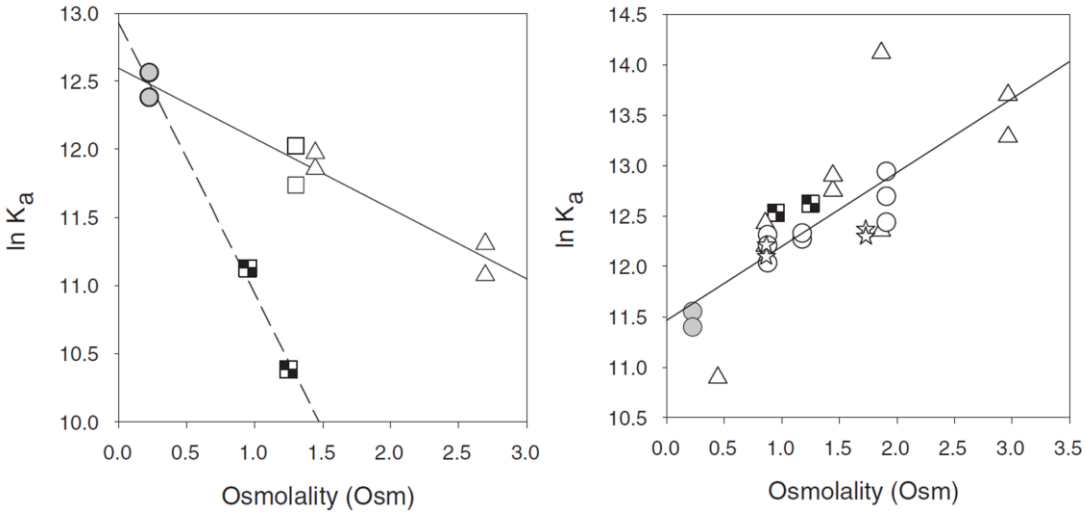

Figure 1-3 Plot of ln K_a versus osmolality
The K_a for DHF binding to R67 DHFR-$NADP^+$ was determined by ITC. Weaker binding and sensitivity to osmolyte identity was observed (left). In contrast, the K_a for NADPH binding to apo R67 DHFR showed a single positive slope. The K_a values for DHF and NADPH binding possess opposite slopes. The results for DHF are consistent with a preferential interaction model while the results for NADPH are consistent with a preferential exclusion model. Data for buffer (gray circle), ethylene glycol (open circle), sucrose (open square), Me_2SO(open circle), glycine betaine (open triangle), and PEG400 (checkerboard) are shown.

When reduction of DHF was investigated using steady state kinetics, the catalytic rate constant, k_{cat}, showed minimal to no variation. However, a significant increase in $K_{M(DHF)}$ values was observed. This combined behavior results in a decrease in catalytic efficiency or $k_{cat}/K_{M(DHF)}$. If K_M equals K_d, this result suggests the drop in catalytic efficiency is due to weaker binding of DHF [1].

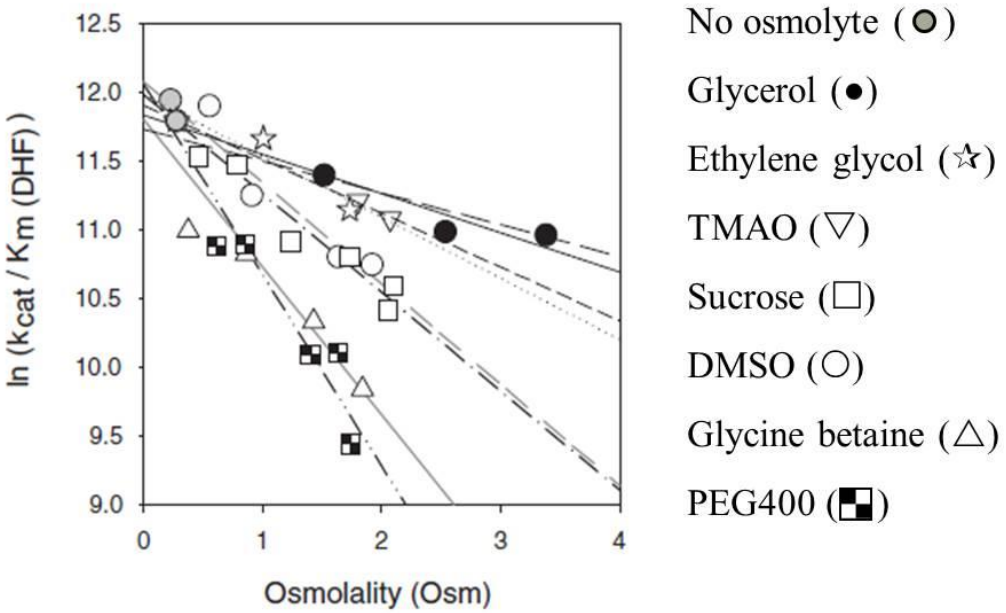

Figure 1-4 A plot of osmolality versus ln $k_{cat}/K_{m\ (DHF)}$ for R67 DHFR.
Steady state kinetic data were obtained at saturating NADPH concentration and varied DHF concentrations in the presence of various osmolytes. Michaelis-Menten plots were used to calculate k_{cat} and $K_{m\ (DHF)}$ values. The units for k_{cat}/K_M (DHF) are s^{-1} M^{-1}. Adopted from [1].

Next, to directly monitor the K_d associated with DHF binding, Chopra et al. titrated DHF into R67 DHFR-$NADP^+$ in the presence of increasing concentrations of sucrose, glycine betaine or PEG400 [1]. Their results showed a steady decline in ln K_a as the osmolyte concentration increased. The use of PEG400 showed a steeper negative slope in the plot

Figure 1-3 Plot of ln Ka versus osmolality above **(**left**)** which correlates with its acting as a crowding agent due to its larger volume [1].

As R67 DHFR possesses 222 symmetry and a single active site pore to bind its ligands, this results in the same site being able to accommodate either cofactor or DHF [8]. This unusual active site allows the Howell lab to use osmotic stress results for NADPH as an internal control which indicates no osmolyte interaction with either NADPH or R67 DHFR. If osmolytes don't interact with R67 DHFR, the likely reason for weaker binding of DHF is a preferential interaction of osmolytes with DHF. This hypothesis led to the cartoon shown in Figure 1-5 (below).

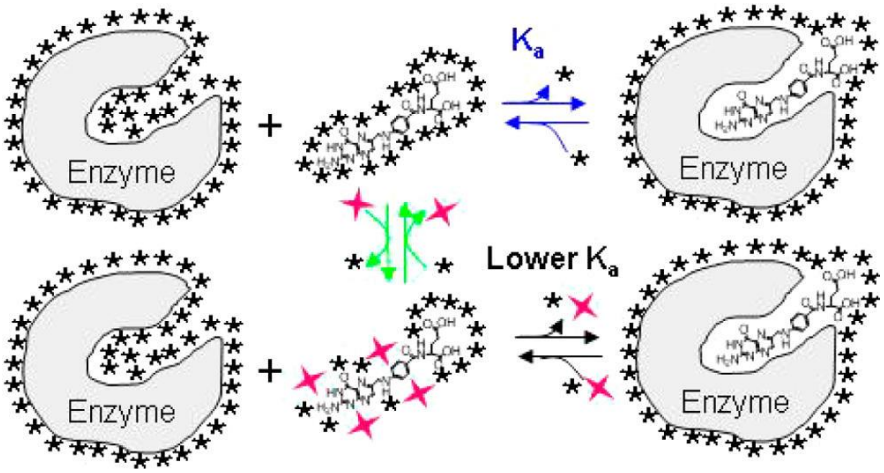

Figure 1-5 Model showing the preferential interaction of osmolytes with free DHF. Removal of water (★) and/or osmolytes (red star) from the solvation shell of DHF is required for the ligand to bind to DHFR. If the DHF-osmolyte association is stronger than the DHF−water interaction, the binding equilibrium will be shifted to the left, favoring the unbound state. This results in a decreased binding affinity of DHF for DHFR. This model does not exclude interactions between osmolytes and the protein. Adopted from [3].

The model of folate/DHF interaction with osmolytes was tested using two additional folate enzymes, chromosomal DHFR from *E. coli* (EcDHFR) [2] and FolM [3]. These enzymes catalyze the DHFR reaction, but they have dissimilar sequences and oligomerization states [3]. For both enzymes studied by steady state kinetics and/or ITC, the K_M for DHF increased and/or the K_a decreased [2, 3]. These results are consistent with the model.

1.2 Osmoprotectants: natural organic solutes generated to rescue cells from osmotic stress.

Osmolytes are low molecular mass compounds. These molecules are compatible or noncompatible with macromolecules. Compatible osmolytes destabilize both the native and unfolded states by their exclusion from the peptide backbone; however, the unfolded state is more affected, resulting in a larger energy difference between the native and unfolded states. This leads to protein folding (see Figure 1-5 above [9]). Noncompatable osmolytes have stabilize denatured form of a protein, thus decreases the thermal stability and activity of the enzyme [10]. Based on their chemical composition, osmolytes are divided into three classes: polyhydric alcohols and

sugars (polyols), amino acids and their derivatives, and methyl ammonium compounds Figure 1-6 (below) [11]. Bacteria and plants generate small organic solutes (osmolytes) or transport them from the environment into the cell to maintain the osmolality of the cell due to external osmotic stress. The internal osmolytes help to compensate for cell volume changes, by stabilizing macromolecules [12] and/or by aiding protein folding [13].

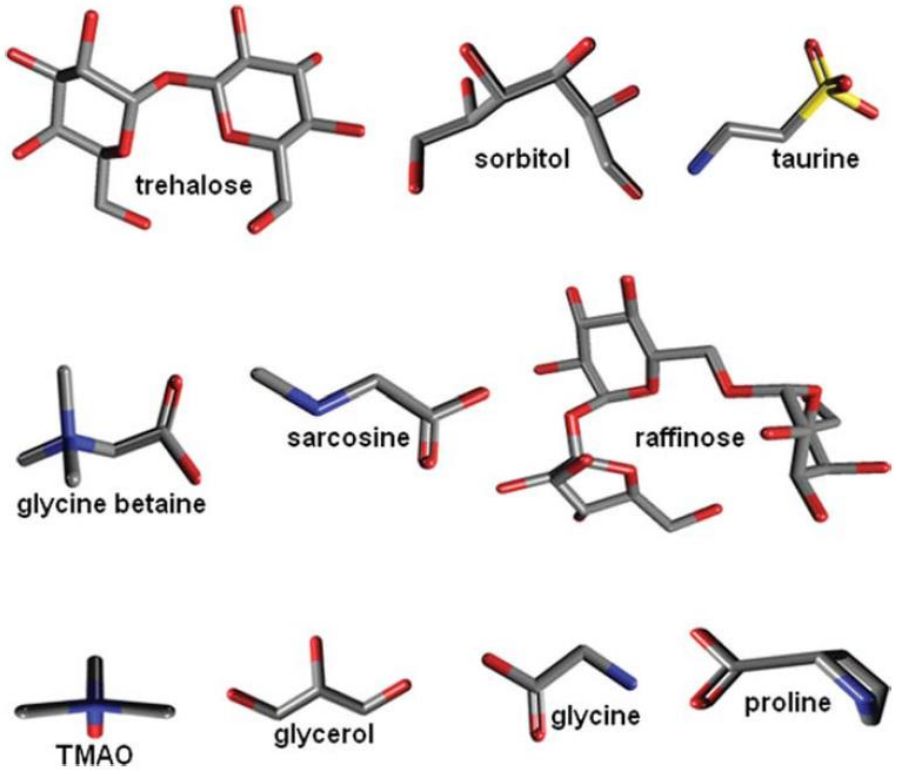

Figure 1-6 Chemical structures of selected naturally occurring osmolytes.
Adopted from [11].

The chemical properties and sizes of osmolytes can be correlated with the number of water molecules (Δn_w) excluded from the hydration shell of proteins [13, 14]. The Record group has provided two excellent reviews of osmoprotectants in bacteria [15, 16].

In the intracellular compartment of bacteria, the total cytoplasmic water content is the sum of 'bound' and 'free/bulk' water. Typically the 'bound' water molecules are not affected by osmotic stress i.e. the organism does not lose bound water but rather 'free' water molecules [17]. In normal circumstances, 'free' water molecules move in and out of the cell. However, if there is a difference in osmotic strength between the internal and external environments, the bacteria face

sudden free water loss and can shrink. To overcome this situation, the bacteria produce intracellular osmolytes to balance the osmolality of the internal environment with that of the outside environment. Thus the intracellular osmolyte(s) concentration increases [17]. Common osmoprotectants in *E. coli* are glycine betaine, glutamate, proline and trehalose.

1.3 Probing the activity of water up on R67 DHFR binding *in vivo*

As betaine is a common osmoprotectant in *E. coli* and as betaine decreases, the catalytic efficiency of R67 DHFR Figure 1-4 (above), Chopra et al. examined the effect of osmotic stress on R67 DHFR function *in vivo.* Both EcDHFR and R67 DHFR reduce folate/DHF to THF, however the chromosomal DHFR is easily inhibited by addition of the antibacterial drug trimethoprim (TMP, K_i = 20 pM) [18]. In contrast, TMP does not inhibit R67 DHFR very well (K_i = 0.15 mM) [19]. Thus, the activity of chromosomal enzyme was inhibited by addition of 20 µg TMP/ml [20]. Then osmotic stress was applied to the host cell by adding sorbitol to a minimal growth media. The ability of *E. coli* DH5α carrying wild type or a mutant (Q69H, K32M, or Y69L) R67 DHFR clones cloned in pUC8 was then assessed [1].

The wild type and two mutant clones rescued the host cells from TMP pressure, but the Y69L mutant clone required an extended growth time [1]. These results correlated with the activity of the type of R67 DHFR enzyme. For example, the host cell carrying wildtype R67 DHFR clone has sufficient enzyme activity to reduce DHF to THF and can enable cell growth. However, host cells carrying the Y69L mutant clone had a lower catalytic efficiency and took a longer time to allow host cell growth. On the other hand, the K32M R67 DHFR clone did not rescue its host cell, suggesting the mutant enzyme did not possess sufficient DHFR activity to rescue the cell from trimethoprim pressure [21].

In the next set of assays, increasing concentrations of sorbitol were added. *E. coli* DH5α and *E. coli* DH5α carrying the wt R67 DHFR-pUC8 clone allowed cell growth in the presence of TMP until the osmolality of the media became ≥ 1.95 Osm. As per the Record lab, this result suggests that the host cell stops growing due to loss of free water in the cytoplasm [17]. In contrast, *E. coli* DH5α carrying the mutant Y69L R67 DHFR-pUC8 clone grew very slowly and stopped growing under much less osmotic stresses (0.92 Osm). This result was interpreted as the

lower activity associated with the Y69L R67 DHFR clone was less able to rescue the host cell; thus its activity could be titrated by osmotic stress. This titration follows the loss of enzyme activity upon osmolyte addition as seen in Figure 1-4 (above).

Titration of the activity of the wt R67 DHFR clone by sorbitol addition was not observed in the above experiments. Since the maximal activity (V_{max}) of an enzyme can be described as k_{cat}* [E_{total}], where [E_{total}] describes the total enzyme concentration, these two parameters need to be considered. The wt enzyme is reasonably active with a k_{cat}/K_m of 2.2 x 10^5 M^{-1} s^{-1}. In addition, the protein is overexpressed due to the high copy number of the pUC8 plasmid. A similar problem of *in vivo* assay for a metabolically essential enzyme with high protein production, but poor enzymatic activity was previously described by the Hilvert lab [22].

1.4 Rationale for a genetic approach

Vapor pressure osmometry studies by the Record group have monitored the interaction of betaine, proline and urea with various small molecules [23-25]. From these studies, they have derived atomistic preferential interaction coefficients (μ_{23}/RT) which allow prediction of whether water or betaine/proline/urea prefers to interact with larger molecules. A positive value indicates exclusion of osmolyte from the molecule; for example, glutamate, phosphate and citrate all exclude betaine from their carboxylate and phosphate atoms. A high value is 1.2. A value of zero for μ_{23}/RT indicates no preference for water vs betaine. A negative value indicates a preference for the molecule to interact with betaine. Capp et al. find a μ_{23}/RT value of -0.091 for the interaction of benzoate with betaine [1]. The Howell lab has used this approach in predicting the interaction of betaine with folate and DHF. The predicted values are in the ballpark of the experimentally measured values, suggesting this approach is reasonable (predicted μ_{23}/RT values are shown in Table 1-1(below). As tetrahydrofolate and its various derivatives possess very similar structures to folate, our prediction is that betaine will also interact with these redox states of folate [23-25]

Table 1-1 Values of predicted μ_{23}/RT: interaction of folate species with betaine.
Predicted μ_{23}/RT values according to Capp et al. [23] that compute the potential interaction preference of betaine with various reduced forms of folate molecules with mono, di, and tri glutamate tails. As betaine is excluded from glutamate, addition of extra glutamates to the tail of the folate molecule results in increases in the predicted value.

	Betaine μ23/RT			
Folate Species	$(glu)_0$	$(glu)_1$	$(glu)_2$	$(glu)_3$
5-formyl-tetrahydrofolate	n/a	0.228	0.579	0.893
5-methyl-tetrahydrofolate	n/a	0.146	0.493	0.806
6-hydroxymethyldihydropterin	-0.024	n/a	n/a	n/a
10-formyl-tetrahydrofolate	n/a	0.287	0.623	0.937
10-methyl-tetrahydrofolate	n/a	0.176	0.524	0.837
6-hydroxymethyl-7,8-dihydropterin pyrophosphate	0.907	n/a	n/a	n/a
Dihydropteroate	-0.166	n/a	n/a	n/a
N5-N10- methenyl-tetrahydrofolate	n/a	0.167	0.512	0.829
N5-N10-methylene-tetrahydrofolate	n/a	0.163	0.509	0.826
p-aminobenzoate	-0.122	0.168	0.47	0.718
Tetrahydropteroate	-0.162	n/a	n/a	n/a
Tetrahydrofolate	n/a	0.133	0.479	0.791
Dihydrofolate	n/a	0.128	0.523	0.766
Folate	n/a	-0.039	0.359	0.685
Glutamate	n/a	0.451	0.744	1.095
Citrate	0.683	n/a	n/a	n/a
Phosphate	0.986	n/a	n/a	n/a
Diphosphate	1.294	n/a	n/a	n/a

[a] Not applicable

To test this prediction, we can purify the relevant enzymes and do *in vitro* osmotic pressure studies. As purifying enzymes and doing *in vitro* osmotic stress studies is quite time-consuming, our hope is that a genetic approach will be faster. This approach will also test whether our model in Figure 1-5 (above) continues to work in the crowded environment of the cell with many other molecules and macromolecules present.

As the growth of various *E. coli* strains is not titrated by increasing concentrations of sorbitol (except for the limit when no free water remains as per Cayley et al. [17]), we need a system that will decrease the total enzyme activity in the cell for folate pathway enzymes. Since a single gene exists per *E. coli* chromosome, a system is needed that will produce less active protein than normally exists per *E. coli* cell. For this type of system, we plan on transforming selected Keio deletant strains [26] with a plasmid with controls on gene expression and protein stability.

1.5 Decreasing the [protein] and/or enzyme rate improve *in vivo* assay

As described by the Hilvert lab, the *in vivo* selection of a chorismate mutase clone with a high protein production, but poor enzymatic activity could be improved by minimizing the protein production level (see Figure 1-7 below) [22]. To address this problem in our system, we will use the pKTS plasmid obtained from the Hilvert lab [4].

The pKTS vector has two ways to control protein production, use of the P_{tet} promoter and a protease degradation tag (SsrA) (see Figure 1-8 and

Figure 1-9(below) [4]. In this vector, the gene of interest is cloned between the tetracycline promoter (P_{tet}) and a SsrA tag. The P_{tet} promoter has a large regulatory window. At the lowest tetracycline concentration, it allows basal expression of a gene to the tune of one mRNA molecule per three cells [27]. In addition, use of a SsrA tag (AANDENYALA) on the C-terminus of the protein, directs the protein to the ClpX protease for degradation [4]. This approach may sufficiently minimize the protein production as to allow titration of enzyme activity by a decreased water activity (see Figure 1-7).

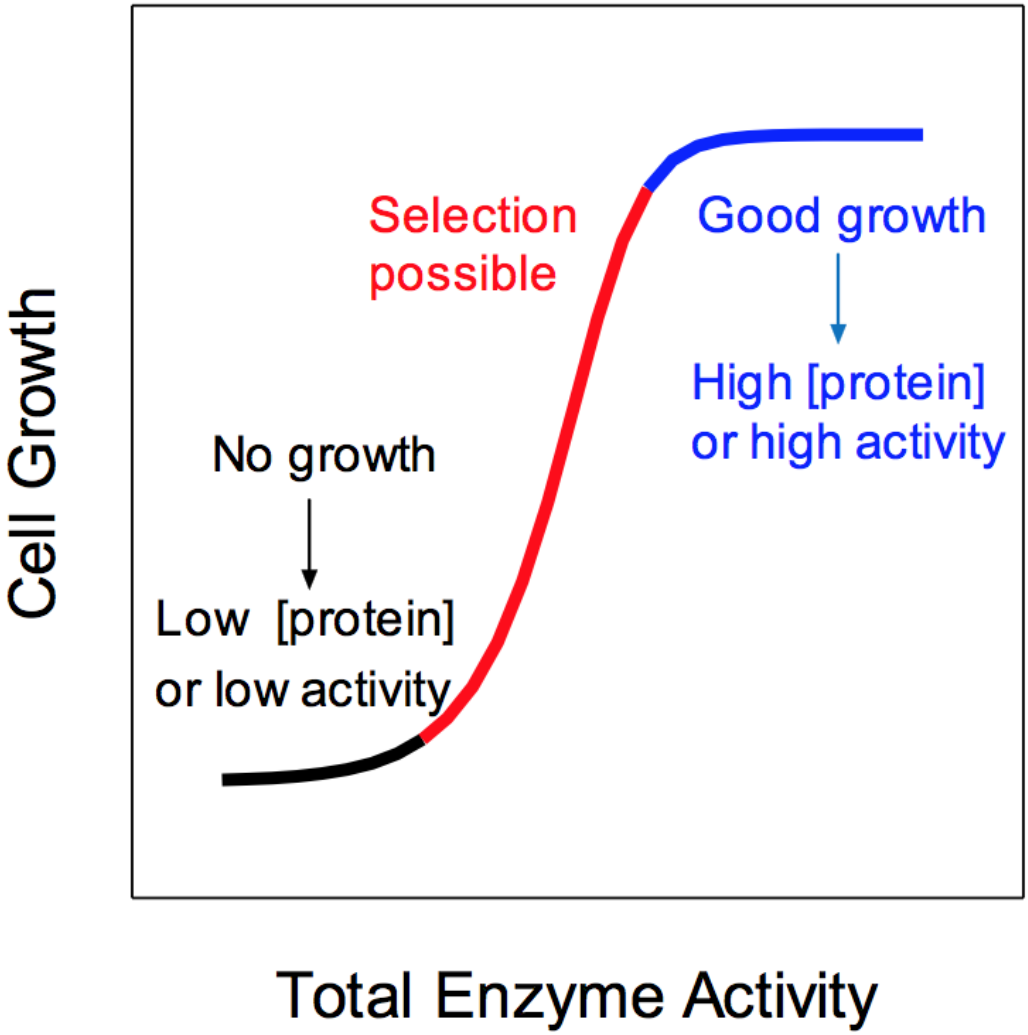

Figure 1-7 Effects of total enzyme activity on cell growth rate.
The best selection window is at the center of the graph. The left hand side of the graph describes conditions where the total enzyme activity is too low to enable growth. The right hand side of the graph describes conditions where selection is not possible due to high expression levels or high activity of the enzyme. Titration of enzyme activity is possible when either a low protein concentration or a low enzyme activity (due to mutation) occurs; the black curve represents the low protein production or enzyme activity, the red curve represents medium protein production where selection is possible, and the blue color represents high protein production where *in vivo* selection is problematic. Adapted from [22].

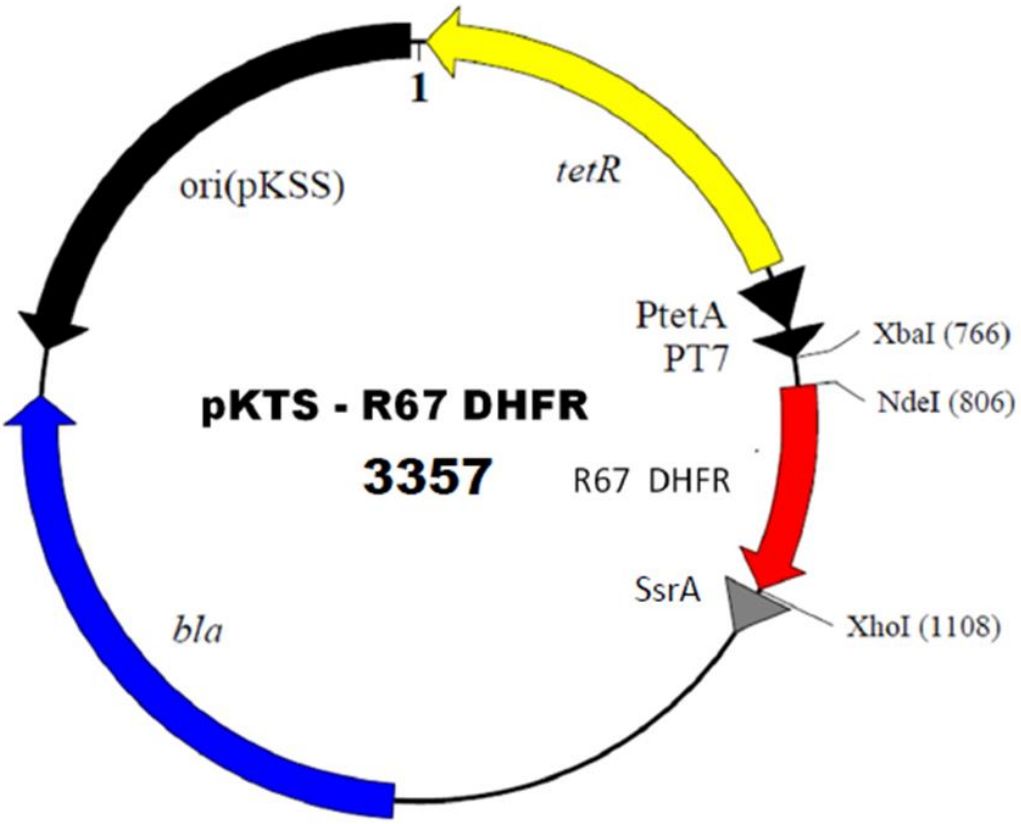

Figure 1-8 Map of the tunable vector pKTS

The gene of interest (for example, R67 DHFR) is cloned into the pKTS vector obtained from the Hilvert lab. In this vector, transcription of the R67 DHFR gene is controlled by the tetracycline repressor (TetR) and tetracycline promoter (P_{tet}). Therefore, while Tc exerted its antibiotic activity in the system, transcription of TetR promotes Tc resistance [28]. As a result, only the basal level of the promoter activity that correlates with the Tc concentration is allowed [29]. In addition to the TetR and P_{tet} system, the SsrA tag at the C- terminal sequence destabilizes the gene product and directs the protein to the ClpX protease for degradation. Adopted from [4].

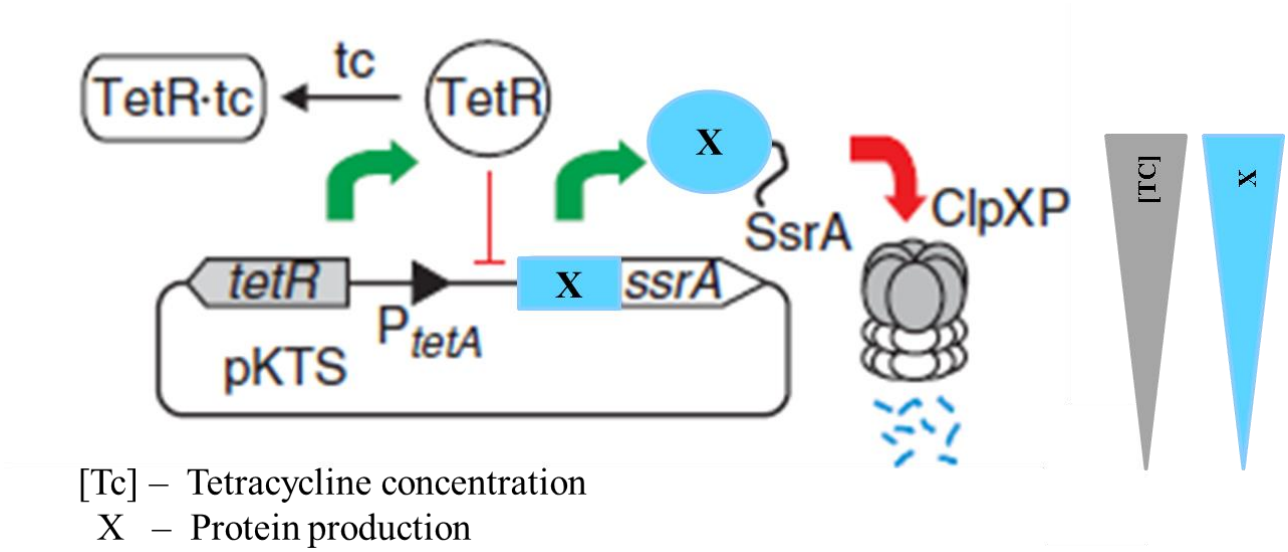

Figure 1-9 pKTS : selection strategies for controlling intracellular [catalyst]
The gene of interest, 'X', is cloned between the P_{tetA} promoter and a sequence encoding a SsrA tag. The pKTS plasmid permits transcriptional control and limits enzyme half-life. The SsrA sequence is fused to the C-terminus of the protein of interest. Minimizing protein production should allow an *in vivo* selection of folate pathway enzyme activity [4].

1.6 *In vivo* osmootic stress study folate enzyme selection criteria

To select candidate enzymes in the folate cycle for these studies, we used the following three criteria. First, the enzyme must be essential and/or selectable;

Table 1-2 (below) lists various genes in the folate pathway and notes whether they are essential (Bold/underlined). Second, the C-terminus and/or N-terminus should not be in a close proximity to the active site as this would block our ability to use the pKTS vector or the pKTR vector (which puts a RepA degradation tag on the N-terminus) to control protein expression levels. And third, we prefer the K_M of the folate derived substrate to be higher than the respective substrate concentration in the cell. We discuss these issues below.

Table 1-2: Folate mediated one-carbon metabolism gene that are essential/letale for *E. coli*

Gene	Enzyme (Abbreviation)	Essential/ Non-essental
folA	Dihydrofolate reductase (EcDHFR)	Yes [21, 26]
folB	Dihydroneopterin aldolase	No
folC	Folylpolyglutamate synthase (FPGS)	Yes [21]
folD	Bifunctional methylene tetrahydrofolate reductase/cyclohydrolase	Yes [21]
folE	GTP cyclohydrolase I	Yes [21, 26]
folK	2-amino-4-hydroxy-6-hydroxymethyl-dihydropteridine pyrophosphokinase (HPPK)	Yes [21, 26]
folM	Pteridine Reductase (FolM)	No [21]
folP	Dihydropteroate Synthase (DHPS)	Uncertain [27]
glyA	Serine Hydroxymethyltransferase (SHMT)	No [21], Yes [26]
metF	Methylenetetrahydrofolate Reductase (MTHFR)	No [21]
purU	Formyl-tetrahydrofolate Deformylase	Yes [26]
thyA	Thymidylate Synthase (TS)	No [21], Yes [26]

Bold/underlined: enzymes selected for *in vivo* osmolality study are in Bold/Underline.

Essential enzymes are required for the survival of a cell. For example, DHFR is essential for synthesis of thymidylate, methionine, glycine, serine and purines in bacteria. Therefore, it was possible to assay the effect of increasing external osmotic stress via a gradual decline in cell growth. We aimed to use a similar approach with other enzymes in the folate mediated one carbon (1C) cycle. As noted in

Table 1-2 (above), there are many essential folate cycle enzymes.

Secondly, since we aimed to use the pKTS plasmid, we were concerned whether the SsrA tag could have an effect on enzyme activity. Therefore, we measured the closest distance between the active site of the selected enzymes and their C-terminus using the Molecular Operating Environment computer program (MOE), version 2012.10 [30]. If the C-terminus is very close to

the active site, we could use an alternative vector, pKTR, that adds an N-terminal RepA degradation tag [22]. The distance range between the active site and the C-terminus is listed Table 1-3 (below). This table also lists whether the C-terminus has been tagged to aid in purification. If a histag has been added, for example, this supports the feasibility of adding a SsrA tag. We also note that if fusion with a SsrA tag impairs enzyme activity, this might be acceptable as we need to have low total activity levels to titrate enzyme activity *in vivo*.

Table 1-3: List of selected enzymes &~ distane between N/C terminus and the active site. selected folate pathway enzymes, PDB file names, oligomerization states, ligands bound in the crystal structure, approximate distances between the active site and the C-terminus and information on whether the protein has been expressed as a histag, GST tag or other fusion.

Protein (PDB)	Oligomeric state	Bound ligands	Distance	Histag or other fusion?
R67 DHFR (1VIE) [8]	Homotetramer	$NADP^+$	≥19 Å	*E. coli* enzyme expressed with a C-terminal histag [31]
Quad4 (n/a)	Monomer	n/a[b]	n/a[b]	*E. coli* enzyme expressed with a C-terminal histag [5]
MTHFR (1ZPT) [32]	Tetramer	Sulfate ion, flavin-adenine dinucleuotide, 1,4-dihydronicotinamide adenine dinucleotide, NADH	≥ 25 Å	*E. coli* enzyme expressed with a C-terminal histag [33]
FPGS (1W78) [34]	Monomer	Lysine NZ-carboxylic acid, magnesium ion, sulfate ion, phosphorylated dihydropteroate, adenosine-5'-diphosphate	≥ 26Å	*E. coli* enzyme expressed with a histag, however not stated whether tag is at N- or C-terminus[35]
SHMT (1DFO) [36]	Dimer	N-Glycine-[3-hydroxy-2-methyl-5 phosphonooxymethyl-pyridin-4-yl-methane], 5-Formyl-tetrahydrofolate, N-pyridoxyl-glycine-5-monophosphate	≥ 25Å	Strep tagged C-terminus for SHMT from *Chlamydia pneumonia [37]*
DHPS (1AJOP) [38]	Monomer	Sulfanilamide, sulfate ion, 2-amino-6-hydroxymethyl-7,8-dihydro-3H-pteridin- 4-one	≥ 22Å	DHPS from *Plasmodium falciparum* tolerates a C-terminal GST tail[39]
HPPK (3KUH)	Monomer	Diphosphomethylphosphonic acid adenosyl ester, 2-amino-6-hydroxymethyl-7, 8-dihydro-3h-pteridin-4-one, magnesium ion, chloride ion, acetate ion	≥ 9 Å	HPPK and DHPS from *Francisella tularensis* exist as a bifunctional HPPK-DHPS fusion [40] ; HPPK from *E. coli* tolerates a C-terminal GST fusion[41]
TS (1AXW)	Dimer	Methotrexate and dUMP	<7 Å[c]	

[a] Distance between active site and C-terminus
[b] Crystal structure is not available

[c] N-formyl-methionine at N-terminus forms H-bonds with T46 and T47

Lastly, if the substrate concentration of the folate metabolite in the cell is much higher than the $K_{M,}$ the active site of the enzyme would be saturated. Thus, it could be difficult to observe measurable effects induced by osmotic stress. To avoid this potential problem, the concentrations of metabolites *in vivo* were identified based on previously published *E. coli* K12 metabolite concentrations [42] and compared to literature K_M values.

1.7 Selected folate cycle enzymes

We considered the following enzymes: Dihydropteroate Synthase (DHPS encoded by the *folP* gene); Folylpolyglutamate Synthase (FPGS encoded by the *folC* gene); R67 dihydrofolate reductase (a type II DHFR that provides resistance to the antibacterial drug trimethoprim); Serine Hydroxymethyl Transferase (SHMT encoded by *glyA*); and Methylenetetrahydrofolate Reductase (MTHFR encoded by *metF*), Figure 1-10 (below).

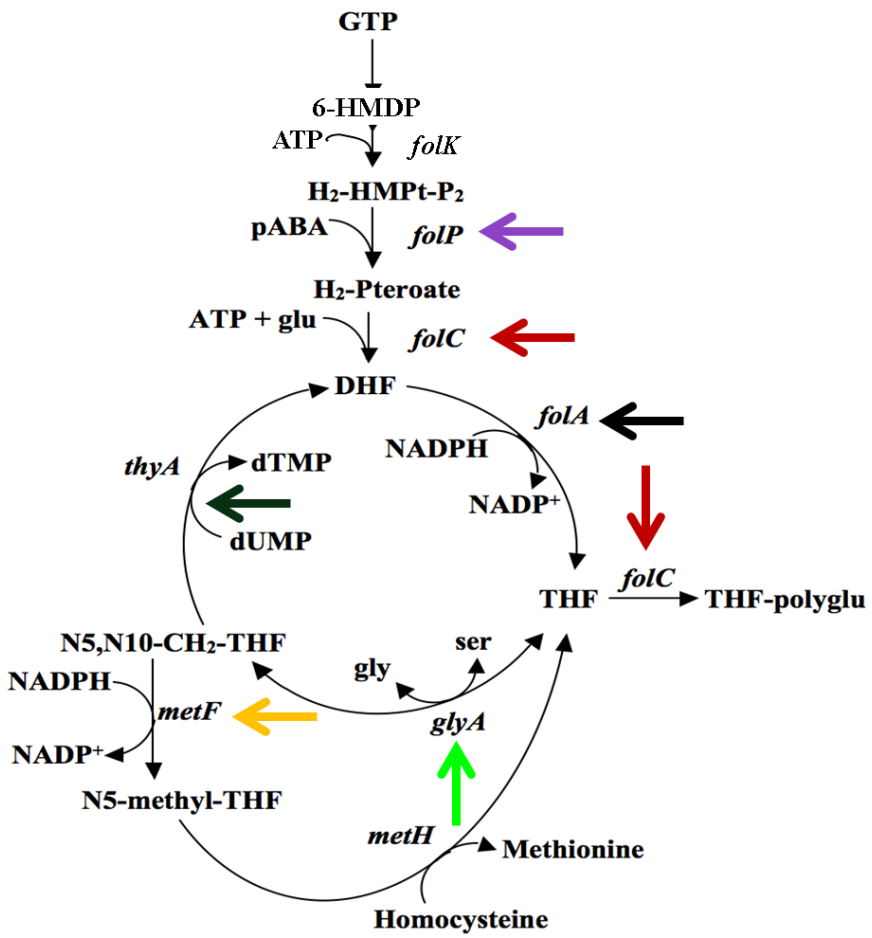

Figure 1-10 Simplified Model of Folate Cycle : Selected enzymes showed in arrows.
The *fol*P gene (**purple arrow**) encodes dihydropteroate synthase or DHPS and this protein forms 7,8-dihydropteroate or H_2-pteroate from 7,8-dihydropterin-methyl diphosphate (H2MPt-P_2) and p-amino benzoic acid**.** The *fol*C gene (**red arrows**) encodes folylpolyglutamate synthase or FPGS and this enzyme has two activities. The first activity adds L-glutamate to dihydropteroate and forms 7,8-dihydrofolate (DHF), while the second activity adds 2-5 glutamates to form polyglutamylated THF species. The *fol*A gene (**block arrow**) encodes dihydrofolate reductase or DHFR; this enzyme catalyzes the NADPH-dependent reduction of 7,8-dihydrofolate (DHF) to 5,6,7,8-tetrahydrofolate (THF). The *gly*A gene (**green arrow**) encodes serine hydroxymethyl transferase or SHMT, which interconverts L-serine to glycine using THF or 5, 10-methylene-THF and pyridoxal phosphate as a cofactor. The *met*F gene (**orange arrow**) encodes methylene-tetrahydrofolate reductase or MTHFR, which reduces N-5, 10-methylene-THF to 5-methyl-THF using NADPH as a cofactor.And, *thy*A gene (**dark green**) encodes thymidylate synthase or TS; this enzyme catalyzes the reductive

1.7.1 Plasmid encoded R67 Dihydrofolate Reductase (R67 DHFR)

R67 dihydrofolate reductase (DHFR), encoded by an R plasmid, provides resistance to the antibacterial drug trimethoprim (TMP) [20]. This enzyme reduces 7,8-dihydrofolate (DHF) to 5,6,7,8-tetrahydrofolate (THF) Figure 1-11 (below). While this is the same reaction catalyzed by EcDHFR, the protein scaffold is different [20]. In *E. coli* K12, the concentration of DHF (glutamate, and diglutamate forms) is 51.02 µM [35]. The K_M is only 5.8 µM [20]. Thus, with this high difference with K_M active site is would be saturated *in vivo* [43].

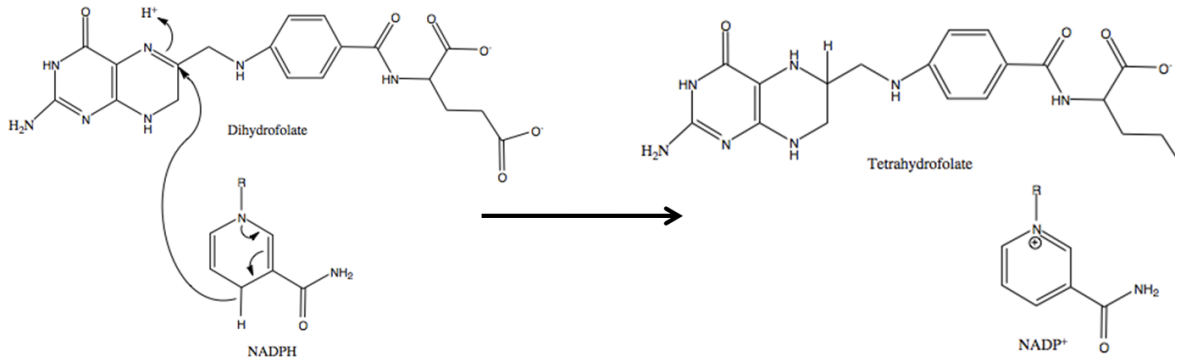

Figure 1-11 R67 Dihydrofolate reductase activity.
R67 Dihydrofolate reductase catalyzes the reduction of 7,8-dihydrofolate (DHF) to 5,6,7,8-tetrahydrofolate (THF) by a stereospecific hydride transfer from the NADPH cofactor to the C6 atom of the pterin ring with a simultaneous protonation at N5.
http://en.wikipedia.org/wiki/Dihydrofolate_reductase

R67 DHFR is a homotetramer (PDB:2RK1) [8]; the active site and the C-terminus are labeled in Figure 1-12 (below). Both DHF (substrate) and NADPH bind in the central active site pore of the enzyme [44]. The distance between the active site and the C-terminus is ≥19 Å.

A tandem array of four fused R67 DHFR genes was previously constructed and a functional enzyme named Quad4 resulted [5] (see Quad4 structure in Figure 1-13 below). In our *in vivo* study, we aim to study the effect of increasing osmolality on Quad4 in parallel to that of R67 DHFR. Quad4 should have a single SsrA tag while R67 DHFR should have four SsrA tags. The $K_{M(DHF)}$ of Quad4 is 5.6 ± 0.3 µM [5], which is comparable to R67 DHFR.

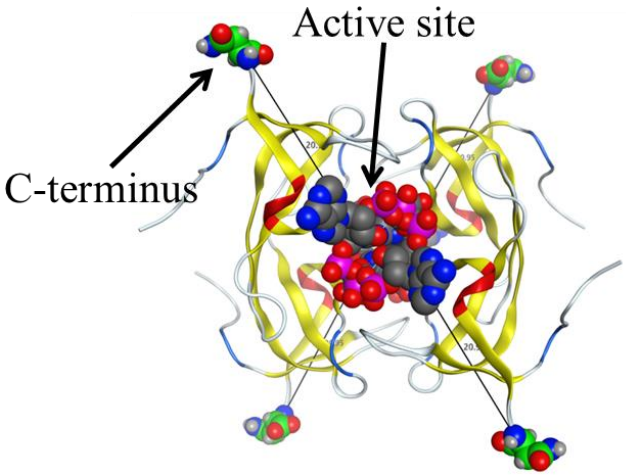

Figure 1-12 Structure of tetrameric R67 DHFR (1VIE).
The crystal structure (PDB:2RK1) [8] of dimeric R67 DHFR shows 17-18 residues are disordered at the N-terminus [45]. When these residues are removed by chymotrypsin treatment, the truncated species crystallizes as the active tetramer [46]. The active site and the C-terminus are labeled above. Both DHF (substrate) and $NADP^+$ are bound in the central active site pore [44]. The distance between the active site and the C-terminus is ≥19 Å.The figure was constructed using Moe, version 2012.10[30].

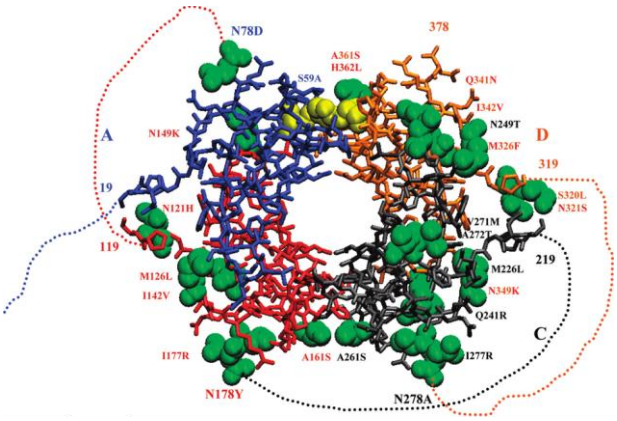

Figure 1-13 Quadruplicated construct of R67 DHFR: Quad4.
The four different colors represent the four fused R67 DHFR domains. The dashed lines imagine the N-terminal 16 amino acids that would serve as the linker between domains. These disordered amino acids are cleaved off to yield a truncated species that crystallizes as the homotetramer [45, 46]. Similar to R67 DHFR, both the substrate and cofactor bind in the central active site pore of the enzyme. The C-terminus is distant from the active site pore and can accommodate a histag.

1.7.2 Folylpolyglutamate Synthase (FPGS)

Folylpolyglutamate Synthase (FPGS) is a product of the *folC* gene [47]. This enzyme (EC 6.3.2.17) catalyzes two distinct reactions: the dihydrofolate synthase reaction adds L-glutamate to dihydropteroate and forms dihydrofolate using ATP as an energy source and the folylpolyglutamate synthase reaction extends the glutamate tail of THF using a γ-linkage

Figure 1-14 (below) [47, 48]. Both THF and 10-formyl-THF are FPGS substrates. These enzymes participate at two separate positions in the folate cycle [34, 47] Figure 1-10 (see red arrows/above).

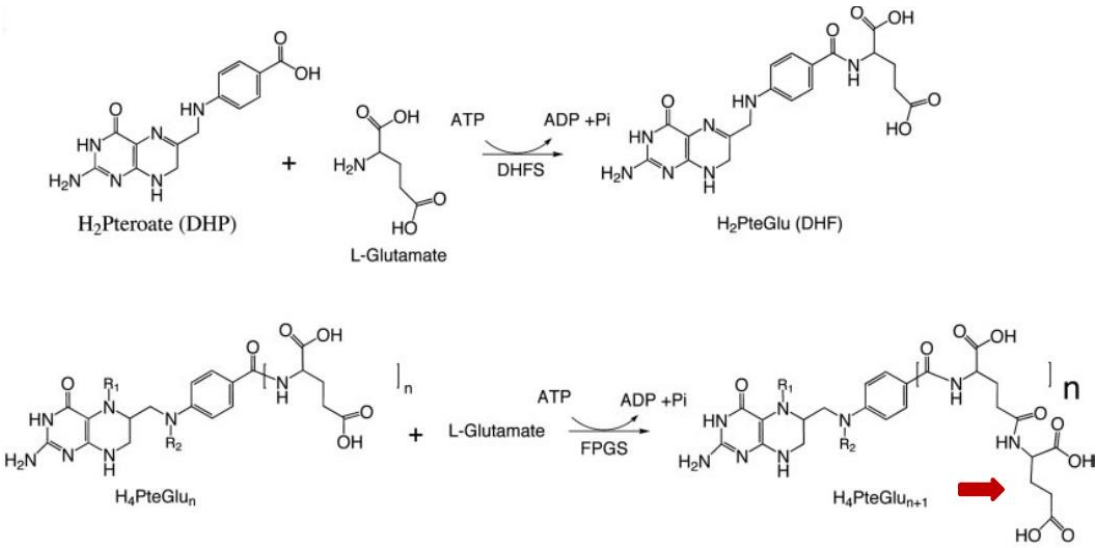

Figure 1-14 Two reactions-one enzyme: bifunctional FPGS.
The first is a dihydrofolate synthase (DHFS) activity. DHFS adds L-glutamate to dihydropteroate to form dihydrofolate (DHF) (TOP). In the second reaction, FPGS extends the glutamate tail using a γ-linkage to form polyglutamylated folates (bottom) [34].

The concentrations of THF and 10-formyl-THF in *E. coli* K12 are 10.02 µM and 6.8 µM, respectively [35]. The K_M of THF for FPGS is 0.9 µM [47], and the K_M of 10-formyl-THF is 17.0 µM [47]. For the latter reaction, the K_M is higher than the concentration of 10-formyl-THF *in vivo*, suggesting the active site of the enzyme may not be saturated.

FPGS is a monomer (PDB: 1W78) [34]. The closest distance between the active site and C-terminus is 26 Å. This great a distance suggests addition of a SsrA tag would be tolerated

Figure 1-15 (below/left)**.** We also note that a C-terminal histag version of the enzyme is available and active [35]. As an alternative to the pKTS cloning, we also obtained two *E. coli* K12 mutant strains SF2 (*folC strA*) and SF4 (*folC strA recA Tn10::srlC*) that carry an A309T mutation in the chromosomal *folC* gene [49] Figure 1-15 (below/right). This mutant enzyme displays a 30 fold increase in K_m for 10-CHO-THF, a 60 fold increase in the K_m for glutamate, a 10 fold increase in the K_m for ATP and a 200 fold increase in the K_m for dihydropteroate [49, 50]. Because of this drastic decrease in enzyme activity, we proposed it might be possible to titrate FPGS activity by osmotic stress in the *E. coli* SF2 (*folC strA*) strain.

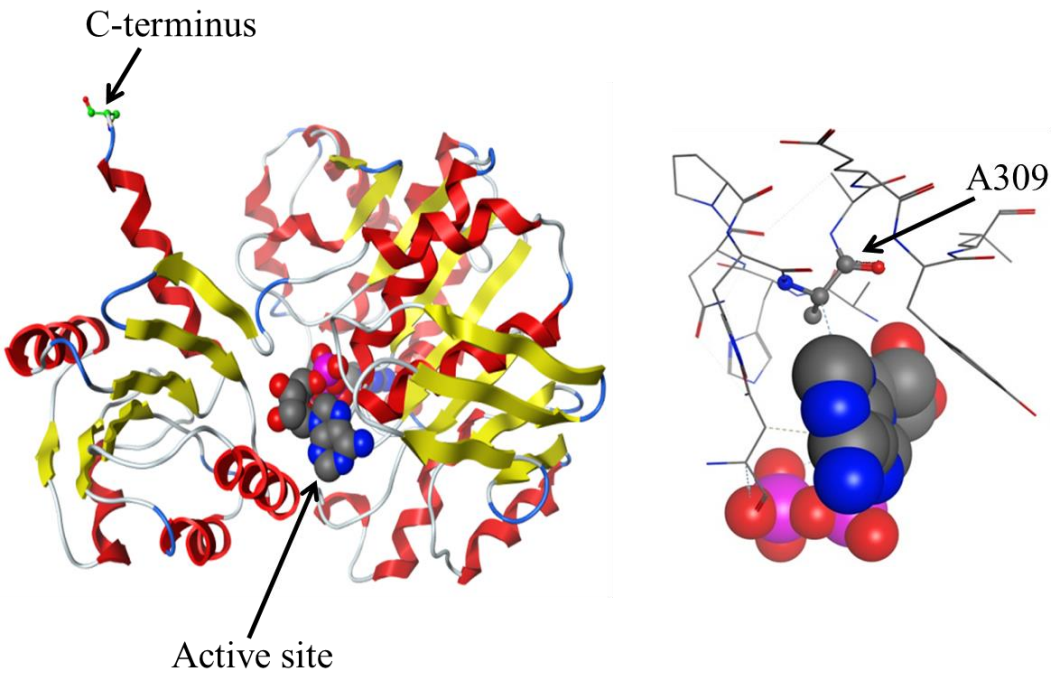

Figure 1-15 The structure of FPGS and the position of SF2 mutation
FPGS is a monomer (PDB:1W78) [34]. Left image: the active site and the C-terminus are labeled. The distance between the active site and the C-terminus is ≥26 Å. Right image: The *E. coli* SF2 strain contains a G925A mutation in the *FolC* gene corresponding to an A309T mutation in FPGS. The figure was constructed using MOE, version 2012.10 [30] .

1.7.3 5,10-Methylenetetrahydrofolate Reductase (MTHFR)

Methylenetetrahydrofolate Reductase (E.C. 1.5.1.20) is encoded by the *metF* gene. This enzyme catalyzes the reduction of 5,10-methylene-THF to 5-methyl-THF using NAD(P)H as a cofactor Figure 1-16 (below) [33, 51]. The 5-methyl-THF product serves as a methyl group donor for the subsequent conversion of homocysteine to methionine by methionine synthase [33]. In *E. coli* K12, the concentration of 5,10-methylene-THF (diglutamate, triglutamate, tetraglutamate and pentaglutamate forms) is 22.24 µM [35]. The K_M is only 0.8 µM [33], suggesting the enzyme will be saturated *in vivo.*

$$CH_2\text{-THF} + NAD(P)H + H^+ \longrightarrow CH_3\text{-THF} + NAD(P)^+ \quad (1)$$

$$\text{MTHFR-FAD}_{ox} + NAD(P)H \longrightarrow \text{MTHFR-FAD}_{red} + NAD(P)^+ \quad (2)$$

$$\text{MTHFR-FAD}_{red} + CH_2\text{-THF} \longrightarrow \text{MTHFR-FAD}_{ox} + CH_3\text{-THF} \quad (3)$$

Figure 1-16 Sequental catalytic mechanism of methylene-tetrahydrofolatereductase (MTHFR). MTHFR catalyzes the reduction of 5,10 methylene-tetrahydrofolate (CH_2-THF) to 5-methyl-tetrahydrofolate (CH_3-THF) using NADPH and flavin adenine dinucleotide (FAD) as coenzymes. MTHFR uses a sequential mechanism in which $NAD(P)^+$ release is followed by the binding of CH_2-THF and the subsequent release of CH_3-THF after reaction with the flavin. Equations from [51].

MTHFR is a tetramer (PDB: 1ZPT)

Figure 1-17 (below) [52]; the closest distance between the active site and C-terminus is 25 Å. Thus, addition of an SsrA tag should not interfere with the activity of the enzyme. Even though all of our criteria were not satisfied, the importance of this enzyme in the folate cycle and its association to heart disease [53 511] made this enzyme an attractive target for our study.

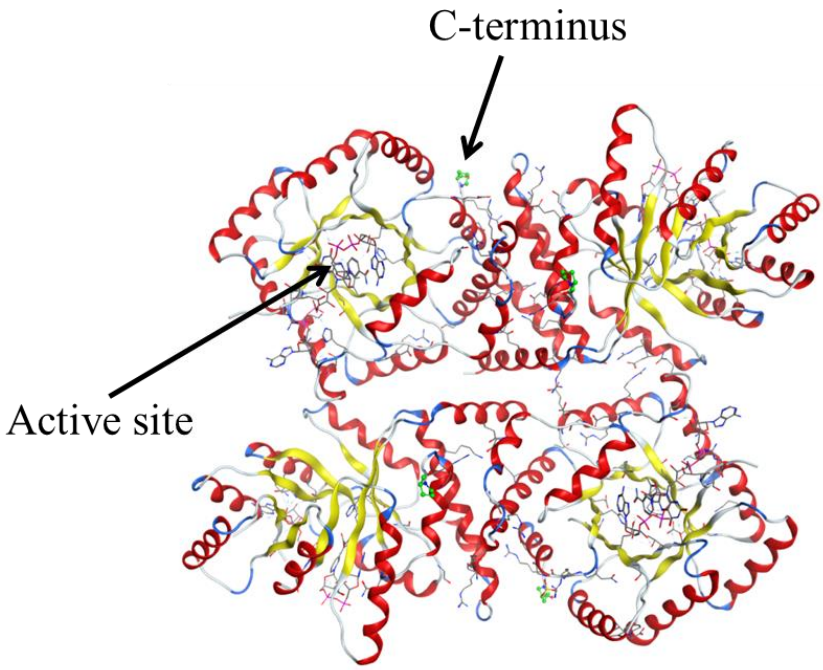

Figure 1-17 Crystal structure methylene-tetrahydrofolatereductase MTHFR
MTHFR is a tetramer (PDB:1ZPT), the active site and C-terminus of a monomer is labeled. The distance between the active site and C-terminus is ≥ 25 Å [32]. The figure was constructed using MOE version 2012.10 [30]

1.7.4 Serine Hydroxymethyl Transferase (SHMT)

Serine hydroxymethyl transferase (SHMT) (EC. 2.1.2.1) is the product of the *GlyA* gene. SHMT converts serine to glycine using pyridoxal phosphate (PLP) as a coenzyme. SHMT catalyzes two coordinated reactions, cleavage of PLP-serine to form PLP-glycine, and condensation of the formaldehyde with THF to form 5,10-methenyltetrahydrofolate [54]. A simplified reaction is shown in Figure 1-18 (below). SHMT is a dimer (PDB = IDFO) Figure 1-19 (below). In *E. coli* K12, the THF concentration (in all glutamylation states) is 10.02 µM [35]. The enzyme follows a sequential reaction mechanism; the K_M for THF is 25 µM [55]. The K_M is higher than the concentration of the metabolites *in vivo* [35], suggesting we may be able to titrate its activity. Finally, the distance between the active site and the C-terminus is ~25 Å, suggesting addition of a SsrA tag would not interfere with the catalytic site of the enzyme.

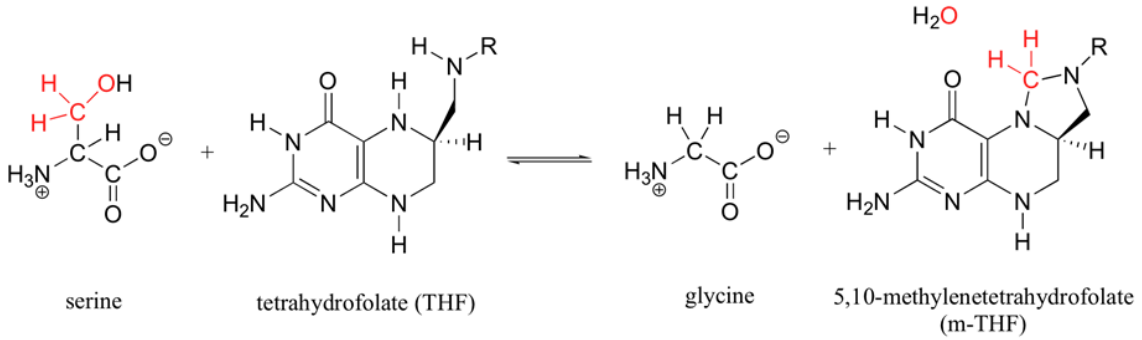

Figure 1-18 Serine hydroxymethyltransferase catalyzes reversible reaction
SHMT catalyzes the THF dependent cleavage of serine to form 5, 10-THF and glycine. Adapted from: http://2012.igem.org/Team:Utah_State/Project.

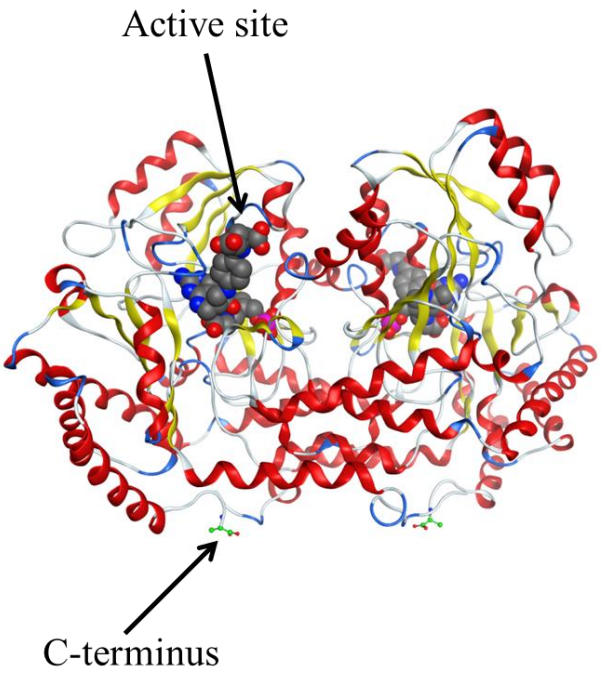

Figure 1-19 Crystal structure Serine hydroxymethyltransferase (SHMT)
SHMT is a dimer (PDB:1DFO). One active site and C-terminus (shown in green) are labeled. The distance between the active site and the C-terminus is ≥25 Å. The figure was constructed using MOE, version 2012.10 [30]

1.7.5 Dihydropteroate Synthase (DHPS)

DHPS (EC 2.5.1.15) catalyzes the formation of dihydropteroate from dihydropteroate-6-pyrophosphate (H_2PtPP) and p-aminobenzoic acid (pABA) Figure 1-20 (below).The *in vivo* pABA concentration is 0.02 µM [35]. The K_Ms for H_2PtPP and pABA are 1.2 ± 0.4 µM and 0.7 ± 0.2 µM, respectively [56]. Dihydropteroate synthase (PDB:1JAO) is a monomer Figure 1-21(below). The distance between the active site and C-terminus is ≥ 22 Å.

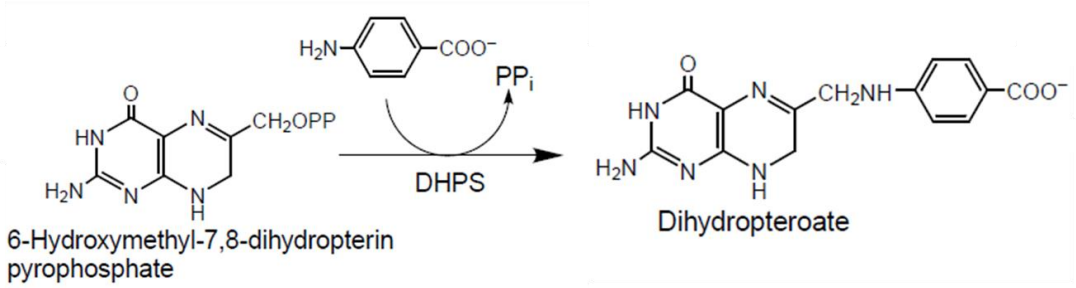

Figure 1-20 Dihydropteroate synthase (DHPS) attached pterin with pABA
This enzyme joins the activated 6-hydroxymethyl-7,8-dihydropterin pyrophosphate (DHPPP) with para-amino benzoic acid (pABA) to produce 7, 8-dihydropteroate [57].

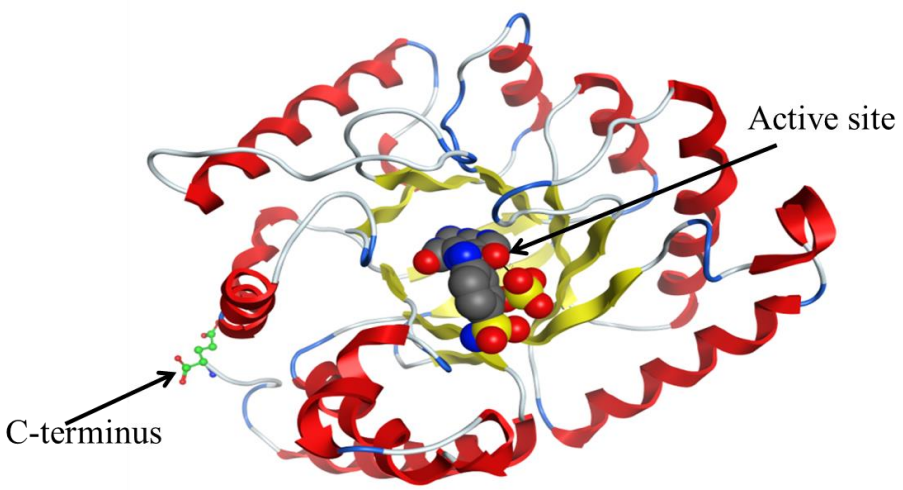

Figure 1-21 Crystal structure Dihydropteroate synthase (DHPS)
DHPS is a monomer, the active site and C-terminus are labeled (PDB: 3KUH). The distance between the active site and C-terminus is ≥22 Å. DHPS is also of interest as it provides resistance to sulfa drugs. The figure was constructed using MOE version 2012.10 [30].

1.7.6 Thymidylate Synthase (TS)

Thymidylate synthase (E.C. 2.1.1.45) catalyzes the conversion of deoxyuridine monophosphate (dUMP) to deoxythymidine monophosphate (dTMP). During this process, the 5,10-CH_2-THF cofactor is converted to DHF. This enzyme is a product of the *ThyA* gene. TS plays a major role in pyrimidine biosynthesis and it is the only de novo source of dTMP Figure 1-22 (below) [48, 58]. In *E.coli* K12, the concentration of 5,10-CH_2-THF is 22.42 µM [48]. The K_M values for CH_2-THF and dUMP are 11 µM [35] and 1.2 µM [42], respectively. However, the enzyme active site is close to the C-terminus and the carboxyl group (-COO^-) is involved in positioning the ligands at the active site [59]. Any additions to the C-terminus inactivate the enzyme. In addition, the N-terminal methionine is formylated and the formyl group forms a hydrogen bond with Thr46 and Thr47 Figure 1-23 (below)**.** Thus, attaching the protease degradation tag at either N-terminus or C-terminus is not possible. In addition, no histag clones exist for this enzyme.

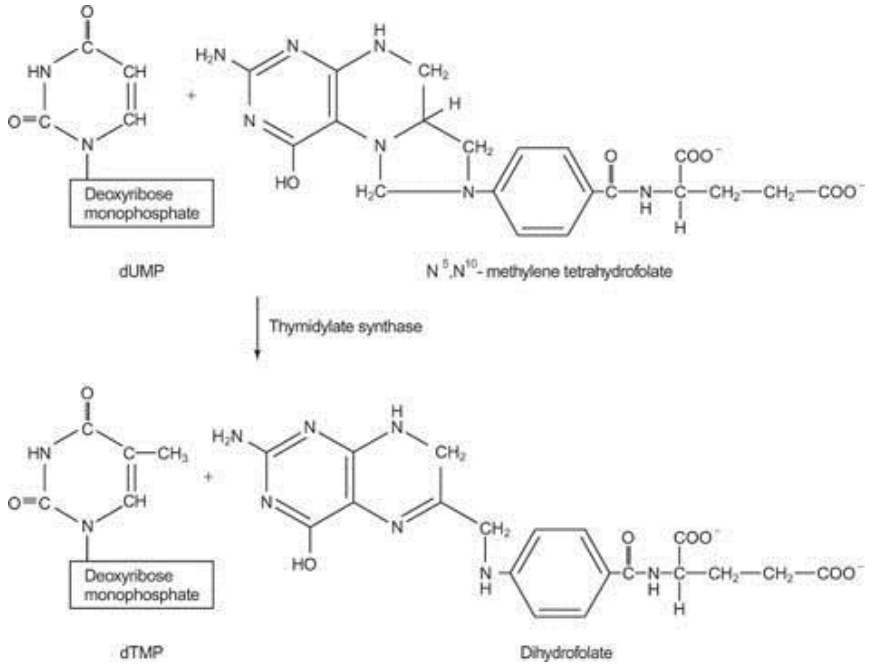

Figure 1-22 Thymidylate synthase (TS) plays a major role DNA synthesis.
This enzyme catalyzes the conversion of deoxyuridine monophosphate (dUMP) to deoxythymidine monophosphate (dTMP) using 5,10-methylene tetrahydrofolate (CH_2THF) as a methyl group donor. From: http://www.cliffsnotes.com/sciences/biology/biochemistry-ii/purines-and-pyrimidines/deoxynucleotide-synthesis

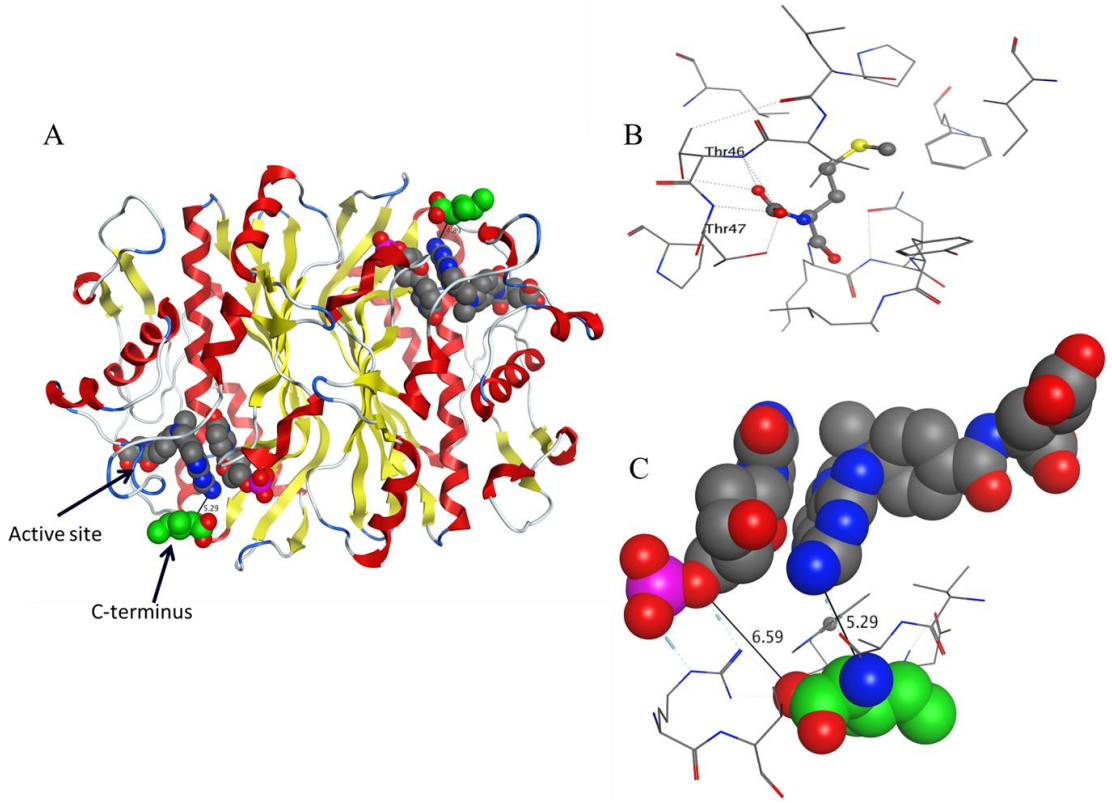

Figure 1-23 Crystal structure thymidylate Synthase (TS)
TS is dimer, (A) the active site and C-terminus are labeled. B-The N-terminus is formlyated; this group forms a hydrogen bond with Thr46 and Thr47. C- The distance between the active site and C-terminus is ≤ 5 Å and the C terminus carboxylate of the enzyme plays a role in adjusting the position of the ligands in the active site (PDB:1AXW) [59].

2 CHAPTER: MATERIALS AND METHODS

2.1 Brief summary and step wise processes and rationales

The flow chart summarizes the theoretical and experimental processes and structure of this thesis. First, we identify and select essential folate enzymes. Second, for the purpose of decreasing the *in vivo* protein production, the coding sequence for selected enzymes was cloned into the tunable plasmid, pKTS. The clones of interest were obtained by introducing NdeI and XhoI recognition sequences within open reading frame of gene via PCR and/or a commercial gene synthesis service. Third, pKTS carrying the gene of interest was transformed into a corresponding knockout *E. coli* strain. Fourth, the desired *in vivo* protein production level that allowed rescue of the auxotrophic strain to prototrophy (regulated via P_{tet} promoter) was determined by tetracycline titration. Fifth, to assess effect of increasing osmolality on the function of the targeted folate pathway enzyme, the internal osmolality of *E. coli* was titrated by sorbitol in minimal growth media. Finally, the effect of increasing osmolality on the function of the enzyme was analyzed based whether the cloned enzyme could maintain prototrophy for the auxotrophic strain. To control for the osmotic fitness of the host cell, parallel cell growth assays were performed on supplemented media. The osmotic fitness of the host cell was estimated based on the osmolality of supplemented growth media where the bacteria stopped growing. The flow chart in Figure 2-1- (below) show the steps in the process.

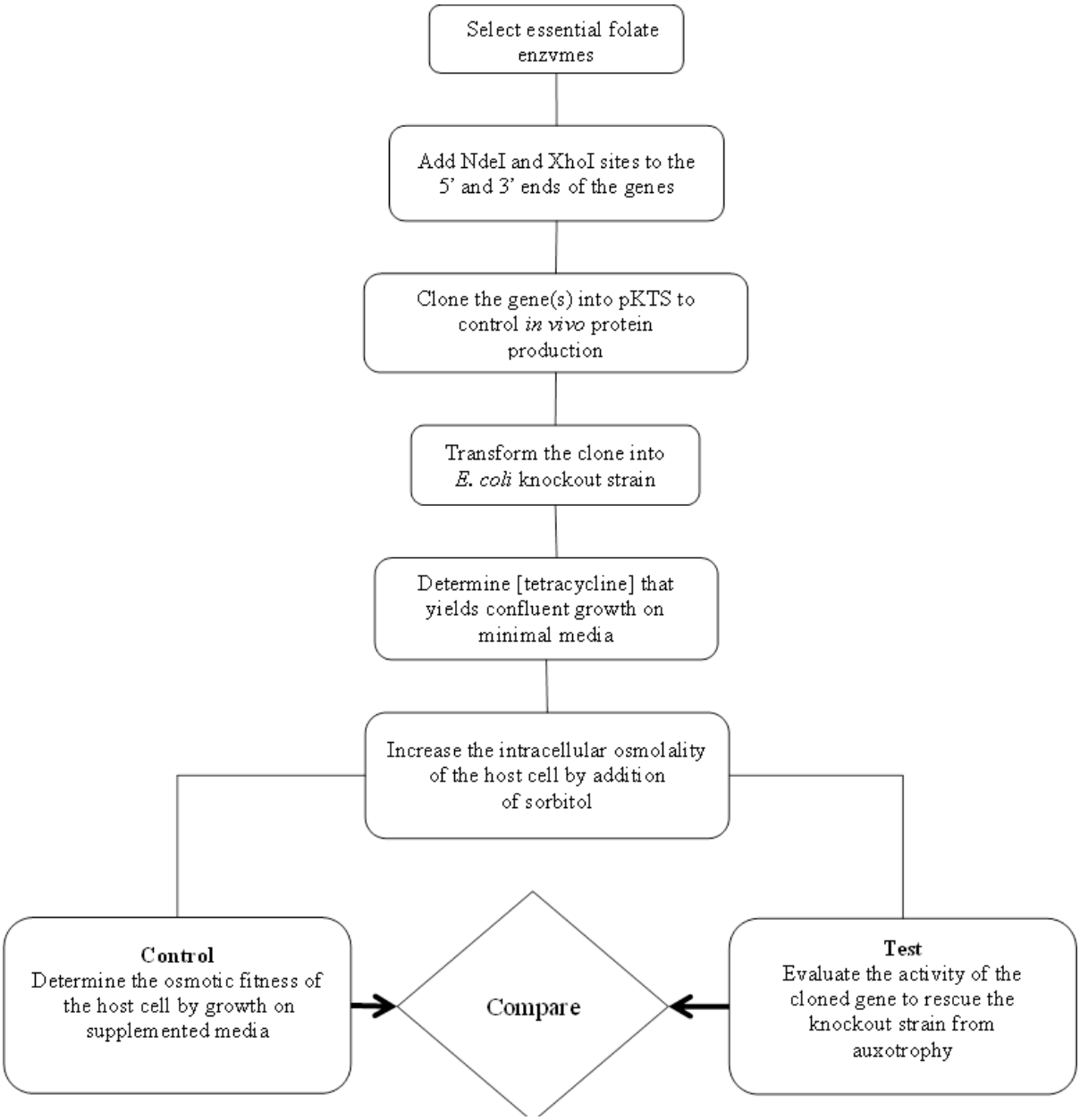

Figure 2-1 Flow chart describing the general work flow.

2.2 Biological Materials

2.2.1 Bacterial strains

Bacterial strains. The *E. coli* strains used in this study are listed in Table 2-1(below). Most strains contain a knockout in a folate pathway enzyme, resulting in some type of folate end product auxotrophy. In this study, the effect of increasing osmolality on the function of the enzyme was evaluated by the ability of the clone to rescue the host cell to prototrophy. Most of the Keio knockout strains [26] were purchased from the Coli Genetic Stock Center (CGSC, see http://cgsc.biology.yale.edu/). Other strains were requested from the lab that constructed the specific gene knockout.

Table 2-1 List of *E. coli* strains, their genotypes, and sources

Strain	Genotype	Source
DH5α	F^- *Φ80lacZΔM15(lacZYA-argF) U169 recA1 endA1 hsdR17* (rK^-, mK^+) *phoA supE44 λ–thi-1 gyrA96 relA1*	Invitrogen [60]
LH18	*Δlac-pro supE hsdRS F' lac(l-ZΔM15)*$^+$ *pro'* Δ*folA::kan*	Howell [61]
W1485	F^+ λ^- *rph-1* (also known as MG1655)	CGSC[26]
SF2	W1485/I-21 (F^- *folC strA*)	Bognar [49, 62]
SF4	F^- λ^- *rph-1 folC strA recA TN10:srlC*	
BW25113	F^- *Δ(araD-araB)567 ΔlacZ4787(::rrnB-3)* λ^- *rph-1 Δ(rhaD-rhaB)568 hsdR514*	CGSC [26]
JW2535-1	BW25113 *ΔglyA725::kan*	CGSC [26]
JW3913-1	BW25113 *ΔmetF728::kan*	CGSC [26]
C600	C600 Δ*folK::tc (thi-1 thr-1 leuB6 lacY1 tonA21 supE44*)	Swedberg [63]
C600	C600 *ΔfolP::kan(thi-1 thr-1 leuB6 lacY1 tonA21 supE44*)	Swedberg [63]
E. coli one shot ®TOP10F competent cells *	F'cells *[lacI*^{q} *Tn10(tet*^{R}*)] mcrA Δ(mrr-hsdRMS-mcrBC) φ80lacZΔM15 ΔlacX74 deoR nupG recA1 araD139 Δ(ara-leu)7697 galU galK rpsL(Str*^{R}*) endA1* λ^-	Invitrogen [64]

* *E. coli* Top 10 cell line was used for TOPO cloning

2.2.2 Plasmids

Clones of the folate pathway enzymes were obtained from various research labs. The source of these clones and some information concerning the clones is given in Table 2-2 (below**)**. The pKTS plasmid was obtained from Donald Hilvert (ETH Zurich) [4]. This plasmid enables gene expression control via the P_{tet} promoter and the SsrA protease degradation tag helps decrease the gene product concentration *in vivo*.

The clones were confirmed via sequencing. Briefly, ~ 40 ng of DNA for each clone was transformed into *E. coli* DH5a (Invitrogen) using the heat shock method. Immediately after the heat shock, 950 µL of S.O.C (2 % tryptone, 0.5 % yeast extract, 10 mM NaCl, 2.5 mM KCl, 10 mM $MgCl_2$, 10 mM $MgSO_4$, and 20 mM glucose) media was added and the samples were placed on a shaker (~200 rpm) at 37 ^{o}C for about one hour. Next 50 µL and 100 µL cells were plated on YT agar media with the appropriate antibiotic added. After overnight growth, three to five colonies were picked and grown in YT broth with 200 µg ampicillin/ml at 37 ^{o}C. Finally, the plasmid DNA was extracted with the Wizard Miniprep DNA purification system and the quality of the genes was confirmed via DNA sequencing at the Molecular Biology Resource facility (University of Tennessee, Knoxville).

Table 2-2 List of folate enzyme clones.

Gene	Enzyme (Abbreviation)	Plasmid Name	Source of cloned gene?
folA	Dihydrofolate reductase (DHFR)	pAG101 (EcDHFR)	Howell [5, 65, 66]
	R67 DHFR (Type II) Trimethoprim resistance Quad4 (Type II)[19]	pUC57	
folC	Folylpolyglutamate synthase (FPGS)	pAC5[a], pAC3[b] and pPM103[c]	Bognar [50, 67]
folP	Dihydropteroate synthase (DHPS) Sulfonamide resistance [68]	pUC19	Swedberg (*E. coli*) Lee (*Staphylococcus aureus*) [63, 69-71]
folK	6-Hydroxymethyl-7,8-dihydropterin pyrophosphokinase	pTT5	Yan [72-74]
glyA	Serine hydroxymethyl transferase (SHMT)	pSGlyA (pBR322), (Bluescript KS)	Contestabile [75-77]
metF	Methylene-tetrahydrofolate reductase (MTHFR)	pCAS30	Trimmer/Matthews [33]
thyA	Thymidylate synthase	Bluescript KS+	Kohen [78], Maley [79]

[a]: pUC9 with folC gene downstream of lac promoter; Amp resistance

[b]: pUC8 with 3.5-kb fragment containing *usg*, *folC*, and *dedD* genes; Amp resistance

[c]: pSC101 temperature sensitive for replication; segregates above 30°C; Tet resistance

The DNA sequences of the above genes were obtained from http://www.genome.jp/kegg-bin/show_organism?org=eco.

Table 2-3 (below) gives the gene sequences and the translated protein sequences [80].

Table 2-3 *E coli* one carbon metabolism genes DNA sequences and their corresponding protein products

Gene (Abbreviation)	DNA and protein sequence
R67 DHFR (type II DHFR)	atgatcaggagctctaatgaagtttcgaatccagttgccggcaattttgtattcccttcg M I R S S N E V S N P V A G N F V F P S aacgccacgtttggtatgggtgaccgcgtacgtaagaaatccggcgccgcctggcaaggt N A T F G M G D R V R K K S G A A W Q G cagattgtcgggtggtactgcacaaatttgacccctgagggctacgccgtcgagtctgag Q I V G W Y C T N L T P E G Y A V E S E gctcacccgggctcagtacagatctatcctgttgcggcgcttgaacgcatcaactaa A H P G S V Q I Y P V A A L E R I N -
Quad4 (Quadruplicated synthetic R67 DHFR)	atgatcaggagctctaatgaagtttcgaatccagttgccggcaattttgtattcccatcg M I R S S N E V S N P V A G N F V F P S aacgccacgtttggtatgggtgaccgcgtacgtaagaaatccggcgccgcctggcaaggt N A T F G M G D R V R K K S G A A W Q G cagattgtcgggtggtactgcacaaatttgacccctgagggctacgccgtcgaggctgag Q I V G W Y C T N L T P E G Y A V E A E gctcatccgggctcagtacagatctatcctgttgcggcgcttgaacgcatcgatatcgat A H P G S V Q I Y P V A A L E R I D I D cagcataacaatggcgttagcaccctggtggcaggtcagtttgccttacctagccatgcg Q H N N G V S T L V A G Q F A L P S H A acctttggcctgggtgaccgcgtccggaaaaagagtggcgccgcttggcagggacaagtc T F G L G D R V R K K S G A A W Q G Q V gtgggctggtattgcaccaagcttaccccggaaggttacgcggtagagagcgaatcgcat V G W Y C T K L T P E G Y A V E S E S H cctggaagcgtgcaaatttatccggtcgctgctctcgagcgaaggtacctcaatgagggc P G S V Q I Y P V A A L E R R Y L N E G aaaaatgaggtgtctacgtctgccgccggccgcttcgccttcccttcgaatgccactttc K N E V S T S A A G R F A F P S N A T F ggtctcggcgatcgtgttcgcaaaaagagcggcgccgcatggcaggggcgtatcgtaggt G L G D R V R K K S G A A W Q G R I V G tggtattgtactaccttaacgccggaggggtatgcagtggaaagtgagagccatccaggg W Y C T T L T P E G Y A V E S E S H P G agtgtccaaatttaccccatgaccgccttagagcgcagggccctgggccagagctctcat S V Q I Y P M T A L E R R A L G Q S S H gaagccaacgccccagtggccggccagttcgccctgcctctgagcgccacgtttggtttt E A N A P V A G Q F A L P L S A T F G F ggcgatcgtgttcgcaagaaatctggcgccgcgtggcaaggcaacgtggttggatggtac G D R V R K K S G A A W Q G N V V G W Y tgtacgaaactcactcccgaaggatatgctgttgaatcggaaagcctcccaggttccgtt C T K L T P E G Y A V E S E S L P G S V cagatctacccagtggcagcactcgaacgaatcaacggaggcggtggtcatcaccatcac Q I Y P V A A L E R I N G G G G H H H H catcac H H
folC (FPGS)	atgattatcaaacgcactcctcaagccgcgtcgcctctggcttcgtggctttcttatctg M I I K R T P Q A A S P L A S W L S Y L gaaaacctgcacagtaaaactatcgatctcggccttgagcgcgtgagcctggtcgcggcg E N L H S K T I D L G L E R V S L V A A cgtcttggcgtcctgaaaccagcgccatttgtgtttaccgttgcgggtacgaatggcaaa R L G V L K P A P F V F T V A G T N G K ggcaccacctgccgtacgctggagtcgattctgatggcggcagggtacaaagtgggcgtc G T T C R T L E S I L M A A G Y K V G V tacagttcgcctcatctggtgcgttataccgagcgcgtacgtgtgcagggccaggaattg Y S S P H L V R Y T E R V R V Q G Q E L ccggaatcggcccacaccgcctcttttgcggagattgaatcggcacgcggtgatatttcc P E S A H T A S F A E I E S A R G D I S ctgacctatttcgagtacggtacgctgtcggcgttgtggctgttcaagcaggcacaactt

	L T Y F E Y G T L S A L W L F K Q A Q L gacgtggtgattctggaagtagggctgggcggtcgtctggacgcaaccaatattgtcgac D V V I L E V G L G G R L D A T N I V D gccgatgtcgcggtagtaaccagtattgcgctggatcataccgactggctgggtccagat A D V A V V T S I A L D H T D W L G P D cgcgaaagtattggtcgcgagaaagcaggcatcttccgcagcgaaaaaccggcaattgtc R E S I G R E K A G I F R S E K P A I V ggtgagccggaaatgccttctaccattgctgatgtggcgcaggaaaaaggtgcactgtta G E P E M P S T I A D V A Q E K G A L L caacgtcggggcgttgagtggaactattccgtcaccgatcatgactgggcgtttagcgat Q R R G V E W N Y S V T D H D W A F S D gctcacggcacgctggaaaatctgccgttgccgcttgtcccgcaaccgaatgccgcaaca A H G T L E N L P L P L V P Q P N A A T gcgctggcggcactgcgtgccagcgggctggaagtcagtgaaaatgccattcgcgacggg A L A A L R A S G L E V S E N A I R D G attgccagcgcaattttgccgggacgtttccagattgtgagcgagtcgccacgcgttatt I A S A I L P G R F Q I V S E S P R V I tttgatgtcgcgcataatccacatgcggcggaatatctcaccgggcgtatgaaagcgcta F D V A H N P H A A E Y L T G R M K A L ccgaaaaacgggcgcgtgctggcggttatcggtatgctacatgataaagatattgccgga P K N G R V L A V I G M L H D K D I A G actctggcctggttgaaaagcgtggttgatgactggtattgtgcgccactggaagggccg T L A W L K S V V D D W Y C A P L E G P cgcggtgccacggcagaacaactgcttgagcatttgggtaacggcaaatcatttgatagc R G A T A E Q L L E H L G N G K S F D S gttgcgcaggcatgggatgccgcaatggcggacgctaaagcggaagacaccgtgctggtg V A Q A W D A A M A D A K A E D T V L V tgtggttctttccacacggtcgcacatgtcatggaagtgattgacgcgaggagaagcggt C G S F H T V A H V M E V I D A R R S G ggcaagtaa G K -
folk (HPPK)	atgacagtggcgtatattgccataggcagcaatctggcctctccgctggagcaggtcaat M T V A Y I A I G S N L A S P L E Q V N gctgccctgaaagcattaggcgatatccctgaaagccacattcttaccgtttcttcgttt A A L K A L G D I P E S H I L T V S S F taccgcaccccaccgctggggccgcaagatcaacccgattacttaaacgcagccgtggcg Y R T P P L G P Q D Q P D Y L N A A V A ctggaaacctctcttgcacctgaagagctactcaatcacacacagcgtattgaattgcag L E T S L A P E E L L N H T Q R I E L Q caaggtcgcgtccgcaaagctgaacgctggggaccacgcacgctggatctcgacatcatg Q G R V R K A E R W G P R T L D L D I M ctgtttggtaatgaagtgataaatactgaacgcctgaccgttccgcactacgatatgaag L F G N E V I N T E R L T V P H Y D M K aatcgtggatttatgctgtggccgctgtttgaaatcgcgccggagttggtgtttcctgat N R G F M L W P L F E I A P E L V F P D ggggagatgttgcgtcaaatcttacatacaagagcatttgacaaattaaacaaatggtaa G E M L R Q I L H T R A F D K L N K W -
folP (DHPS)	atgaaactctttgcccagggtacttcactggaccttagccatcctcacgtaatggggatc M K L F A Q G T S L D L S H P H V M G I ctcaacgtcacgcctgattccttttcggatggtggcacgcataactcgctgatagatgcg L N V T P D S F S D G G T H N S L I D A gtgaaacatgcgaatctgatgatcaacgctggcgcgacgatcattgacgttggtggcgag V K H A N L M I N A G A T I I D V G G E tccacgcgcccaggggcggcggaagttagcgttgaagaagagttgcaacgtgttattcct S T R P G A A E V S V E E E L Q R V I P gtggttgaggcaattgctcaacgcttcgaagtctggatctcagtcgatacatccaaacca V V E A I A Q R F E V W I S V D T S K P gaagtcatccgtgagtcagcgaaagttggcgctcacattattaatgatatccgctccctt E V I R E S A K V G A H I I N D I R S L tccgaacctggcgctctggaggcggctgcagaaaccggtttaccggtttgtctgatgcat S E P G A L E A A A E T G L P V C L M H atgcagggaaatccaaaaaccatgcaggaagctccgaagtatgacgatgtctttgcagaa M Q G N P K T M Q E A P K Y D D V F A E gtgaatcgctactttattgagcaaatagcacgttgcgagcaggcgggtatcgcaaaagag V N R Y F I E Q I A R C E Q A G I A K E aaattgttgctcgaccccggattcggtttcggtaaaaatctctcccataactattcatta K L L L D P G F G F G K N L S H N Y S L

	ctggcgcgcctggctgaatttcaccatttcaacctgccgctgttggtgggtatgtcacga L A R L A E F H H F N L P L L V G M S R aaatcgatgattgggcagctgctgaacgtggggccgtccgagcgcctgagcggtagtctg K S M I G Q L L N V G P S E R L S G S L gcctgtgcggtcattgccgcaatgcaaggcgcgcacatcattcgtgttcatgacgtcaaa A C A V I A A M Q G A H I I R V H D V K gaaaccgtagaagcgatgcgggtggtggaagccactctgtctgcaaaggaaaacaaacgc E T V E A M R V V E A T L S A K E N K R tatgagtaa Y E -
glyA (SHMT)	atgttaaagcgtgaaatgaacattgccgattatgatgccgaactgtggcaggctatggag M L K R E M N I A D Y D A E L W Q A M E caggaaaaagtacgtcaggaagagcacatcgaactgatcgcctccgaaaactacaccagc Q E K V R Q E E H I E L I A S E N Y T S ccgcgcgtaatgcaggcgcagggttctcagctgaccaacaaatatgctgaaggttatccg P R V M Q A Q G S Q L T N K Y A E G Y P ggcaaacgctactacggcggttgcgagtatgttgatatcgttgaacaactggcgatcgat G K R Y Y G G C E Y V D I V E Q L A I D cgtgcgaaagaactgttcggcgctgactacgctaacgtccagccgcactccggctcccag R A K E L F G A D Y A N V Q P H S G S Q gctaactttgcggtctacaccgcgctgctggaaccaggtgataccgttctgggtatgaac A N F A V Y T A L L E P G D T V L G M N ctggcgcatggcggtcacctgactcacggttctccggttaacttctccggtaaactgtac L A H G G H L T H G S P V N F S G K L Y aacatcgttccttacggtatcgatgctaccggtcatatcgactacgccgatctggaaaaa N I V P Y G I D A T G H I D Y A D L E K caagccaaagaacacaagccgaaaatgattatcggtggtttctctgcatattccggcgtg Q A K E H K P K M I I G G F S A Y S G V gtggactgggcgaaaatgcgtgaaatcgctgacagcatcggtgcttacctgttcgttgat V D W A K M R E I A D S I G A Y L F V D atggcgcacgttgcgggcctggttgctgctggcgtctacccgaacccggttcctcatgct M A H V A G L V A A G V Y P N P V P H A cacgttgttactaccaccactcacaaaaccctggcgggtccgcgcggcggcctgatcctg H V V T T T T H K T L A G P R G G L I L gcgaaaggtggtagcgaagagctgtacaaaaaactgaactctgccgttttccctggtggt A K G G S E E L Y K K L N S A V F P G G cagggcggtccgttgatgcacgtaatcgccggtaaagcggttgctctgaaagaagcgatg Q G G P L M H V I A G K A V A L K E A M gagcctgagttcaaaacttaccagcagcaggtcgctaaaaacgctaaagcgatggtagaa E P E F K T Y Q Q Q V A K N A K A M V E gtgttcctcgagcgcggctacaaagtggtttccggcggcactgataaccacctgttcctg V F L E R G Y K V V S G G T D N H L F L gttgatctggttgataaaaacctgaccggtaaagaagcagacgccgctctgggccgtgct V D L V D K N L T G K E A D A A L G R A aacatcaccgtcaacaaaaacagcgtaccgaacgatccgaagagcccgtttgtgacctcc N I T V N K N S V P N D P K S P F V T S ggtattcgtgtaggtactccggcgattacccgtcgcggctttaaagaagccgaagcgaaa G I R V G T P A I T R R G F K E A E A K gaactggctggctggatgtgtgacgtgctggacagcatcaatgatgaagccgttatcgag E L A G W M C D V L D S I N D E A V I E cgcatcaaaggtaaagttctcgacatctgcgcacgttacccggtttacgcataa R I K G K V L D I C A R Y P V Y A -
metF (MTHFR)	atgagctttttcacgccagccagcgggatgccctgaatcagagcctggcagaagtccag M S F F H A S Q R D A L N Q S L A E V Q gggcagattaacgtttcgttcgagtttttcccgccgcgtaccagtgaaatggagcagacc G Q I N V S F E F F P P R T S E M E Q T ctgtggaactccatcgatcgccttagcagcctgaaaccgaagtttgtatcggtgacctat L W N S I D R L S S L K P K F V S V T Y ggcgcgaactccggcgagcgcgaccgtacgcacagcattattaaaggcattaaagatcgc G A N S G E R D R T H S I I K G I K D R actggtctggaagcggcaccgcatcttacttgcattgatgcgacgcccgacgagctgcgc T G L E A A P H L T C I D A T P D E L R accattgcacgcgactactggaataacggtattcgtcatatcgtggcgctgcgtggcgat T I A R D Y W N N G I R H I V A L R G D ctgccgccgggaagtggtaagccagaaatgtatgcttctgacctggtgacgctgttaaaa L P P G S G K P E M Y A S D L V T L L K gaagtggcagatttcgatatctccgtggcggcgtatccggaagttcacccggaagcaaaa

	E V A D F D I S V A A Y P E V H P E A K agcgctcaggcggatttgcttaatctgaaacgcaaagtggatgccggagccaaccgcgcg S A Q A D L L N L K R K V D A G A N R A attactcagttcttcttcgatgtcgaaagctacctgcgttttcgtgaccgctgtgtatcg I T Q F F F D V E S Y L R F R D R C V S gcgggcattgatgtggaaattattccgggaattttgccggtatctaactttaaacaggcg A G I D V E I I P G I L P V S N F K Q A aagaaatttgccgatatgaccaacgtgcgtattccggcgtggatggcgcaaatgttcgac K K F A D M T N V R I P A W M A Q M F D ggtctggatgatgatgccgaaacccgcaaactggttggcgcgaatattgccatggatatg G L D D D A E T R K L V G A N I A M D M gtgaagattttaagccgtgaaggagtgaaagatttccacttctatacgcttaaccgtgct V K I L S R E G V K D F H F Y T L N R A gaaatgagttacgcgatttgccatacgctgggggttcgacctggtttataa E M S Y A I C H T L G V R P G L -
thyA (TS)	atgaaacagtatttagaactgatgcaaaaagtgctcgacgaaggcacacagaaaaacgac M K Q Y L E L M Q K V L D E G T Q K N D cgtaccggaaccggaacgctttccatttttggtcatcagatgcgttttaacctgcaagat R T G T G T L S I F G H Q M R F N L Q D ggattcccgctggtgacaactaaacgttgccacctgcgttccatcatccatgaactgctg G F P L V T T K R C H L R S I I H E L L tggtttctgcagggcgacactaacattgcttatctacacgaaaacaatgtcaccatctgg W F L Q G D T N I A Y L H E N N V T I W gacgaatgggccgatgaaaacggcgacctcgggccagtgtatggtaaacagtggcgcgcc D E W A D E N G D L G P V Y G K Q W R A tggccaacgccagatggtcgtcatattgaccagatcactacggtactgaaccagctgaaa W P T P D G R H I D Q I T T V L N Q L K aacgacccggattcgcgccgcattattgtttcagcgtggaacgtaggcgaactggataaa N D P D S R R I I V S A W N V G E L D K atggcgctggcaccgtgccatgcattcttccagttctatgtggcagacggcaaactctct M A L A P C H A F F Q F Y V A D G K L S tgccagctttatcagcgctcctgtgacgtcttcctcggcctgccgttcaacattgccagc C Q L Y Q R S C D V F L G L P F N I A S tacgcgttattggtgcatatgatggcgcagcagtgcgatctggaagtgggtgattttgtc Y A L L V H M M A Q Q C D L E V G D F V tggaccggtggcgacacgcatctgtacagcaaccatatggatcaaactcatctgcaatta W T G G D T H L Y S N H M D Q T H L Q L agccgcgaaccgcgtccgctgccgaagttgattatcaaacgtaaacccgaatccatcttc S R E P R P L P K L I I K R K P E S I F gactaccgtttcgaagactttgagattgaaggctacgatccgcatccgggcattaaagcg D Y R F E D F E I E G Y D P H P G I K A ccggtggctatctaa P V A I -

2.3 Cloning

2.3.1 Competent cell preparation

2.3.1.1 Chemically competent cell preparation.

Chemically competent cells for each *E. coli* strain of interest, in particular the knockout strains listed in Table 2-1 (above), were made following general molecular biology techniques. Briefly a starter culture of the *E. coli* knockout strain was grown in 10 mL YT broth with selective antibiotic and required folate end product(s). (The list of required folate end products for each enzyme is given in Table 2-5 (below). Next, 1% of starter culture was transferred into 50 mL fresh YT broth with antibiotic. After the cells reached an OD_{600} of ~0.4-0.6, the cell suspension was spun down in a Sorvall RC-6 Plus centrifuge using a SS-34 rotor at 6100 rpm for 5 minutes. The pellet was washed twice with wash buffer (5 mM Tris-HCl pH 7.6, 10 mM $MgCl_2$ and 50 mM NaCl) and re-suspended twice. Then, the cell pellet was re-suspended in a $CaCl_2$ buffer (10 mM Tris-HCL pH 7.6, 10 mM $MgCl_2$, and 10 mM $CaCl_2$) and incubated for 30 min on ice. Next, the cells were spun down and $CaCl_2$ buffer was removed. The pellet was re-suspended with ice cold storage buffer ($CaCl_2$ buffer with 15% glycerol) and 100 µL cell suspensions were aliquoted into sterile 1.5 mL microfuge tubes. These samples were snap frozen with dry ice and stored at -80°C [81].

2.3.1.2 Electrocompetent cell preparation

Electrocompetent cells of each *E. coli* knockout strain of interest were made following the protocol in the Micropulser™ electroporation apparatus operation manual (cat 165-2100) [82]. Briefly, a 10 ml starter culture of a knockout strain was grow in of 50 mL SOB-Mg^- (without Magnesium) 0.5 % tryptone, 0.5 % yeast extract, 10 mM NaCl, 1.34 mM KCl) broth with selective antibiotic and required folate end product(s). Next, 1% of starter culture was transferred into 50 mL fresh YT broth with antibiotic and required folate end product(s). After the cells reached an OD_{600} of ~0.5-0.7, they were centrifuged in a Sorvall centrifuge using a SS-34 rotor at 6,100 rpm. The pellet was washed twice with ice-cold 10 % glucose solution. Then, the cells were re-suspended in a final volume of 1-2 mL with ice-cold 10 % glucose solution and 100 µL cells were

aliquoted into sterile 1.5 mL microfuge tubes. These samples were snap frozen with dry ice and stored in the -80°C freezer.

2.3.2 Introduction of NdeI and/or XhoI recognition sequences

The pKTS plasmid has NdeI and XhoI cloning sites between the P_{tet} promoter and the SsrA degradation tag. These two restriction enzyme sites were introduced at the 5' and 3' ends of the gene, respectively. Two methods were used to introduce the sequences, as described below.

2.3.2.1 Chemical Synthesis

Chemical Synthesis: For R67 DHFR and Quad4 genes, NdeI and XhoI recognition sites were added to the 5' and 3' ends of these genes by chemical synthesis by Genscript (USA, Inc.). The genes were supplied as clones in pUC57.

To decrease the activity of DHPS, a 'pessimal' DNA sequence was designed in collaboration with Mike Gilchrist (Ecology and Evolutionary Biology department, University of TN, Knoxville). A pessimal sequence is the opposite of an optimized sequence as low frequency use codons are utilized in the design process. The 'pessimal' sequence with NdeI and XhoI recognition sites was chemically synthesized and supplied as a clone in the pET 3a vector by Genscript (USA, Inc). The gene sequence is shown below:

```
atgaagctatttgcccaaggaacatcactagatctaagtcatccccatgtcatgggaata
 M  K  L  F  A  Q  G  T  S  L  D  L  S  H  P  H  V  M  G  I
ctaaatgtcacacccgattcattttcagatggaggaacacataattcactaatagatgcc
 L  N  V  T  P  D  S  F  S  D  G  G  T  H  N  S  L  I  D  A
gtcaagcatgccaatctaatgataaatgccggagccacaataatagatgtcggaggagag
 V  K  H  A  N  L  M  I  N  A  G  A  T  I  I  D  V  G  G  E
tcaacaagacccggagccgccgaggtcagtgtcgaggaggagctacaaagagtcataccc
 S  T  R  P  G  A  A  E  V  S  V  E  E  E  L  Q  R  V  I  P
gtcgtcgaggccatagcccaaagatttgaggtctggatatcagtcgatacatcaaagccc
 V  V  E  A  I  A  Q  R  F  E  V  W  I  S  V  D  T  S  K  P
gaggtcataagagagtcagccaaggtcggagcccatataataaatgatataagatcacta
 E  V  I  R  E  S  A  K  V  G  A  H  I  I  N  D  I  R  S  L
tcagagcccggagccctagaggccgccgccgagacaggactacccgtctgtctaatgcat
 S  E  P  G  A  L  E  A  A  A  E  T  G  L  P  V  C  L  M  H
atgcaaggaaatcccaagacaatgcaagaggcccccaagtatgatgatgtctttgccgag
 M  Q  G  N  P  K  T  M  Q  E  A  P  K  Y  D  D  V  F  A  E
gtcaatagatattttatagagcaaatagccagatgtgagcaagccggaatagccaaggag
 V  N  R  Y  F  I  E  Q  I  A  R  C  E  Q  A  G  I  A  K  E
aagctactactagatcccggatttggatttggaaagaatctatcacataattattcacta
 K  L  L  L  D  P  G  F  G  F  G  K  N  L  S  H  N  Y  S  L
ctagccagactagccgagtttcatcattttaatctacccctactagtcggaatgtcaaga
 L  A  R  L  A  E  F  H  H  F  N  L  P  L  L  V  G  M  S  R
```

```
aagtcaatgataggacaactactaaatgtcggaccctcagagagactaagtggaagtcta
 K  S  M  I  G  Q  L  L  N  V  G  P  S  E  R  L  S  G  S  L
gcctgtgccgtcatagccgccatgcaaggagcccatataataagagtccatgatgtcaag
 A  C  A  V  I  A  A  M  Q  G  A  H  I  I  R  V  H  D  V  K
gagacagtcgaggccatgagagtcgtcgaggccacactatcagccaaggagaataagaga
 E  T  V  E  A  M  R  V  V  E  A  T  L  S  A  K  E  N  K  R
tatgagtaa
 Y  E  -
```

2.3.2.2 PCR Method

PCR method: For the other two folate genes encoding *metF* and *glyA*, NdeI and/or XhoI restriction sites were introduced with the polymerase chain reaction (PCR). For *metF*, the forward and reverse primers were designed following the protocol described on the Oxford Genetics website [83]. Briefly, upstream from the start codon of *metF*, the NdeI recognition sequence 'CAT' and six non-complementary TA bases were added. Then 21 coding bases for *metF* were included. The T_M of the primer was estimated using the New England BioLabs (NEB) T_M calculator [84]. In the *metF* clone, a XhoI restriction site was already present at the end of the gene. Therefore, the reverse primer was designed using 25 complementary bases that were upstream of the XhoI site. The annealing temperature was calculated by subtracting 5 ^{0}C from the lowest T_M estimated for the forward and reverse primers. The sequences of the primers are listed in Table 2-4 (below).

The PCR primers for the *glyA* gene were designed by a similar approach. The forward primer possessed 39 bases from the coding sequence with an added Nde1 site. Similarly, the reverse primer was designed with 20 complementary bases upstream of the stop codon. Then a XhoI recognition sequence was added as well as an extended 'GC' sequence. The T_M values for the primers were estimated using the New England BioLabs (NEB) T_M calculator [84] . The sequences of the primers are listed in Table 2-4(below).

The PCR amplification reaction was carried out in 50 μl reaction volumes using 0.50 μM forward and reverse primers, 200 mM dNTPs (Fisher), 1.5 mM $MgCl_2$ and 1X PCR buffer (100 mM Tris-HCl, pH 9.0; 500 mM KCl; 15 mM $MgCl_2$) (Fisher) and 1 Unit Taq DNA polymerase (Fisher) and 5 to 100 ng DNA template. The reaction was carried out in a 0.2 μl PCR tube in a DNA thermal cycler (Bio-Rad). The reaction conditions were 95 ^{o}C for 5 minutes, with 35 cycles

of (95 ^{o}C for 30 seconds, annealing temperature (~the lowest of the T_M – 5 ^{0} C) as listed in Table 5 for 45 seconds, 72 ^{o}C for 1-2 minute), and a final extension of 72 ^{o}C for 15 minutes.

Table 2-4 List of PCR primer sequences used to introduce Nde1 and/or Xho1 restriction enzyme sites with their calculated T_M values.

Enzyme name	Primer sequences with the introduced restriction enzyme sequence underlined	Annealing Temperature (^{0} C)
MTHFR (pCAS30) [33]	5'TATTTACATATGAGCTTTTTTCACGCCAGC 3' (NdeI) T_m= 56°C, 30 mer with 22 complementary bases (forward primer)	51 ^{o}C
	5'AAGGGGTTATGCTAGTTATTGCTCA 3' T_m= 56°C, 25 bp complementary sequence (reverse primer)	
SHMT (pBSGlyA) [75-77]	5'GGGAGGAGGCATATGTTAAAGCGTGAAATGAACAT TGCCGATTATGATGCC 3' (NdeI) T_m= 64 ^{o}C, 51 mer with 39 complementary bases (forward primer)	50 ^{o}C
	5'GAGAGAGAGCTCGAGTGCGTAAACCGGGTAACGTG C 3' (XhoI) T_m= 56°C, 36 mer with 20 complementary bases (reverse primer)	

2.3.3 TOPO TA cloning

Cloning the PCR product into the TOPO TA vector pCR®2.1

Following PCR amplification, the PCR products of *metF* and *glyA* were cleaned with the Gene JET PCR Purification Kit (Thermo Scientific) following the manufacturers protocol. The resulting PCR products were cloned into the pCR 2.1 vector based on the Taq DNA polymerase reaction. This polymerase provides A-overhangs on the PCR fragment which allows ready ligation with the TOPO TA kit (Invitrogen). The resulting ligation mixture was transformed into Top10 One Shot chemically competent listed in Table 2-1 (above) [64] using a standard heat shock method and 20 µL and 50 µL aliquots were plated on YT agar media with 50 µg /ml kanamycin to select for cells carrying the TOPO vector. 40 µg/mI 5-bromo-4-chloro-3-indolyl-β-D-galactopyranoside (X-gal) was added to select for colonies carrying the vector with the insert using a white/blue colony selection. The plates were incubated overnight at 37°C. After overnight cell growth, ten white colonies were selected and grown in YT broth with 200 µg/mL ampicillin. The

plasmid DNA was extracted using the Wizard Miniprep DNA purification system and the identity of the insert was confirmed by DNA sequencing.

2.3.4 Sample cleaning processes

Preparing the insert and vector DNA fragments for cloning

The plasmid DNA for each clone and the pKTS vector were linearized with NdeI and XhoI following the manufacturer's protocol with minor modifications. Briefly, the restriction enzyme digest was performed in a 20 µL volume containing 1-2 µg of DNA, 1X Cutsmart™ buffer (50 mM potassium acetate, 20 mM Tris-acetate, 10 mM magnesium acetate, and 100 µg/mL BSA pH 7.9 g) with 5 to 10 units of NdeI (NEB) and XhoI (NEB). Then the samples were incubated at 37 ^{o} C from 3 hours to overnight. The digested DNA samples were electrophoresed on a 1% SeaKem® LE agarose (Rockland, ME) gel using modified Tris-acetate EDTA (TAE) buffer (1 mM NaEDTA,40 mM Tris acetate, pH 8). The DNA fragments were visualized by staining the gel with 0.5 µg ethidium bromide/ ml (Sigma). The correct sized DNA fragments were determined under a long wave UV light using a 1 kb plus DNA ladder as a standard. Then, the correct DNA fragment, based on the fragment size, was excised and purified with the Ultrafree®-DA and Wizard clean up systems (Millipore) according to the manufacturer's protocol. The desired DNA fragments were precipitated with 7.5 M ammonium acetate plus ethanol and suspended with filtered (0. 22 µm syringe filter, Millipore) and autoclaved Milli-Q Water. The DNA concentration was estimated with the NanoDrop 1000 Spectrophotometer (Thermo Scientific). The insert:vector ratio was calculated using Equation 1.

$$\text{ng of insert} = \frac{\text{ng vector} \times \text{kb size of inset}}{\text{kb size of vector}} \times \text{molar ratio of } \frac{\text{insert}}{\text{vector}}$$

Equation 1

2.3.5 Ligation and transformation

Linearized and cleaned DNA fragments were cloned using the DNA Ligation System Ver.2.1 kit (Takara Bio Inc.) following the manufacturer's instructions. Briefly, the insert and vector DNA molecules were mixed in a 1:1, 1:3, and 1:5 ratio and equal volumes of Solution 1 (Takara Bio Inc.) were added. The samples were incubated over night at 16 ^{0}C. Next, the ligation mixture was divided into two parts. The first half of the DNA mixture was directly transformed into chemically competent cells of the appropriate knockout strains. The other half of the ligated DNA was precipitated with 7.5 M ammonium acetate plus ethanol and resuspended with 10 µL filtered (0. 22 µm syringes filter, Millipore) and autoclaved Milli-Q Water for electroporation.

Chemically competent cells of knockout *E. coli* strains were made and the ligation mixture was transformed as described above. Electroporation was performed on electrocompetent cells following the manufacturers protocol (Bio Rad). Briefly, 1- 4 µL of ligated and precipitated DNA mixture was mixed with 40 µL electrocompetent cells and gently mixed. The cell suspension was transferred into an electroporation cuvette of 1 mm inter-electrode gap (BTX Technologies Inc. Hawthorne, NY). Electroporation was performed by a single pulse at the setting 1 E.C that corresponds to 1.8 kV. The sample preparation and set-up of cuvettes, plasmid DNA and electrocompetent cells were kept on ice. Immediately after electroporation, 1 ml of S.O.C. media was added to the electroporation cuvette and the cells were transferred into a sterile 1.5 mL Eppendorf tube. The mixture was shaken at ~200 rpm at 37 ^{o}C for one to three hours. ~ 50 µL and 100 µL cells were plated as described below.

To identify the correct clones, the selection used the ability of the clone to rescue the knockout host strain to prototrophy. The plates were Bonner-Vogel (BV) minimal media containing 1xBV salt: 0.00038 M $MgSO_4.7H_2O$, 0.0094 M citric acid•H_2O, 0.0574 M K_2HPO_4, 0.0167 M NH_4NaHPO_4•$4H_2O$), 0.2% glucose/mL, 50.0 µg histidine/mL, 40.0 µg guanine/mL, 50.0 µg tyrosine/mL 50.0 µg tryptophan/mL, and 1.0 µM thiamine. An alternate selection used YT agar media with selective antibiotic. The former selection is based on the ability of the clones to rescue the host to prototrophy and the latter selection allows for the antibiotic resistance selection associated with the pKTS vector. The *E. coli* LH18 strain carrying the DHFR clone was selected

on BV minimal media consisting of BV minimal media plus 50.0 μg thymidine/mL. The correct clones were further verified by DNA sequencing.

Table 2-5 The folate end products added as supplement(s) to BV minimal media

Gene	Folate end product supplement
folA	30.3 μg adenine /mL, 50.0 μg glycine /mL, 50.0 μg methionine/mL and 10.0 μg pantothenate/mL
glyA	50.0 μg glycine /mL and 50.0 μg serine /mL
metF	50.0 μg methionine/mL
folP	50.0 μg thymidine/mL
folC	50.0 μg glycine /mL and 50.0 methionine μg /mL,

2.4 Tetracycline titration

To assess the ability of the folate pathway gene carried in pKTS to rescue the appropriate knockout strain from auxotrophy, the optimal tetracycline concentration that supports a minimal but confluent cell growth was determined by streaking an overnight cell culture on plates containing increasing concentrations of tetracycline. The concentration range used was 0 (no tetracycline, control), 10 ng tetracycline/ml, 25 ng tetracycline/ml, 50 tetracycline/ml, 75 ng tetracycline/ml, 100 ng tetracycline/ml, 200 ng tetracycline/ml and 500 ng tetracycline/ml ng tetracycline/ml in either M9 minimal media or Bonner-Vogel (BV) minimal media. The tetracycline concentration that supports confluent cell growth was determined.

2.5 Sorbitol titration

Effects of osmotic stress on the *in vivo* activities of folate pathway enzymes.

E.coli knockout strains carrying the appropriate folate enzyme cloned in pKTS were plated on BV minimal agar with the optimal tetracycline concentration that supported confluent bacterial growth. Then, a sorbitol titration (0 to 1.50 M) was performed to determine if increasing osmolality *in vivo* can interfere with the ability of the enzyme to rescue the host cell to prototrophy.

A positive control involved plating the cells on BV supplemented media. This allows discrimination between the lack of cell growth due to loss of free water in the cell from the effect of osmolytes on enzyme activity [85]. Folate end product(s) supplements for each enzyme are listed in Table 2-5 (above).

2.5.1 Quantifying osmolality of a media

Water activity measurements: The water activity of BV agar containing 0, 0.25, 0.50, 0.75, 1.00, 1.25 or 1.05 M of sorbitol was measured at room temperature using an AquaLab dew point water activity meter 4TE (Decagon Devices, Inc., Pullman, WA). Then, the osmolality (Osm) was calculated using Equation 2

$$\text{Osmolality (Osm)} = \frac{\ln a_{H2O}}{-0.018}$$

Equation 2

2.6 Effects of osmolality on the function of plasmid encoded R67 DHFR and/or quad4 to rescue E. coli from TMP pressure

The activity of EcDHFR is inhibited by trimethoprim (TMP) (K_i = 20 pM) [18], but R67 DHFR provides resistance to this drug (K_i = 0.15 mM) [19]. Thus, the activity of R67 DHFR and Quad4 in the presence of increasing osmolality was assessed by the ability of the clones to allow DH5α to grow on M9 media containing 200 µg ampicillin/mL, 20 µg TMP/mL, 100 ng tetracycline, and various concentrations of sorbitol (0 to 1.50 M). The plates were incubated at 37 ^{0}C and the cell growth was observed for 2 to 5 days. As a control to evaluate the optimal external osmotic pressure that blocked DH5α growth, cells were grown on M9 media titrated with sorbitol, but without antibiotics.

2.7 Effects of osmolality on the activity of folylpolyglutamate synthase (FPGS)

The effect of osmolality on the function of FPGS was assayed in the *E. coli* SF2 strain (F^- *folC strA*). The *FolC* chromosomal lesion carries a G925A mutation corresponding to an A309T

mutation in FPGS [49, 50]. This strain is auxotrophic for methionine and its growth is stimulated by glycine [49]. Thus, the activity of FPGS in the presence of increasing osmolality was assessed by the ability of the pAC3, pAC5 and pPM103-FolC plasmids Table 2-2(above) to rescue *E. coli* SF2 (F^- *folC strA*) from methionine and/or glycine auxotrophy on BV minimal media lacking these components. Cell growth was compared to that of the *E. coli* SF2 parent strain E. *coli* MG1665.

3 CHAPTER: RESULTS

We propose that increased osmolality will titrate the activity of folate pathway enzymes due to preferential interactions of osmolytes with folate redox states. This hypothesis can be probed genetically via restoration of prototrophy to the appropriate knockout strains. A challenge to this approach is controlling the enzyme turnover rate and/or protein production level [1, 4]. To address these issues, the gene for the enzyme of interest was cloned into a controllable pKTS vector [4]. This plasmid was transformed into the appropriate knockout *E. coli* strain and osmotic stress titrations were performed.

3.1 Assessing the activity of R67 DHFR and/or Quad4 clones in the presence of increasing osmolality *in vivo*

Our first gene of interest was R67 DHFR. This target was selected as we previously performed osmotic stress titrations of the Y69L mutant clone [1]. At that time, the activity of the wt R67 DHFR clone was too high to titrate *in vivo*. To decrease the activity of the enzyme as well as the protein life time, our first step was cloning the R67 DHFR gene into the pKTS plasmid. An additional tandem array of 4 fused R67 DHFR genes (named Quad4) was also cloned into pKTS.

3.1.1 Construction of R67 DHFR-pKTS and Quad4-pKTS

The pKTS vector has NdeI and XhoI cloning sites for gene insertion [4]. This vector was sent to us with a chorismate mutase insert. To facilitate cloning of R67 DHFR and Quad4 genes into pKTS, synthetic genes with NdeI and XhoI restriction enzyme recognition sequences at the 5' and 3' ends of the genes were synthesized by GenScript. These constructs were purchased as clones in the pUC57 vector. Prior to constructing the desired plasmids, the R67 DHFR-pUC57, Quad4-pUC57, and chorismate mutase-pKTS DNA were transformed into DH5α and colonies were selected on YT agar media with 200 μg ampicillin/ml. Four to six colonies were grown in YT liquid media with 200 μg ampicillin/ml. Next, the plasmid DNA of individual colonies was extracted and the DNA sequences were confirmed via DNA sequencing.

Then, the plasmid DNA encoding R67 DHFR, Quad4, and pKTS were double digested with NdeI and XhoI. As can be seen in Figure 3-1 (below), the DNA was separated on a 1% agarose gel, which also removed the restriction enzymes. The correct sized DNA fragments for the

R67 DHFR or/and Quad4 genes were excised from the gel, cleaned and ligated into pKTS. The ligation mixture was transformed into *E. coli* DH5α and plated on YT agar media with 200 μg ampicillin/ml. After overnight cell growth, single colonies were inoculated into YT broth with 200 μg/ml ampicillin. After overnight cell growth, the plasmid DNA was extracted and the R67 DHFR-pKTS or/and Quad4-pKTS clones were verified by sequencing.

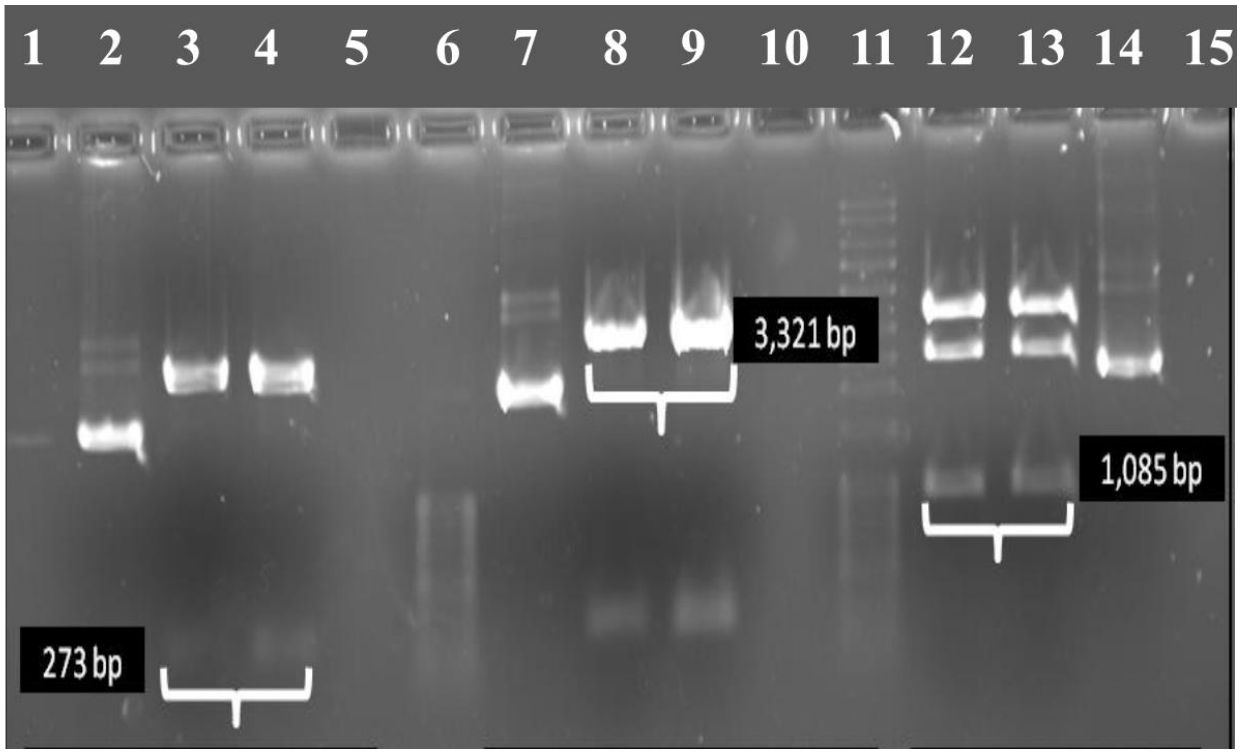

Figure 3-1 Restriction enzyme digested R67 DHFR, pKTS. and pKTS DNA
Lane 2: uncut R67 DHFR-pUC57, Lanes 3 and 4: NdeI and XhoI digested clone, insert size = 273bp. Lane7: uncut chorismate mutase-pKTS, Lanes 8 and 9: NdeI and XhoI digested chorismate mutase-pKTS (3,321 bp). Lanes 12 and 13: NdeI and XhoI digested Quad4-pUC75 clone, insert size 1,085 bp, Lane14 uncut Quad4-pKTS. The DNA samples were separated on a 1% agarose gel. DNA ladders are also shown in lane 6 and 11 (100 bp and 1000 bp plus, respectively). Brackets show the bands used in cloning.

3.1.2 Tetracycline dependent *E. coli* DH5α and/or *E. coli* LH-18 (*ΔFolA::Kan*) growth on M9 and/or Bonner-Vogel minimal selective media

3.1.2.1 Tetracycline concentration required to produce sufficient R67 DHFR and/or Quad4 activity in vivo to confer TMP resistance to E. coli DH5α.

To determine the minimum tetracycline concentration required to obtain confluent cell growth of DH5α carrying R67 DHFR-pKTS and/or Quad4-pKTS, cells were plated on M9

minimal media without antibiotics (control) or with 200 μg ampicillin/ml, 20 μg/ml TMP and various concentrations of tetracycline/ml (e.g. 0, 10, 25, 50, 75, 100, 200 and 500 ng/ml). The growth of the streaks on each plate was examined for three days (the third day plate images are shown in Figure 3-2 (below). After 24 hours, confluent cell growth was observed on the M9 minimal plate without antibiotic. Also *E.coli* DH5α carrying R67 DHFR-pKTS and/or Quad4-pKTS showed incremental cell growth that correlates with the tetracycline concentration added to induce expression from the P_{tet} promoter. As can be seen in Figure 1-2 (below) cells carrying the R67 DHFR-pKTS clone showed confluent cell growth at 50 ng tetracycline/ml, while Quad4-pKTS showed confluent cell growth at 10 ng tetracycline/ml. The need for a slightly higher concentration of tetracycline for a confluent growth in the R67 DHFR-pKTS clone is likely related to four SsrA tags associated with tetrameric R67 DHFR vs. one SsrA tag associated with monomeric Quad4.

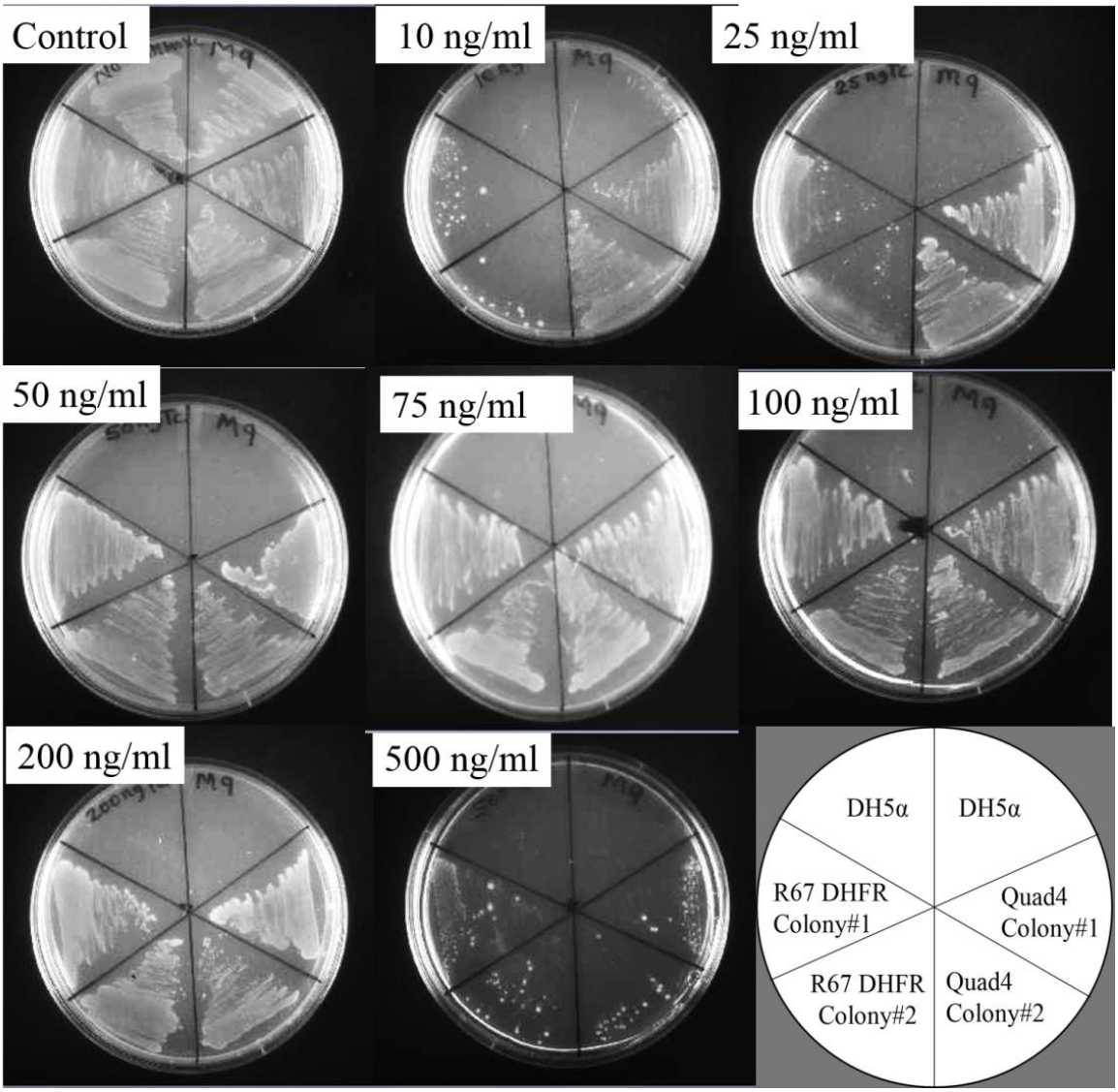

Figure 3-2 Tetracycline dependent *E. coli* DH5α growth on M9 media.
The optimal tetracycline concentration required to induce the P_{tet} promoter to produce sufficient DHFR activity to support confluent cell growth was determined from the tetracycline dependent cell growth pattern of *E. coli* DH5α carrying R67 DHFR-pKTS and Quad4-pKTS. The cartoon in the lower right shows how the constructs are streaked on the plates.

3.1.2.2 Tetracycline concentration required to induce sufficient R67 DHFR and/or Quad4 production to allow confluent growth of E. coli LH-18 (ΔFolA::Kan) on Bonner-Vogel minimal media.

Prior to tetracycline titration, we evaluated the growth pattern of the *E. coli* LH-18 (Δ*folA::kan*) strain which is auxotrophic for folate end products [61]. The cells were grown in YT and/or glucose liquid media with 20 µg kanamycin /ml plus 50 µg thymidine /ml. The next day, cells were streaked on Bonner-Vogel (BV) minimal agar supplemented with folate end products (30 µg adenine/ml, 10 µg pantothenate/ml, 50 µg glycine/ml, and 50 µg methionine/ml) [61]. Kanamycin (25 µg/ml) was also added to select for the deletant strain. Cells were additionally plated on BV minimal media (lacking the folate end product supplements) plus kanamycin. The plates were incubated at 37 ^{o}C. As can be seen in the 24 hours cell growth in Figure 3-3 (below), cell growth was observed on BV supplemented media, but not on BV minimal media. The results are consistent with previous studies that this strain is auxotrophic for folate end products [61].

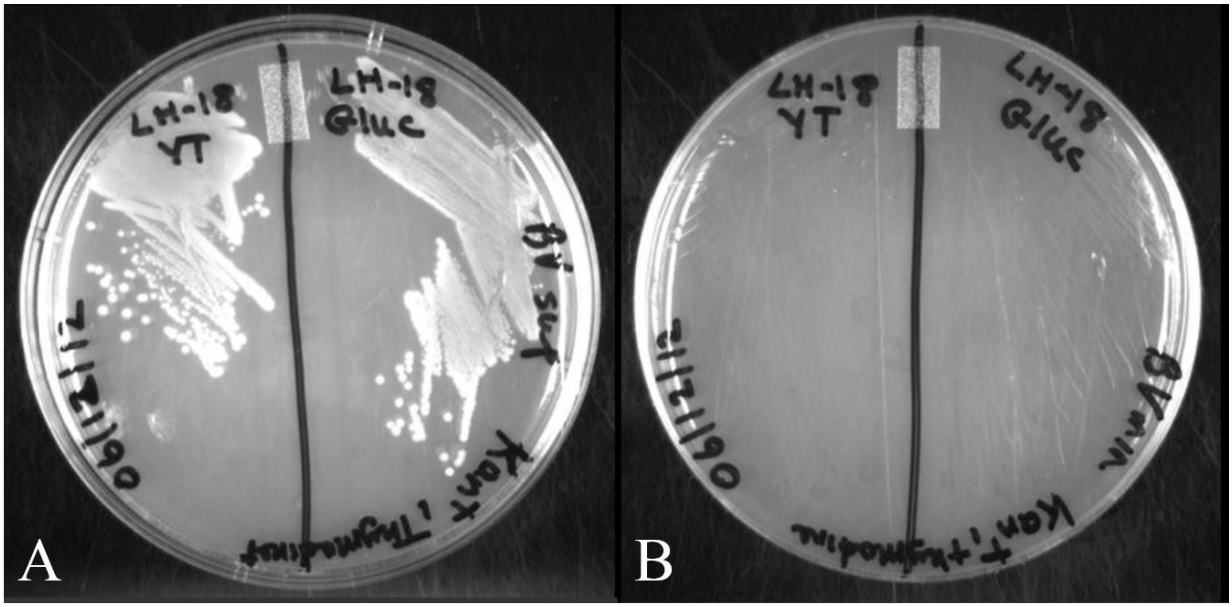

Figure 3-3 Growth pattern of *E. coli* LH-18 in BV supplemented (A) and minimal (B) media. *E. coli* LH-18 cells grew in BV supplemented media but not the minimal media. The 48 hour plate image is shown.

To determine the minimum tetracycline concentration required to obtain confluent growth of *E. coli* LH-18 carrying R67 DHFR–pKTS or Quad4-pKTS, cells were plated on BV minimal media with 25 μg kanamycin/ml, 200 μg ampicillin/ml, and various concentrations of tetracycline/ml (10, 25, 50, 75, 100, 200 and 500 ng/ml ng/ml). The plates were examined for three days. As can be seen from the third day image Figure 3-4 (below), the growth of *E. coli* LH-18 carrying R67 DHFR-pKTS and/or Quad4-pKTS reflects an incremental cell growth that correlates with the tetracycline concentration. The R67 DHFR clone supported confluent LH-18 growth with 50 to 200 ng tetracycline/ml. On the other hand, Quad4 supported confluent cell growth from 10 up to 200 ng tetracycline/ml. As can be seen in Figure 3-2 (page 48), a similar cell growth pattern was observed for the TMP resistance titration performed in DH5α. These results suggest that titration of TMP resistance or of restoration of prototrophy to an auxotrophic strain are related and both depend on the level of R67 DHFR activity present.

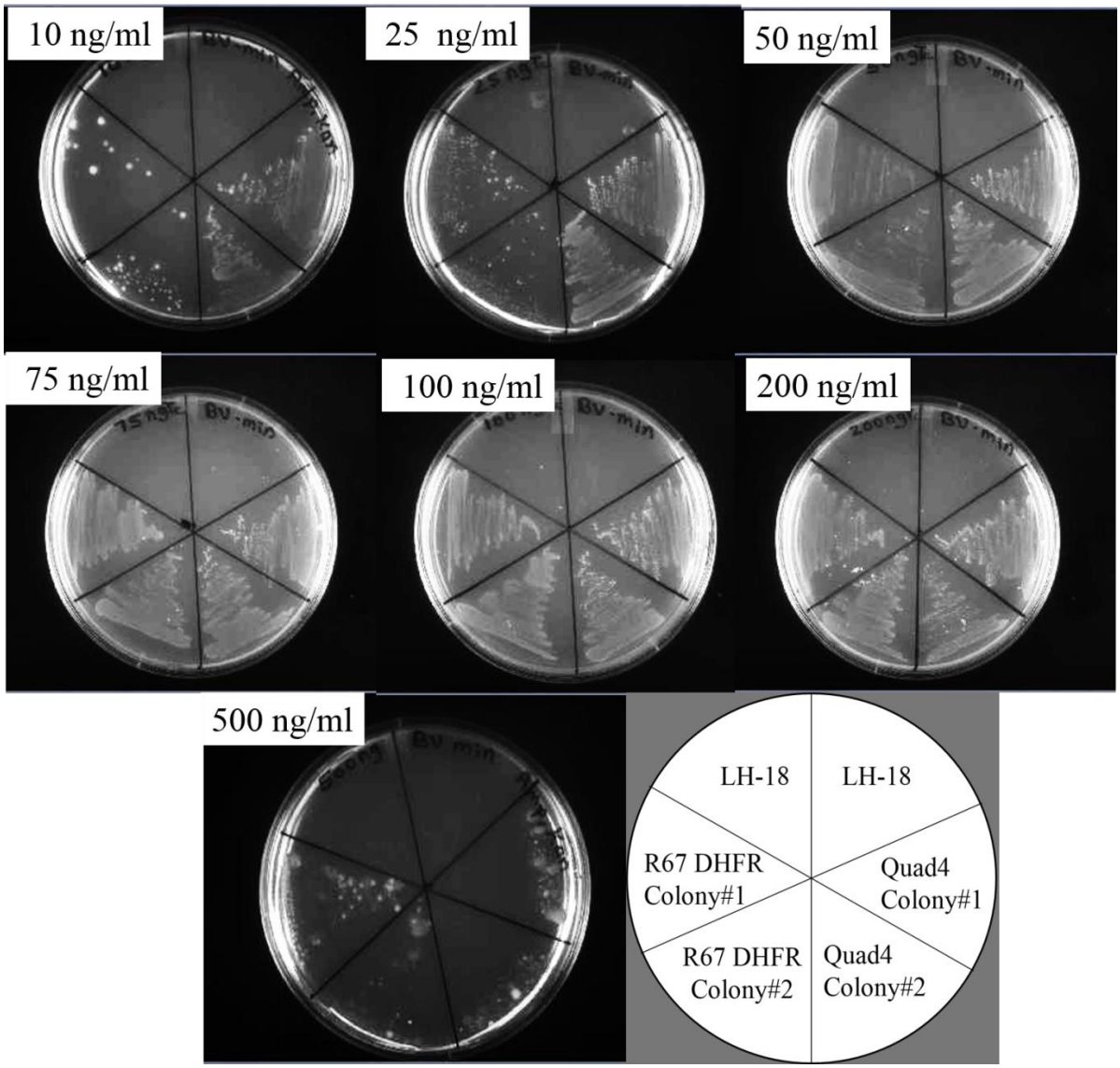

Figure 3-4 Tetracycline dependent *E. coli* LH-18 growth on BV minimal media
The optimal tetracycline concentration required to induce the P_{tet} promoter to support confluent cell growth was determined on BV minimal media containing 200 µg ampicillin/ml, 25 µg/ml kanamycin and various concentrations of tetracycline. The cartoon on the lower right shows how the constructs are streaked on the plates.

3.1.3 Effect of osmolality on the ability of the R67 DHFR and/or Quad4 to provide TMP resistance to *E.coli DH5α*

External osmotic stress causes cytoplasmic water loss which can slow and eventually cause bacterial growth to cease [17]. To examine the effect of increasing external osmotic pressure on *E. coli* DH5α, cells were plated on M9 media without antibiotic and the following osmolalities: 0.54, 0.79, 1.07, 1.28, 1.64, 1.90, and 2.42 Osm. Osmolality was increased via sorbitol titration. This set of plates was used to determine the osmotic fitness of DH5α. As can be seen in Figure 3-5 (below), DH5α growth decreased at 1.90 Osm and completely stopped at 2.42 Osm. At this level of osmotic stress, the bacteria were unable to grow due to loss of free water in the cell somewhere between 1.90 Osm and 2.42 Osm. This is similar to the observation of Cayley et al. where *E. coli* growth stopped at ~ 1.95 Osm [85, 86].

To assess the effect of increasing osmolality *in vivo* on the function of R67 DHFR and/or Quad4*, E.coli DH5α* carrying R67 DHFR-pKTS and/or Quad4-pKTS clones were plated on M9 minimal media with 200 μg ampicillin/ml and 20 μg TMP/ml, while the *in vivo* protein production was controlled with 100 ng tetracycline/ml. The external osmolality was increased by adding of 0 to 1.50 M of sorbitol in 0.25 M increments. The osmolalities of the M9 plates without added sorbitol were 0.45 Osm and 0.50 Osm. The osmolalities of the plates with added sorbitol were 0.78, 0.81, 1.28, 1.60, 1.93, and 2.23 Osm. As can be seen in Figure 3-6 (below), R67 DHFR production rescued DH5α on 0.78, 0.81 and 1.28 Osm plates, but the cell growth was sparse under 1.28 Osm and stopped ≥ 1.60 Osm. On the other hand, Quad4 provided sufficient DHFR activity to allow confluent growth of DH5α under 0.78, 0.81, 1.28, and 1.60 Osm, and totally stopped at 1.93 Osm. The lesser efficiency of the R67 DHFR clone to allow growth could be explained by a lower protein stability/life time which derives from its homo-tetrameric structure, which adds 4X higher SsrA tags per protein than monomeric Quad4 which carries only 1X SsrA tag per protein.

To assess the effects of osmolytes on the ability of R67 DHFR and/or Quad4 to rescue the host cell from TMP resistance, it is important to evaluate the effect of increasing osmolyte concentrations on the viability of the cells. This was achieved by comparing the growth patterns of control and test plates seen in Figure 3-5 and Figure 3-6 (below). On the control plates, DH5α stopped growing somewhere between 1.90 Osm and 2.43 Osm. However the R67 DHFR clone stopped growing between 1.28 Osm and 1.60 Osm while the Quad4 clone stopped growing

between 1.60 Osm and 1.93 Osm. In both cases the bacteria ceased growth at a lower osmolality than the control. Considering our lab's previous *in vitro* observation [23], the loss of activity of both R67 DHFR and Quad4 could be due to the preferential interactions of osmolytes with DHF which weaken bindings and results in loss of sufficient DHFR activity to rescue the cell.

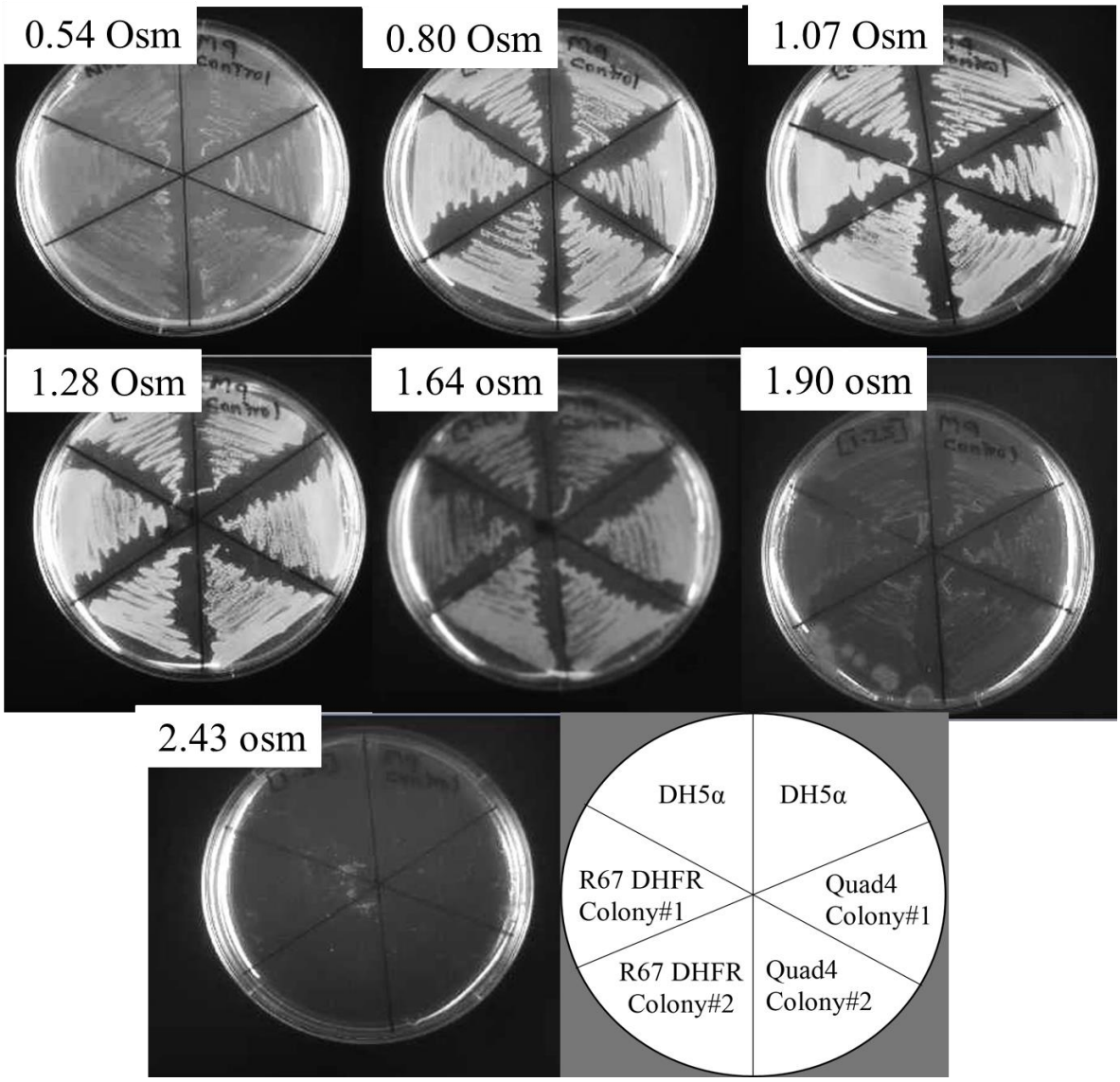

Figure 3-5 Effect of osmolality on *E. coli* DH5α viability.
An assessment of the ability of *E. coli* DH5α carrying R67 DHFR-pKTS or/and Quad4-pKTS to grow in the presence of increasing concentration of sorbitol. The cells were plated on M9 minimal medium without antibiotics and different concentrations of sorbitol were added. Confluent growth was observed up to 1.90 Osm, cell growth stopped on the 2.43 Osm plate, suggesting the bacteria ceased growing due to free water loss. The lower right cartoon shows the pattern of cells streaked on the plates.

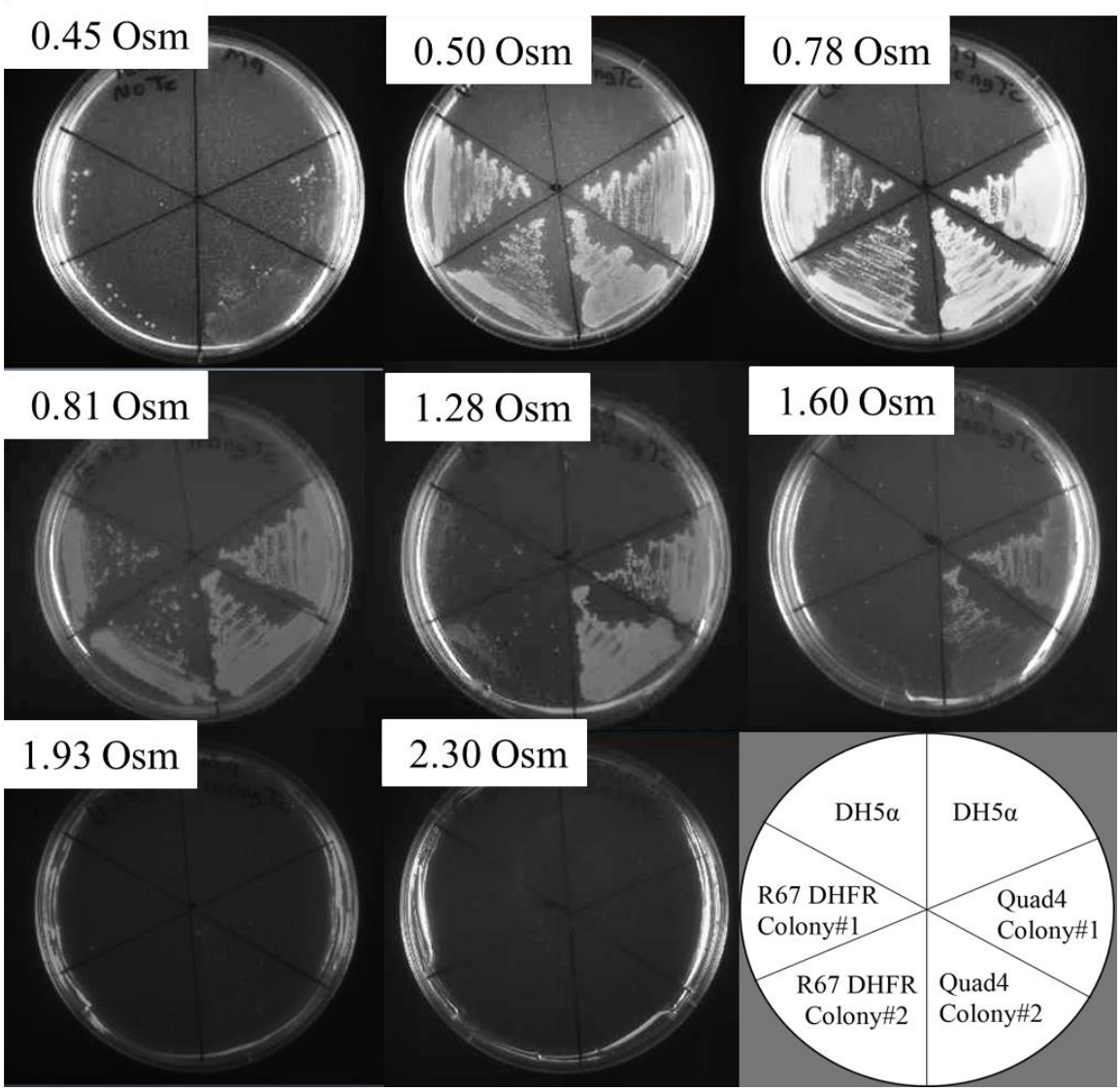

Figure 3-6 Effect of Osmolality on R67 DHFR and/or Quad4 to rescue DH5α from TMP^R . The ability of R67 DHFR and/or Quad4 to provide TMP resistance to DH5α on M9 minimal media with 200 µg ampicillin/ml, 20 µg TMP/ml and 100 ng tetracycline/ml was assessed on M9 minimal media with osmolalities from 0.78 to 2.29 Osm. The R67 DHFR clone supported confluent *E. coli* DH5α growth on M9 agar media with 0.78, and 0.81 Osm. On the other hand, the Quad4-pKTS clone supported confluent *E. coli* DH5α growth on M9 media with 0.78, 0.81, 1.28, and 1.60 Osm. The lower right cartoon shows how the various cultures are streaked on the plates.

3.1.4 Effect of osmolality on the ability of R67 DHFR and/or Quad4-pKTS clones to rescue *E.coli* LH-18 to prototrophy

Our first set of cell growth assays assessed how increasing *in vivo* osmolality affected the ability of R67 DHFR and/or Quad4 to provide TMP resistance to DH5α. To test our hypothesis directly on the activity of DHFR, we used *E. coli* LH18 (Δ*folA::kan).* For LH-18 to grow, it either requires addition of folate end products into the media or should be complemented with a functional DHFR gene [61].

The first set of cell growth assays was aimed to assess the osmotic fitness of LH-18 on BV supplemented media with 25 µg kanamycin/ml and 0.78, 1.06, 1.34, 1.50, 2.12, and 2.32 Osm. As can be seen in Figure 3-7 (below), LH-18, with and without the plasmid, had similar confluent growth patterns from 0.77 Osm to 1.50 Osm, but the growth was slightly less under 1.50 Osm, and growth stopped on the plates with ≥ 2.12, Osm. These observations suggested that the bacterium no longer had free cytoplasmic water and ceased to grow.

Next, to probe the effects of increased osmolality on DHFR activity supplied by the R67 DHFR and/or Quad4-pKTS clones, external osmotic stress were applied to LH-18. The osmolality of each plates were 0.52, 0.85, 1.04, 1.37, 1.68, 2.10, and 2.23 Osm. As can be seen in Figure 3-8 (below), the R67 DHFR clone rescued LH-18 on BV minimal plates with 0.50, 0.85, and 1.04 Osm, however cell growth on the 1.04 Osm plate was sparse, and growth was not observed on 1.37 Osm plate. And, Quad4-rescued LH-18 under 0.50, 0.85, 1.04, 1.37 and 1.68 Osm, growth was stopped 2.10 Osm. Confluent cell growth was observed on the first four plates, but cell growth on the 1.68 Osm plate was sparse.

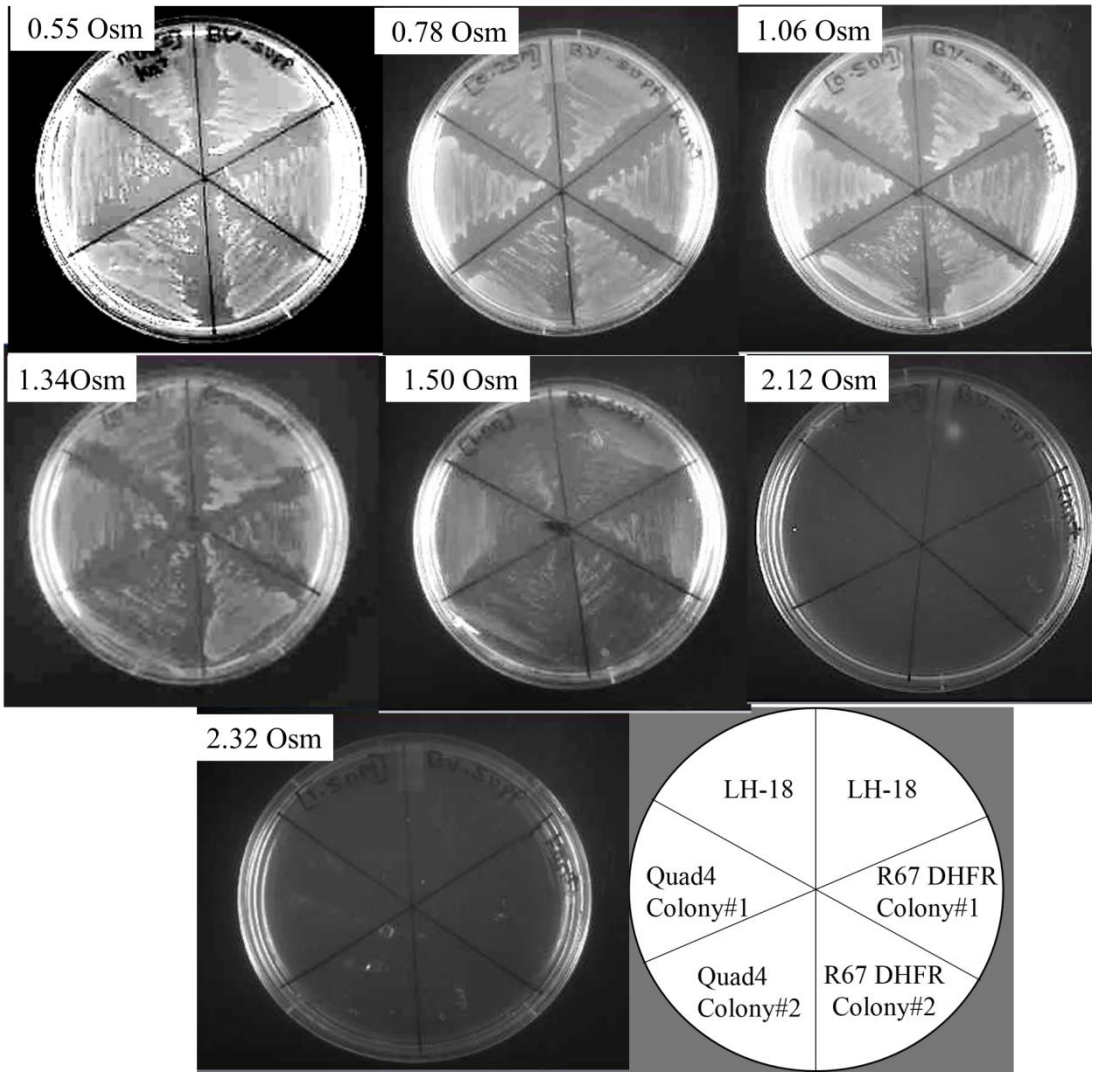

Figure 3-7 Effect of osmolality on *E. coli* LH-18 viability.
The ability of *E. coli* LH-18, and *E. coli* LH-18 carrying R67 DHFR-pKTS or/and Quad4-pKTS clones to grow in the presence of increasing concentrations of sorbitol was assessed on BV supplemented media. Added folate end products are 3.03 mg adenine /ml, 1.0 mg pantothenate/ml, and 50 µg glycine /ml with 50 µg thymidine/ml. 25 µg kanamycin/ml was added to select for the Δ*folA::kan* lesion. Sorbitol addition led to plates possessing osmolalities of 0.55, 0.77, 1.06, 1.34, 1.50, 2.12, and 2.32 Osm. Confluent bacterial growth was observed until 1.50 Osm. *E. coli* LH-18 did not grow on BV supplemented plates with an osmolality of ≥ 2.12 Osm, suggesting no free cytoplasmic water was present which blocked cell growth. The lower right cartoon shows how the various cultures are streaked on the plates.

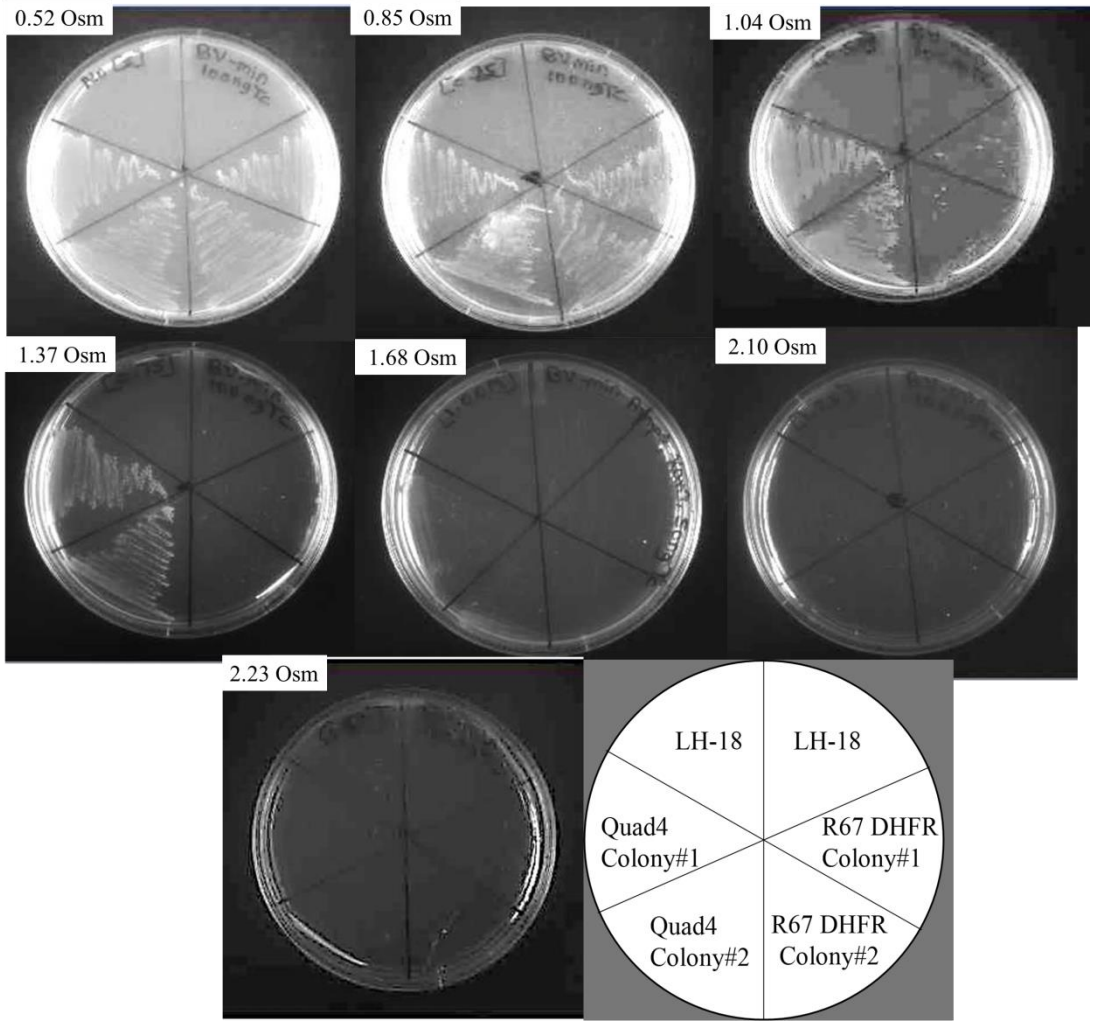

Figure 3-8 Effect of osmolality on R67 DHFR and/or Quad4 activity on BV minimal plates. The ability of R67 DHFR or/and Quad4-pKTS clones to rescue LH-18 from folate end product auxotrophy was assessed on BV minimal media containing 200 µg ampicillin/ml, 25 µg kanamycin/ml, 100 ng tetracycline/ml and sorbitol additions such that the osmolality was 0.52, 0.85, 1.04, 1.37, 1.68, 2.10, and 2.23 Osm. The R67 DHFR-pKTS clone rescued LH-18 on BV minimal plates with 0.50, 0.85, and 1.04 Osm, however cell growth on the 1.04 Osm plate was sparse. The Quad4-pKTS clone rescued LH-18 on BV minimal plate possessing osmolality of 0.50, 0.85, 1.04, 1.37 or 1.68 Osm. The lower right cartoon shows how the various cultures are streaked on the plates.

As described above, two different aspects of DHFR activities were assessed, to confer TMP resistance upon host bacteria and to rescue a DHFR knockout strain from folate end product auxotrophy. As can be seen from Figure 3-6 and Figure 3-8 (above), both of these assays showed sensitivity to increasing osmotic stress with loss of cell growth under high osmolalities. The control titrations with media lacking TMP or with supplemented media (Figure 3-5 and Figure 3-7 above) indicate that the cells can grow to higher osmolality. This difference in growth suggests that DHFR activity can be titrated *in vivo.* These observations are also consistent with the *in vitro* assays of Chopra et al. [1] where addition of osmolytes weakens binding of substrate to DHFR and decreases the overall activity of the enzyme under limiting substrate conditions.

3.2 Can osmotic stress affect the *in vivo* activity of the *folC* gene product, FPGS?

To continue probing our hypothesis that osmolytes will interact with many folate redox states and shift the equilibria towards the free species; we next examine the effect of increasing osmolality on the function of folylpolyglutamate synthase (FPGS), the product of the *folC* gene. This enzyme adds L-glutamate to dihydropteroate; it also extends the glutamate tail of THF using a γ-linkage. Both THF and 10-formyl-THF are FPGS substrates [34].

3.2.1 *E. coli*: SF2 *(F^- folC strA,)* a mutant strain with a lower activity of FPGS

A previous study by the Bognar lab has reported two mutant *folC* strains of *E. coli*: SF2 *(F- folC strA)* and SF4 *(F- folC strA recA TnI0:srlC)* [50]. These strains carry a G925A mutation in the *folC* chromosomal gene [50] that corresponds to an A309T amino acid change in the protein. This mutant protein displays a 30 fold increase in K_M for 10-CHO-THF, a 60 fold increase in the K_M for glutamate, a 10 fold increase in the K_M for ATP and a 200 fold increase in the K_M for dihydropteroate [49, 50]. The reduced FPGS activity results in the absolute requirement for methionine in the growth media; added glycine further increases the growth rate [49]. Since the activity of this mutant strain is already compromised, we asked if the FPGS activity of the SF2 strain could be titrated by osmotic pressure.

The parent strain of SF2, known as MG1655, grew on both BV minimal and supplemented plates without and with complementation. SF2 grew on BV supplemented plates, but not on BV minimal plates as shown in Figure 3-9 (below) where SF2 carrying a functional *folC* gene in trans

grows on both BV minimal and supplemented plates suggesting the FPGS activity of the clones rescues SF2 to prototrophy. Several different FPGS containing plasmids were used, pAC5 and pPM103 [50] (see Table 2 in the Methods section). Similar growth patterns of the parent strain with and without the *folC* clone suggested multiple copies of *folC* are not detrimental to the cells.

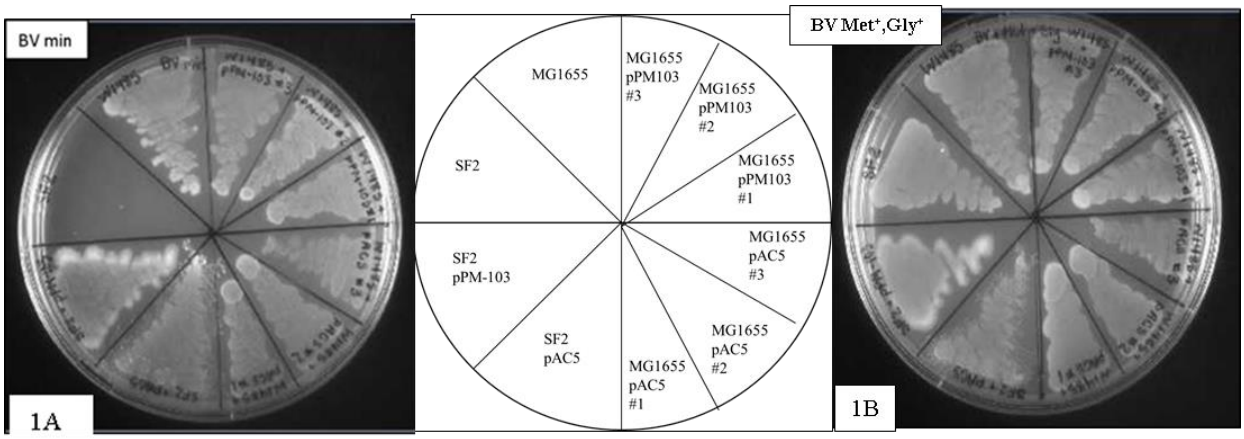

Figure 3-9 The growth pattern of the *folC* mutant strain, SF2, and its parent strain MG1655. Panel A shows their growth patterns on BV minimal agar while panel B shows the growth of on a BV plate supplemented with 50 µg methionine/ml and 50 µg glycine/ml plates. SF2 did not grow on BV minimal media. However, both SF2 carrying a functional *folC* gene and the parent strain grew on BV minimal and supplemented plates. The middle panel shows how the various cultures were streaked on the plates.

3.2.2 Effect of osmolality on the function of *fol*C

3.2.2.1 Osmotic Stress effects on the growth of the SF2 strain on BV media supplemented with excess methionine and glycine/ml

Next, we asked if an increasing *in vivo* osmolality could impact the ability of the SF2 strain to grow on BV supplemented media; i.e. if osmolytes weakly interact with dihydropteroate and/or tetrahydrofolate based substrates, this can weaken their binding to FPGS and potentially titrate the activity of the A309T mutant enzyme. Since loss of FPGS activity is lethal to the cell [67], this could block cell growth. This hypothesis was tested by plating SF2 and SF2 carrying pAC5 and/or pPM103-FolC plasmids as well as the MG1655 parent strain without and with the pAC5 and/or pPM103-FolC plasmids on BV media supplemented with 50 µg methionine/mL and 50 µg glycine/mL. The osmolality of the media was gradually increased via sorbitol in 0.25 M increments from 0 to 1.50 M. Also to stimulate FPGS protein synthesis that is controlled by the

Lac promoter in the pAC5 plasmid, 1 mM IPTG was added. As seen in Figure 3-10 (below), the MG1655 strain carrying either the pAC5 or pPM103-*folC* plasmid allowed confluent growth on media containing up to 1.25 M sorbitol. Cell growth ceased on 1.50 M sorbitol. On the other hand, SF2 and SF2 carrying either pAC5 or pPM103-FolC plasmids grew confluently up to 0.75 M sorbitol and decreased in the presence of 1.00 M sorbitol, and completely stopped on a 1.25 M sorbitol Figure 3-10 (below).

The differences in cell growth patterns between the parent strain and SF2 carrying a functional *folC* in Figure 3-10 were unexpected. If the difference between the parent strain and SF2 is only a A309T mutation in the *folC* gene, we assumed the wild type clone would complement the lost activity and allow similar growth as the parent strain under higher osmotic stress.

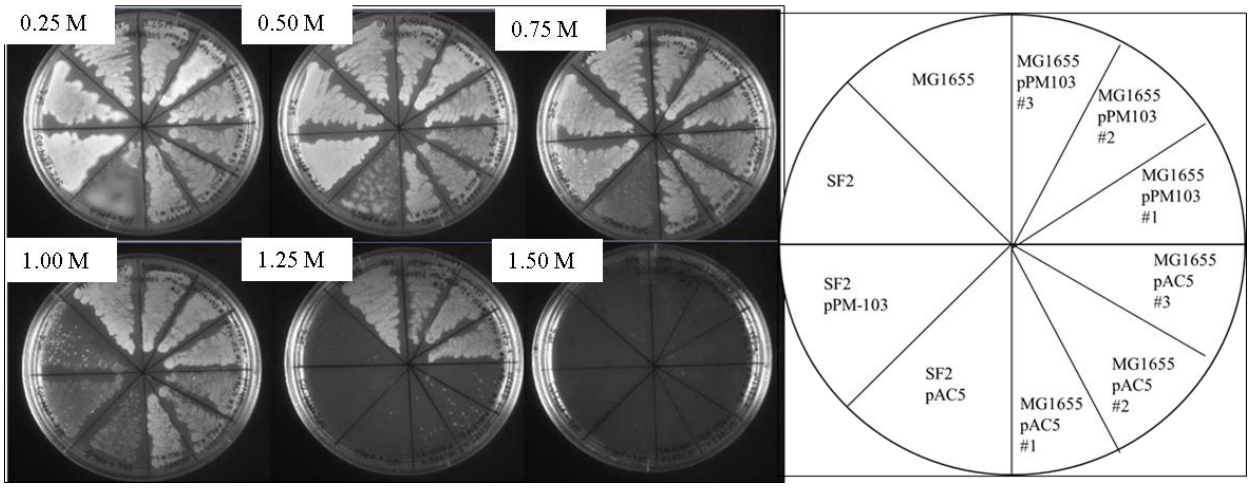

Figure 3-10 The effect of increasing osmolality on the growth of *E. coli* SF2.
Assessing the effect of increasing osmolality on the growth of SF2 with and without complementation. All cultures were streaked on BV minimal media supplemented with 50 µg methionine/mL and 50 µg glycine/mL with various concentrations of sorbitol (0.25 M, 0.50 M, 0.75 M, 1.00 M, 1.25 M or 1.50 M). The right panel shows how the various cultures were streaked on the plates.

3.2.2.2 Growth of the SF2 strain on BV media supplemented with a sub-optimal concentration of methionine

In another series of experiments, we asked if decreasing the methionine and/or glycine concentration from an optimal level would increase the pressure on the enzyme to function under increasing osmotic pressure and allow an osmotic pressure titration of FPGS activity. For the first trial, since methionine is absolutely required for SF2 growth [49], the optimal methionine concentration methionine was determined by titrating different concentrations of methionine ranging from 0 to 50 µg /ml. Minimal growth of SF2 was observed on a BV media supplemented with 7.46 µg methionine /ml (data not shown). Then, the activity of SF2 under increasing osmolality was assessed by plating various cultures on BV media supplemented with only 7.46 µg methionine /ml and 50 µg glycine/ml. Interestingly, the cell growth patterns of the parent strain and the parent strain carrying three different plasmid were able to show confluent growth up to 1.25 M sorbitol plate.. The cell growth was slightly decreased under 1.50 M plates (see Figure 3-11 below). On the other hand, SF2 with and without complementation showed confluent growth up to 1.00 M sorbitol and the cell growth was decreased under 1.25 M and stopped on 1.50 M plate, while SF2 growth showed slight improvement from Figure 3-10 (above). Minimizing the methionine concentration did not allow titration of SF2 growth by osmotic stress as compared to MG1655. These results suggested that other mutations may be present in the SF2 strain to make it more sensitive to osmotic stress. As SF2 was created by treating MG1655 with ethylmethane sulfonate [49], this seems a likely possibility. Our inability to titrate FPGS activity by osmotic stress indicates either that FPGS is not sensitive to osmotic pressure or that the FPGS activity is still sufficient to rescue the cell.

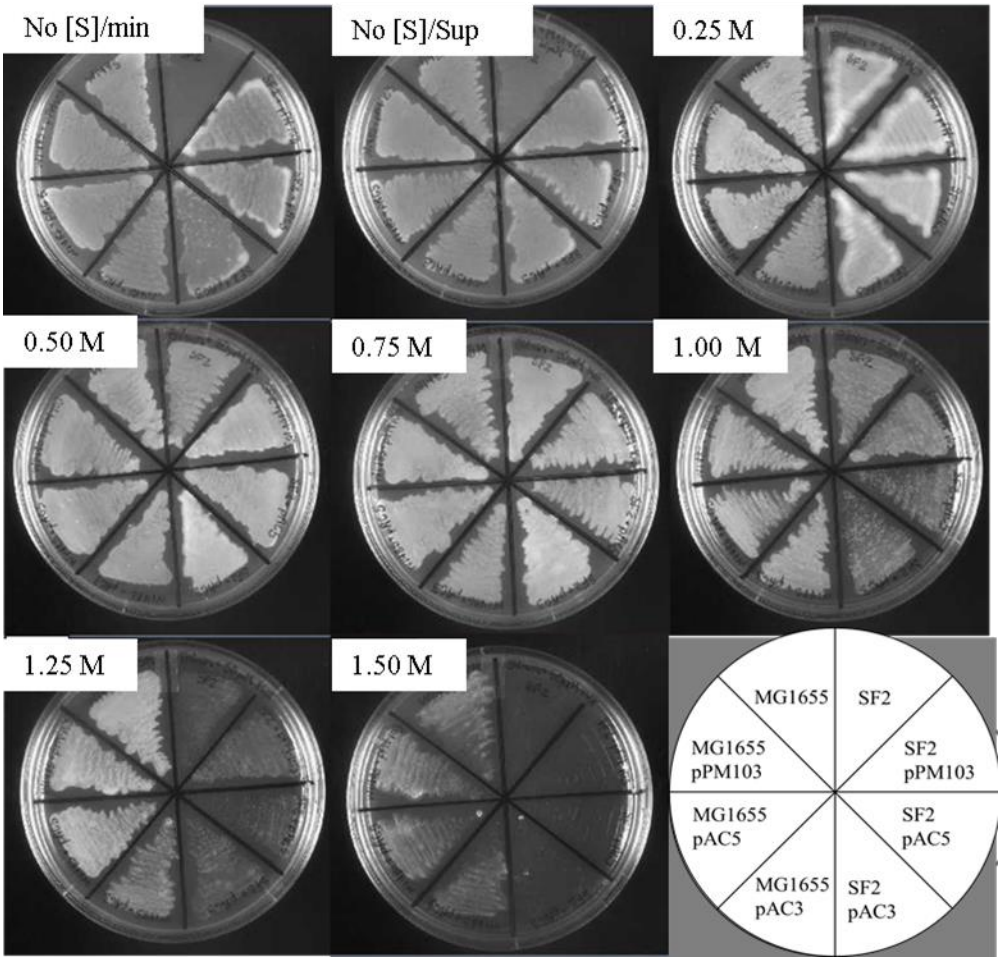

Figure 3-11 Assessing the effect of increasing osmolality on the ability of SF2 to grow in the presence of a sub-optimal methionine concentration.
Assessing the effect of increasing osmolality on the growth of MG1655 and SF2 growth on BV agar media with 7.46 µg methionine/ml and 50 µg glycine/ml and various concentrations of sorbitol (0.25 M, 0.50 M, 0.75 M, 1.00 M, 1.25 M or 1.50 M) and 1 mM IPTG. The bottom right panel shows how the various cultures are streaked on the plates.

3.3 Cloning the Methylenetetrahydrofolate Reductase (MTHFR) gene (*metF)* into pKTS

Next, to continue probing the effect of osmolality on the activity of folate enzymes, MTHFR was selected. This enzyme reduces 5, 10-methylene-THF to 5-methyl-THF using NAD(P)H as a cofactor [33, 51]. If osmolytes weakly interact with 5, 10-methylene-THF, the *in vivo* activity of MTHFR can be titrated and assessed by its ability to rescue a knockout to prototrophy. This

section describes how a *metF*-pKTS construct was made, the auxotrophy of the *E. coli* JW3913-1 (Δ*metF::kan*) strain was tested and the tetracycline dependent growth characteristics of JW3913-1 carrying *metF*-pKTS. These experiments are ongoing in the lab to determine the effect of increasing concentration of osmolytes on the activity of MTHFR by the ability of the *metF*-pKTS clone to rescue *E. coli* JW3913-1 (Δ*metF::kan*) to prototrophy.

3.3.1 Designing a primer, PCR amplification and cloning into the pCR 2.1 TOPO TA vector

A clone of the MTHFR gene was a gift from Dr. Elizabeth Trimmer from Grinnell College. Her pCAS-30 clone is a derivative of the pET2-3b plasmid [33]. To assess the quality of the DNA and cloning sites of the gene, the plasmid was transformed, selected and sequenced with T7 and T7 terminator primers. The sequence alignment results showed the *metF* open reading frame was cloned between XbaI and XhoI sites. A sequence encoding a C-terminal His_6 tag was present. To introduce an NdeI restriction sequence via PCR, a forward primer that adds a NdeI restriction sequence was used along with a primer near the T7 terminator site. Primers were designed as described in the Material and Methods section of this thesis (Table 5). The primers were synthesized by Invitrogen, Carlsbad, CA.

Next, for the purpose of adding an 'A' overhang into the PCR product of *metF* which would enable cloning into the TOPO TA pCR 2.1 (Invitrogen), Taq polymerase was used [87]. The PCR product is shown in Figure 3-12 (below). The PCR product was cleaned with the GeneJET PCR Purification Kit (Thermo Scientific), cloned into the TOPO TA vector and transformed into TOP10 *E. coli* cells. The cell suspension was plated on YT agar with 50 µg kanamycin /ml. Use of the X-gal blue/white colony [87] screening technique allowed selection of six white colonies carrying a plasmid with an insert. These cells were individually grown in YT liquid media, and the plasmid DNA was extracted and sequenced with M13 Forward and M13Reverse primers. A total of five correct colonies were found.

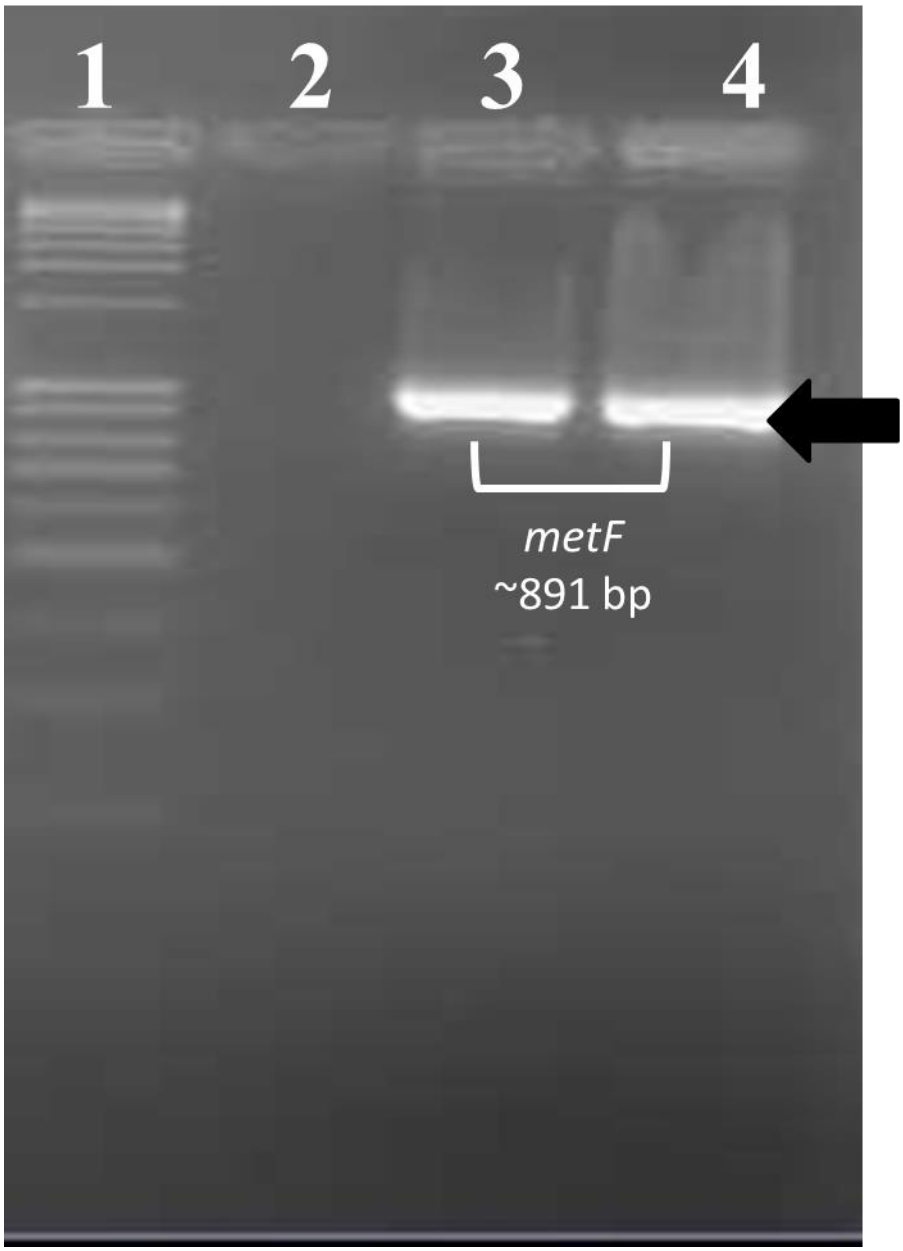

Figure 3-12 PCR amplification of the *metF* gene.
An Nde1 restriction site was introduced at the 5' end of the gene. The expected length of the PCR product was 891 bp. The PCR product was electrophoresed on a 1% agarose gel. Lane 1:1Kb plus DNA ladder and Lanes 3 and 4: the PCR product of *metF* of expected size.

3.3.2 Construction of the metF-pKTS plasmid

To clone the *metF* gene into pKTS, a correct *metF*-pCR 2.1 clone and the pKTS-chorismate mutase plasmid were double digested with NdeI and XhoI restriction enzymes. The DNAs were separated on a 1% agarose gel (see Figure 3-13 below). The correct sized DNA fragments for the *metF* gene and the pKTS plasmid were excised from the gel and ligated with T4 DNA ligase (TaKaRa). The ligation mixture was transformed into the *E. coli* (Δ*metF::kan*) strain. This strain is auxotrophic for methionine, thus it will grow only on minimal media supplemented with methionine or when complemented with a plasmid carrying a functional *metF* gene. The ligation mixture was transformed into JW3913-1 (Δ*metF::kan*) and the cells plated on either YT agar with 200 μg/ml ampicillin, 25 μg/ml kanamycin/ml and μg methionine/ml or BV minimal agar with 200 μg/ml ampicillin, 25 μg/ml kanamycin/ml and 80 ng/ml tetracycline. The next day, tiny colonies started to appear on the YT plates and within 48 hours, colonies developed. On BV minimal media, colonies started to appear after 48 hours. After 48 hours, six colonies from the YT plate were selected and individually inoculated into YT broth with 200 μg/ml ampicillin. After overnight growth, the plasmid DNA from six colonies were purified and the identity of the insert was confirmed by DNA sequencing with T7 and T7 terminator primers. On the BV minimal plate ~ a total of 50 colonies were detected, suggesting the clone rescued JW3913-1 to prototrophy.

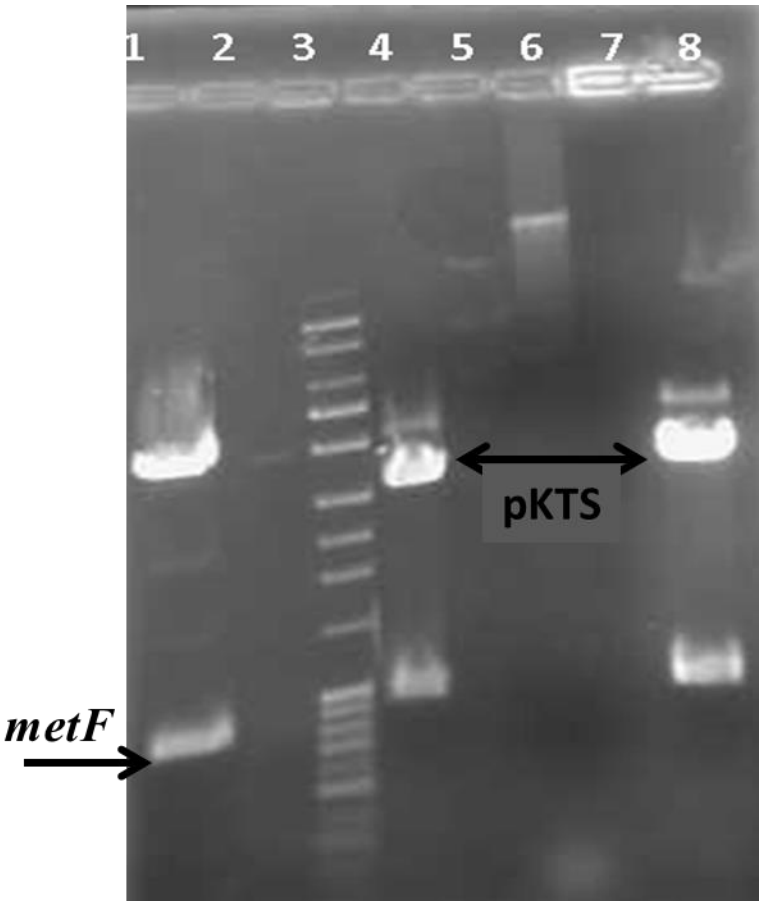

Figure 3-13 NdeI and XhoI digested *metF*-pCR 2.1 and pKTS.
Restriction enzyme digested *metF*-pCR 2.1 and pKTS-chorismate mutase. The plasmids were digested with NdeI and XhoI and the DNA fragments were electrophoresed in a 1% agarose gel. Lane1: *metF*-pCR 2.1, Lane3, 1,000 bp plus DNA ladder, Lanes 4 and 8, pKTS vector with a chorismate mutase gene insert. The correct DNA fragments are shown by the arrow: *metF* ~891 bp and pKTS ~3.9 kb.

3.3.3 Assessing the growth pattern of *E. coli* JW3913-1 (Δ*metF::kan*)

To characterize the growth pattern of E. *coli* JW3913-1 (Δ*metF::kan*), the cells were grown in YT liquid media with 25 µg kanamycin/mL and 50 µg methionine/ml. The next day, the cells were plated on BV agar supplemented with 50 µg methionine /ml and 25 µg kanamycin/mL or BV minimal media with 25 µg kanamycin/ml. The plates were checked for five consecutive days. Cell growth was observed on BV supplemented media after 24 hours, but E. *coli* JW3913-1 (Δ*metF::kan*) did not grow on BV minimal media**.** The image of the plate at 48 hrs. is shown in Figure 3-14 (below)**.** This assay confirmed that *E. coli* JW3913-1 (Δ*metF::kan*) is auxotrophic for methionine.

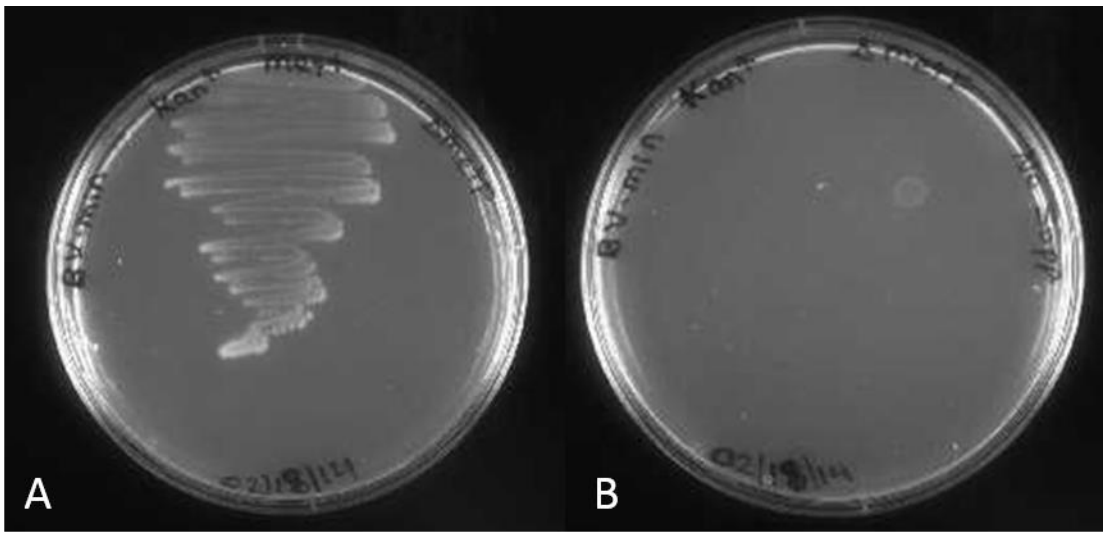

Figure 3-14 The growth pattern of the *metF* knockout strain *of E. coli* JW3913-1.
Panel A shows growth of *E. coli* JW3913-1 (Δ*metF::kan*) on BV supplemented media while panel B shows no growth on BV minimal media.

3.3.4 Tetracycline concentration required to induce sufficient MTHFR production to rescue *E. coli* JW3913- (Δ*metF::kan*)

To determine the minimum tetracycline concentration that will allow confluent cell growth of *E. coli* JW3913-1 (Δ*metF::kan*) carrying the *metF*-pKTS clone, several cell stocks plasmid were grown in a YT liquid media with 200 μg ampicillin/ml and 25 μg kanamycin/ml. Next the cells were plated on BV minimal media with 200 μg ampicillin/ml, 25 μg kanamycin/ml and various concentrations of tetracycline (10, 25, 50, 75, 100, 200 and 500 ng/ml ng/ml). The plates were examined for three days. After 18 hours, confluent cell growth was observed (the second day plate images are shown in Figure 1-15 (below). Sparse cell growth was observed on BV media with no tetracycline and 10 ng tetracycline/ml. Confluent growth was obtained on the plates with 25 to 200 ng tetracycline/ml. Cell growth became sparse on a 500 ng tetracycline/ml plate (Figure 3-15 below) suggesting 500 ng tetracycline/ml is cytotoxic to the host cell [88].

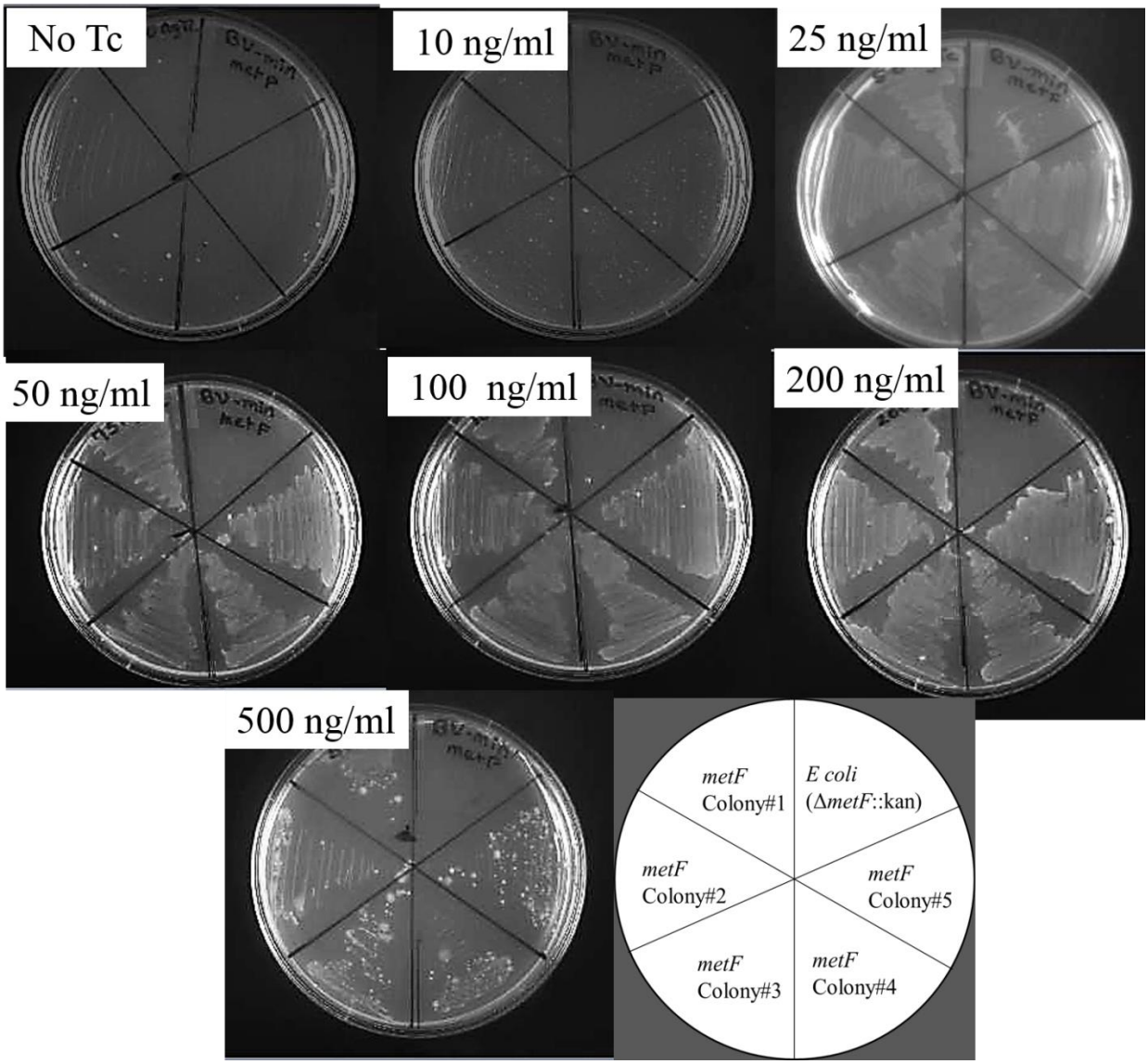

Figure 3-15 Tetracycline dependent *metF* production rescues JW3913-1 (Δ*metF*::kan) carrying the *metF*-pKTS plasmid.

The cells were grown on BV minimal media and the concentration of tetracycline that allowed cell growth was monitored. Confluent cell growth was observed at concentrations ≥ 25 ng tetracycline/ml. The highest tetracycline concentration (500 ng/ml) showed punctate growth, suggesting the concentration was too high. The bottom right panel shows how the various cultures are streaked on the plates.

3.4 Initial experiments to explore the effect of *in vivo* osmotic stress on serine hydroxymethyl transferase activity

The next folate pathway enzyme we considered was serine hydroxymethyl transferase (SHMT). This enzyme is encoded by the *glyA* gene and the protein catalyzes the reversible conversion of serine and tetrahydrofolate to glycine and 5,10-methylene tetrahydrofolate[36]. If osmolytes preferentially interact with either THF and/or 5, 10-methylene tetrahydrofolate, increasing the osmolyte concentration *in vivo* would weaken the catalytic efficiency of the enzyme. To test this hypothesis, the *glyA* gene was cloned into pKTS. Experiments are ongoing in the lab to determine the effect of increasing concentration of osmolytes on the activity of SHMT by the ability of *glyA*-pKTS to rescue *E. coli* JW 2535-1 (*Δgly::kan*) to prototrophy.

3.4.1.1 Designing a primer, PCR amplification and cloning into the pCR 2.1 TOPO TA vector

We obtained the *E. coli glyA* gene cloned in the pBlueScript KS vector from [75]. The DNA was transformed into *E. coli* DH5α and plated on YT agar with ampicillin. After overnight growth, five colonies were selected and grown, the plasmid DNA was purified and sequenced with M13 Forward and M13 reverse primers. The open reading frame of the *glyA* gene was cloned between PstI and BamHI cloning sites. Next, to introduce NdeI and XhoI restriction sequence via PCR, primers were designed. The primer sequences are given in the Materials and Methods section. The primers were synthesized by Invitrogen (Carlsbad, CA).

Next, for the purpose of adding an 'A' overhang into the PCR product of *glyA* that would enable cloning using the TOPO TA kit (Invitrogen), Taq polymerase was used. The PCR product is shown in Figure 1-16 (below). The PCR product was cleaned with the GeneJET PCR Purification Kit (Thermo Scientific), cloned into the TOPO TA vector and transformed into TOP10 *E. coli* cells. Half of the transformed cells were plated on YT agar with 50 µg kanamycin /ml. The other half of the transformed cell mixture was plated on agar containing X-gal and IPTG for blue/white screening. Eight individual white clones were grown in YT liquid media, the plasmid DNA extracted and the DNA sequenced with M13F/M13Rev primers. Five clones were identified with a *glyA* insert.

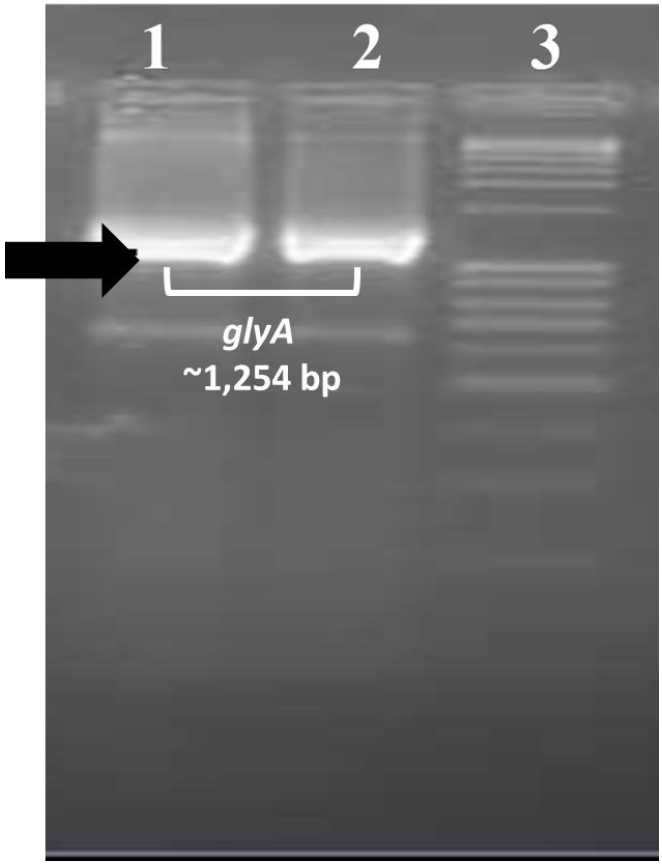

Figure 3-16 *glyA* PCR product.
Introduction of Nde1 and Xho1 restriction enzyme sites into the *glyA* gene by PCR amplification. The primer pair specific to *glyA* that enabled addition of NdeI and XhoI sites was used to amplify the coding region of *glyA* (1,254 bp). The PCR product was electrophoresed on a 1% agarose gel. Lanes 1 and 2: *glyA* PCR product and Lane 3: 1Kb plus DNA ladder. The PCR product appears in the position expected for its size.

3.4.1.2 Construction of the glyA-pKTS plasmid

The next step was to digest the correct *glyA*-pCR2.1 clone with NdeI and XhoI and separate the fragments on a 1% agarose gel see Figure 1-17 (below). The double digest of *glyA*-pCR2.1 revealed three bands. The top band was about 3.9 kb, which is the size of TOPO plasmid pCR2.1 vector. The bottom two bands were approximately 900 bp and 300 bp. Assessment of the *glyA* sequence found an internal XhoI site at 906 bp which suggested the ~ 900 bp and ~300 bp fragments came from the *glyA* insert.

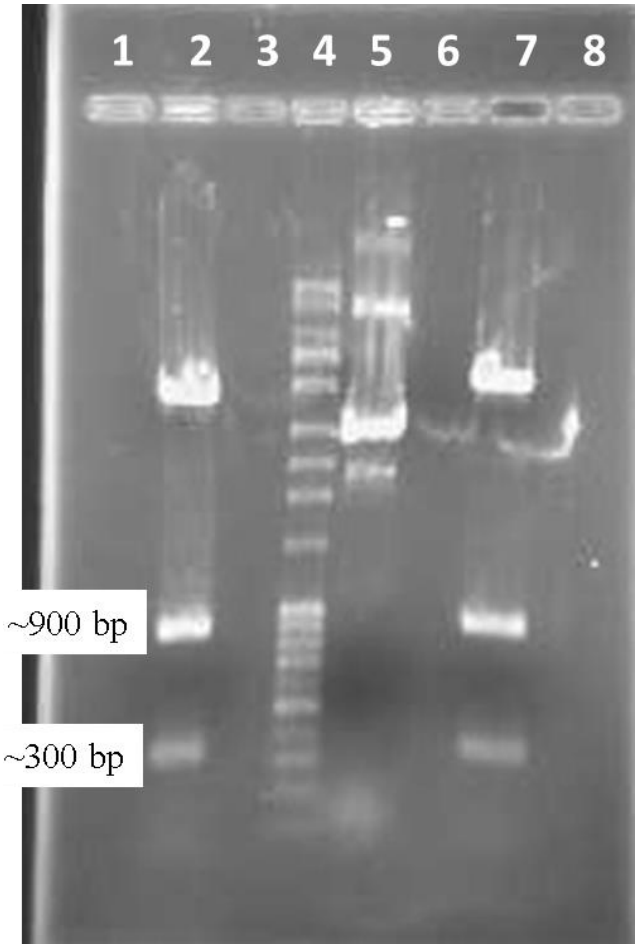

Figure 3-17 NdeI and XhoI digested *glyA.*
TOPO TA cloned glyA-pCR 2.1 was digested by NdeI and XhoI and separated on a 1% agarose gel. Lanes 2 and 7: double digested *glyA*-pCR 2.1, Lane 4: 1 kb plus DNA ladder, and Lane 5: Uncut *glyA*-pCR 2.1. The double digested *glyA*-pCR 2.1 plasmid released ~3.9 bp, 900 bp and 300 bp fragments. The 3.9 bp fragment corresponded to the pCR 2.1 vector. However instead of the expected ~1.2 bp *glyA* DNA fragment, ~ 900 bp and 300 bp fragments were detected. The lack of the correct sized *glyA* fragment led to noticing the presence of an internal XhoI site at 906 bp position that cut *glyA* into two fragments with ~ size 906 bp and 348 bp.

Two commonly utilized techniques to obtain a complete DNA fragment from a vector carrying multiple undesired restriction sites are partial digestion of the vector to obtain a full length fragment and/or changing the undesired restriction enzyme recognition site via site specific mutagenesis technique. For the latter method, codon redundancy could allow use of an alternative DNA sequence which does not change the protein sequence.

After assessing our options, we elected to use the partial digestion protocol of Bloch and Grossmann [89]. Briefly, ~ 9 µg *glyA*-pCR 2.1 plasmid DNA was re-suspended in 90 µL sterile milli-Q H_2O. Then, we added 1X CutSmart™ buffer (NEB) and 20 Unit/µl (2µl) of NdeI enzyme and incubated the sample at 37 ^{o}C for 1 hour. After an hour, the sample was kept on ice and transferred into five sterile eppendorf tubes labeled one to five with the following order and volume: Tube1: 30 µL, Tube 2: 20 µL, Tube 3: 20 µL, Tube 4: 20 µL, and Tube 5: 10 µL. Next, 100 Units/µl (2 U/) of XhoI were added to the first tube and gently mixed. Then, 10 µL samples were transferred, mixed and again a10 µL sample was transferred to the next tube. In other words a 10 µL sample was serially diluted until the 5th tube. Finally, the tubes were incubated at 37 ^{o}C for 30 minutes. Immediately after removing the samples from the incubator, each sample was loaded on a 1% agarose gel and separated. The electrophoresed DNA sample image is shown in Figure 1-18 (below).

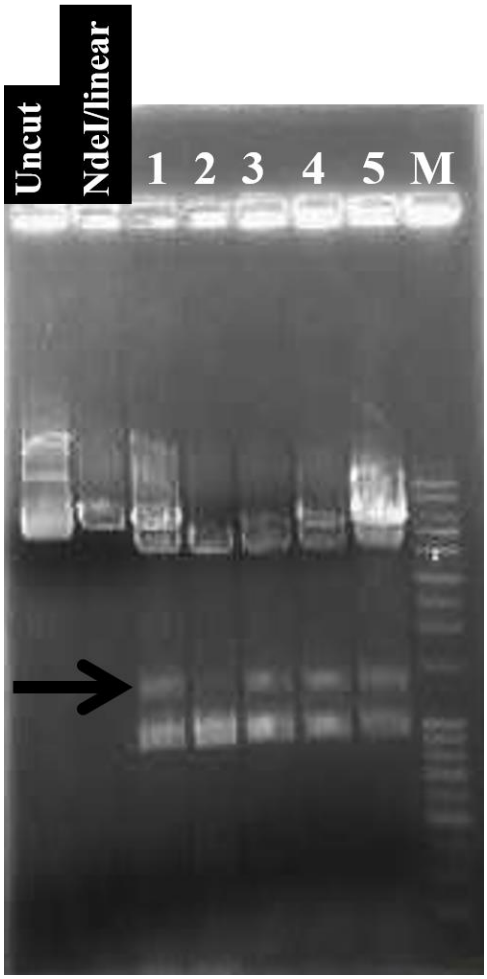

Figure 3-18 Partially digested *glyA*.plasmid
The *glyA*-pCR 2.1 vector was fully digested with NdeI and partially digested with XhoI. Fragments were separated on a 1% agarose gel. Lane 1: Uncut *glyA*-pCR 2.1, Lane 2: NdeI digested *glyA*-pCR 2.1, Lanes 3 to 7 (partial digest tubes numbered 1 to 5) partially digested *glyA*-pCR 2.1, and Lane 8:1 kb plus DNA ladder. Lane 1 shows the supercoiled *glyA*-pCR 2.1 and Lane 2 shows the approximate size of vector plus insert, which is ~ 5,000 bp. Lanes 4 to 7: from partially digested NdeI digest *glyA*-pCR 2.1, an additional partial digest band was found, shown by the arrow. The size of the top fragment was between 4,000- 5,000 bp. The next fragment was slightly lower than the 1,500 bp marker and the bottom DNA fragment was ~1,000 bp. Since the middle fragment (black arrow) was closer to the expected *glyA* size of 1,254 bp, the DNA from all five lanes was excised and used for cloning.

3.4.1.3 Assessing the growth pattern of E. coli JW2535-1 (ΔglyA::kan)

After receiving *E. coli* JW2535-1 (Δ*gly::kan*) from the Coli Genetic Stock Center, we tested it for glycine and serine auxotrophy [26]. The cells were grown in YT liquid media with added 50 µg glycine /ml, 50 µg serine /ml, and 25 µg kanamycin/ml. The overnight culture was streaked on BV agar media supplemented with 50 µg glycine /ml, 50 µg serine /ml, and 25 µg kanamycin/mL and/or BV minimal media with 25 µg kanamycin/ml. The plates were incubated at 37 ^{o}C and checked for five consecutive days. After 24 hours, cell growth was observed on BV supplemented media, but cells did not grow on BV minimal media for two days. Slight cell growth was observed after 72 hours. The image for 48 hours growth is shown in Figure 1-19 (below). These results suggest that *E. coli* JW2535-1 (Δ*glyA::kan*) is auxotrophic for glycine and serine.

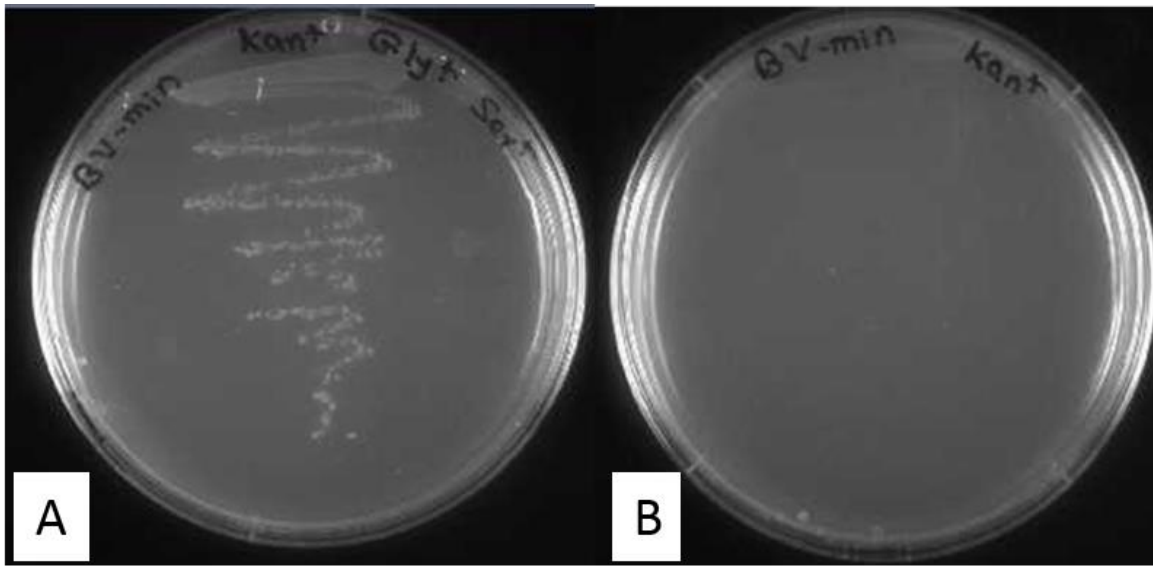

Figure 3-19 The growth pattern of *E. coli* JW2535-1 (*ΔglyA::kan*).
Panel A shows growth on BV supplemented media while Panel B shows growth on supplemented media. *E. coli* JW2535-1 (Δ*glyA::kan*) did not grow on the BV minimal media (right), but it did grow on BV media supplemented with glycine and serine (left).

3.4.1.4 Identification of the tetracycline concentration required for sufficient in vivo SHMT production to rescue E. coli JW2535-1 (ΔglyA::kan) to prototrophy

To determine the minimum tetracycline concentration that allows confluent cell growth of *E. coli* JW2535-1 carrying the *glyA*-pKTS plasmid, cells were grown in YT liquid media with 200 μg ampicillin/ml and 25 μg kanamycin/ml. Next the cells were plated on BV minimal media with 200 μg ampicillin/ml, 25 μg kanamycin/ml and various concentrations of tetracycline (10, 25, 50, 75, 100, 200 and 500 ng/ml). The plates were examined for four days. After 48 hours, confluent cell growth was observed. Images of cell growth at 72 hours are shown in Figure 1-20 (below). Confluent growth was obtained on the plates with 10 to 100 ng tetracycline/ml, but the cell growth became sparse on 200 and 500 ng tetracycline/ml plates.

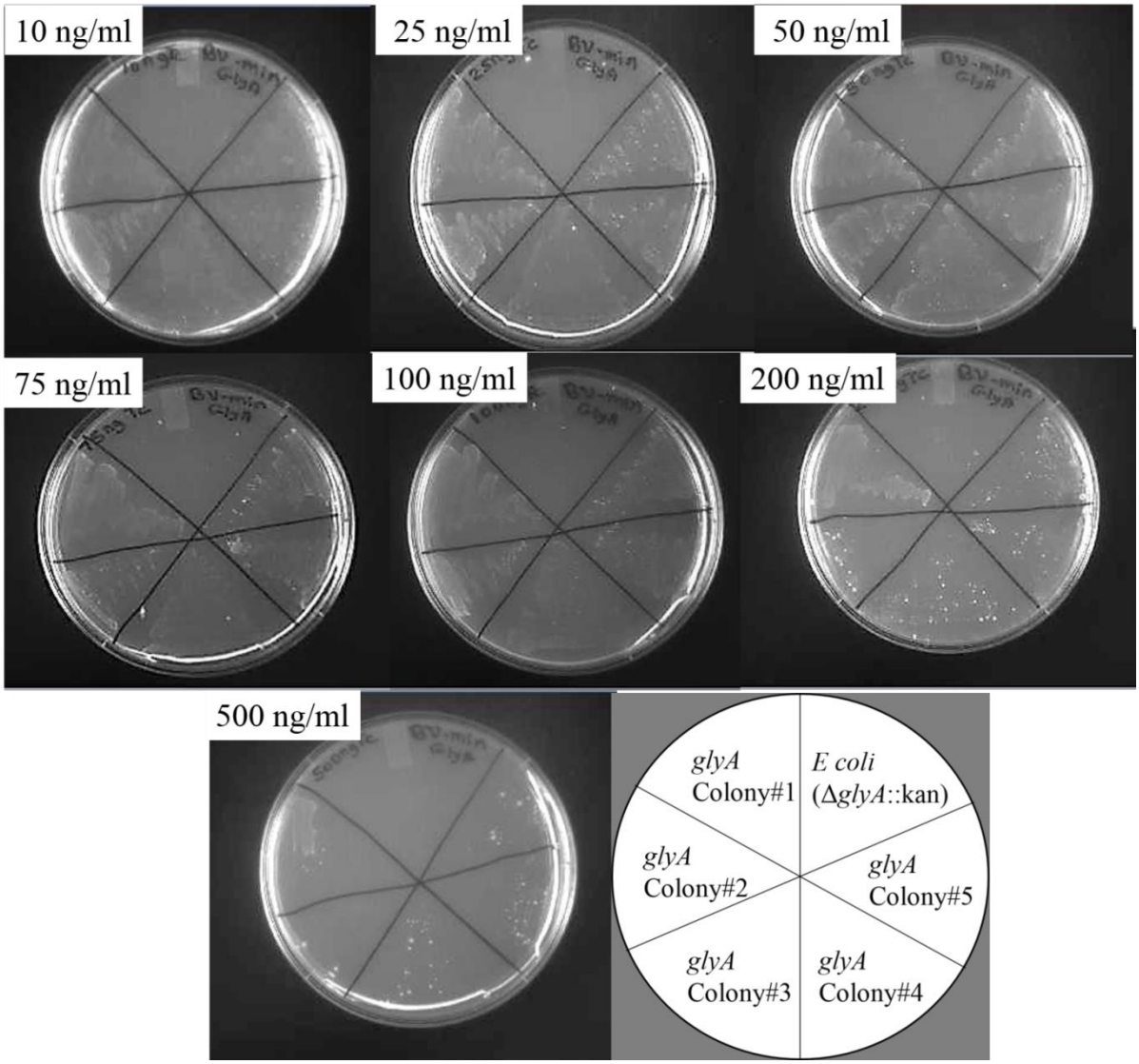

Figure 3-20 Tetracycline dependent *glyA* production.
The optimal tetracycline concentration required to induce production of sufficient SHMT to rescue *E. coli* JW2535-1 (Δ*glyA::kan*) carrying the pKTS-*glyA* plasmid from glycine and serine auxotrophy was determined. Increasing concentrations of tetracycline were added to BV minimal media containing 200 µg ampicillin/ml and 25 µg/ml kanamycin. Confluent cell growth was achieved on plates with 10-100 ng tetracycline/ml. The bottom right panel shows how the various cultures are streaked on the plates.

3.5 Beginning steps to clone the dihydropteroate synthase gene into the pKTS plasmid

Dihydropteroate synthase **(**DHPS) is encoded by the *folP* gene. The protein catalyzes the formation of 7,8-dihydropteroate by linking 6-hydroxymethyl-7,8-dihydropterin pyrophosphate (H_2PtPP) and ρ-aminobenzoic acid (pABA) [56]. If osmolytes preferentially interact with either substrate, the catalytic efficiency of DHPS is predicted to decrease. As an initial step to test this hypothesis, we obtained a *fol*P-pUC19 clone and the knockout *E. coli* strain *(ΔfolP::kan*) from Dr. Swedberg [90]. Progress was made as described below.

3.5.1 Assessing the quality of the *folP* clone and assessing the cloning sites in the gene

The plasmid DNA received from Dr. Swedberg was sequenced using M13 forward and M13 reverse primers. The sequence alignment show the *folP* open reading frame was cloned between HindIII and BamHI cloning sites of pUC19. To introduce an NdeI restriction site sequence via PCR, a primer was designed as described in the Materials and Methods section. While the primers worked as sequencing primers, several attempts to PCR amplify the gene were not successful**.**

As an alternate strategy, we decided to design a "pessimal" DNA sequence encoding *folP*. As codon optimization is a frequent strategy to increase protein production, we took the opposite approach and designed a "worst" sequence to minimize protein production. The sequence design was done in collaboration with Mike Gilchrist from the Ecology and Evolutionary Biology Department [91, 92]. The resulting sequence was synthesized by GenScript. The construct was sent to us as a *folP* gene inserted in the pET3a plasmid using the NdeI and XhoI restriction enzyme sites. This construct was transformed into DH5α cells. Individual colonies were selected on YT agar media with 200 μg ampicillin/ml. Four colonies were grown up, the plasmid DNA extracted and the DNA sequenced.

In an initial experiment, the plasmid DNA of *folP*-pET3a was double digested with NdeI and XhoI. The DNAs were separated on a 1% agarose gel Figure 3-21(below). The correct sized DNA fragments were excised. However ligation and transformation reactions did not yield colonies. This is an ongoing project in the lab.

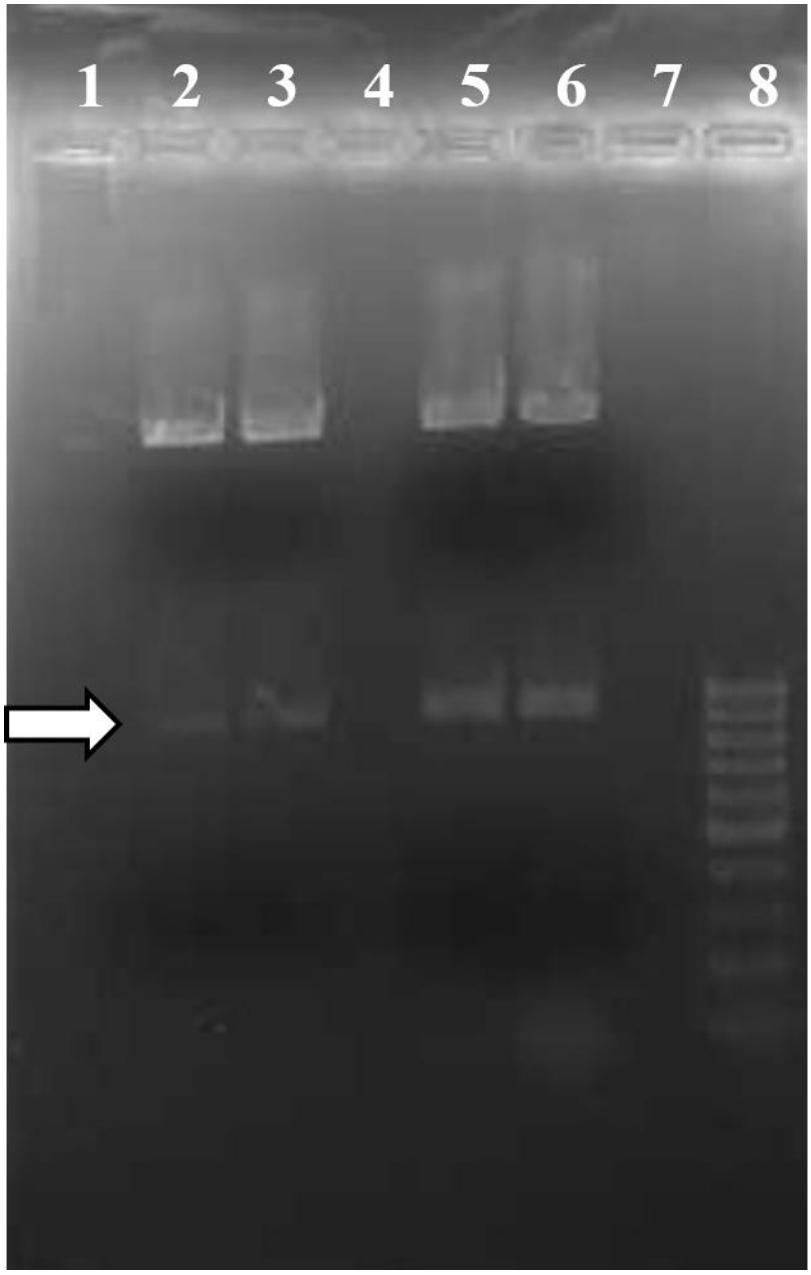

Figure 3-21 NdeI and XhoI digested *folP*.
Digestion of *folP*-pET3a DNA by NdeI and XhoI. The reaction was electrophoresed in a 1% agarose gel. Lanes 2, 3, 5 and 6: digested *folP*-pET3a, Lane 8: 100 bp DNA ladders. Lanes 2, 3, 5 and 6 showed the expected DNA fragment size (849 bp) for *folP* digestion by NdeI and XhoI. The arrow shows the band of interest.

4 CHAPTER: DISCUSSION

These *in vivo* genetic studies were designed to test our model presented in Figure 1-5page 5) that proposes osmolytes interact with folate and its various redox states. Table 1 (below) shows our progress for 6 folate pathway enzymes. Not all enzymes were cloned and screened, however our success with the wild type R67 DHFR clone provides a proof of concept for using the pKTS plasmid to decrease protein expression levels so that a genetic selection can be implemented that responds to osmotic stress. Each enzyme will be discussed briefly below.

Table 1. Summary of results for several folate metabolism enzymes.

	R67 DHFR and Quad4 (LH18)	R67 DHFR and Quad4 (TMP^R)	MTHFR (metF)	SHMT (glyA)	DHPS (folP)	HPPK (folK)	FPGS (folC)
Receive gene and knockout strain	✔	✔	✔	✔	✔	✔	✔
Clone gene into pKTS plasmid	✔	✔	✔	✔	-	-	-
Find [tetracycline] that relieves auxotrophy of the rescued strain	✔	n/a [a]	✔	✔	-	-	-
Find [tetracycline] that provides TMP resistance	n/a [a]	✔	n/a [a]	n/a [a]	n/a [a]	n/a [a]	n/a [a]
Sorbitol titration	✔	✔	- [b]	- [b]	-	-	-
In vivo osmotic stress titration of enzyme activity or antibiotic resistance?	Yes	Yes	- [b]	- [b]	-	-	-

[a] not applicable.

[b] continued by Deepika Nambiar. Deepika sees a clear osmotic stress effect for MTHFR.It is too early to tell for SHMT.

4.1.1 R67 DHFR and/or Quad4

Success in titrating the *in vivo* R67 DHFR activity using osmotic stress was previously achieved using a Y69L mutant and using resistance to the EcDHFR active site directed inhibitor, trimethoprim. In this thesis, we extend this osmotic stress titration to the wt R67 DHFR enzyme using the controllable P_{tet} promoter and a SsrA tag encoded by the pKTS plasmid. To monitor enzyme activity directly, we used a knockout strain where the *folA* gene was replaced by a kanamycin resistance marker. This strain, LH18, was rescued by the pKTS-R67 DHFR or pKTS-Quad4 plasmids.

The pKTS-R67 DHFR construct required an ~2.5x higher concentration of tetracycline to provide sufficient DHFR activity to confer TMP resistance and/or rescue LH18 from folate end product auxotrophy. The tetracycline titration images are shown in Figure 3-2page-50 and Figure 3-4 page-53. As described in the Methods section, the ability of an enzyme to rescue the host cell from the missing metabolic activity and/or to confer resistance to TMP is dependent on the catalytic activity as well as the *in vivo* concentration of the enzyme. As R67 DHFR and Quad4 have similar catalytic efficiencies [5], this is unlikely to be the parameter involved.

The other main difference between R67 DHFR and Quad4 is their oligomerization states; R67 being a homotetramer and Quad4 being a monomer. Therefore R67 DHFR would carry four SsrA tags in comparison to one per Quad4. This scenario predicts the *in vivo* concentration of R67 DHFR will be lower than for Quad 4 as the SsrA tag targets the protein to the ClpX protease. More tags are expected to increase targeting. This is likely the reason for the increased tetracycline concentration required to provide TMP resistance or growth to the knockout strain for the pKTS-R67 DHFR clone as compared to the pKTS-Quad4 clone.

Confluent cell growth of DH5α and LH18 carrying the pKTS-R67 DHFR and pKTS-Quad4 clones was observed on the minimal plates up to 200 ng tetracycline/ml. However cell growth became sparse at in the presence of 500 ng tetracycline/ml. This result suggested this concentration of tetracycline was above a threshold and became toxic to DH5α and LH18. Similar observations were reported by Neuenschwander et al. when using the green fluorescent protein (GFP) gene cloned into pKTS and expressed in XL1-Blue and DH5α *E. coli* strains [88]. In XL-1-Blue, GFP production was increased until a concentration of 5,000 ng tetracycline/ml was reached.

But in DH5α, GFP production was increased until 100 ng tetracycline/ml was reached; however GFP production started to decline at higher tetracycline concentrations [88]. Neuenschwander proposed individual strains have different tolerances to higher tetracycline concentrations.

Under normal conditions, bacterial cells maintain turgor pressure, which is a higher internal osmotic pressure than their surrounding environment/medium. However when the outside osmotic pressure becomes higher than the intracellular pressure, bacteria generate their own internal osmoprotectants and/or transport osmolytes from the environment [93]. As a result, the cytoplasmic water concentration and growth rate decrease [94]. In 2003, Cayley and Record showed that as the external osmotic pressure rises, the cytoplasmic free water concentration decreases as does the cell growth rate of *E. coli* [17].When no free water remains, cell growth stops. This is the upper limit for our osmotic stress assays.

To establish a baseline to assess the activity of R67 DHFR and Quad4 rescuing DH5α and/or LH18 from TMP resistance and/or folate end product auxotrophy, bacterial osmolality fitness was measured by adding increasing concentrations of sorbitol to the growth media. The media supplied all the metabolic needs of the bacteria, and bacterial fitness was identified based on the osmolality of the plate where the bacteria stopped growing. DH5α growth was decreased under 1.90 Osm and completely stopped at 2.43 Osm (Figure 3-5, page 56), while LH18 (Figure 3-6page 57) growth decreased at 1.50 Osm and stopped at 2.12 Osm (**Error! Reference source not found.**, page 59). Previous differences in osmotic fitness between strains and organisms have been reported [95, 96].

When DH5a carrying pKTS-R67 DHFR (Figure 3-6page-57) was examined, the cells were able to grow on media containing TMP up to 1.23 Osm and the pKTS-Quad4 clone enabled growth up to 1.60 Osm. These results showed the increased viability associated with the pKTS-Quad4 clone compared to that of pKTS-R67 DHFR containing cells. In addition, *E. coli* LH18 (Δ*folA::kan*) carrying pKTS-R67 DHFR and/or pKTS-Quad4 allows cell growth up to 1.37 Osm and 1.68 Osm, respectively (Figure 3-8, page-60). These different limits indicate the Quad4 clone provides a selective advantage.

A scenario consistent with our model suggests that upon addition of sorbitol, the *E. coli* cells synthesize their own osmoprotectants, including betaine [17]. As betaine addition decreases the catalytic efficiency of R67 DHFR, the R67 DHFR activity is titrated such that insufficient

activity remains to allow cell growth. This titration is seen *in vitro* in Figure 1-4, page 4. Other osmolytes and crowding molecules may be present in the cell and their potential effects add complicating layers to the analysis. Cayley and Record find that betaine is the predominant osmoprotectant in *E. coli* grown in a minimal MOPS media with added 1mM betaine [17]. A future experiment will test the effect of this media on our titrations.

When we compare the *in vivo* osmotic stress titrations of R67 DHFR and Quad4 activities, we find the Quad4 clone confers a growth advantage. Both enzymes have similar protein scaffolds and enzyme activities; however the pKTS-Quad4 construct likely allows a higher cytoplasmic protein concentration as it possesses fewer SsrA tags. Quad4 may be considered to be an internal control for R67 DHFR as a higher Quad4 protein concentration leads to growth at higher sorbitol concentrations. This comparison supports our contention that sorbitol addition results in higher osmoprotectant concentrations inside the cell, which then decreases the catalytic efficiency of R67 DHFR such that it can longer support cell growth.

Several other experiments can be explored to test our hypothesis. For example, if R67 DHFR concentration is the important variable, we can perform a tetracycline titration at sorbitol concentrations that block cell growth. For example, LH18 carrying pKTS-R67 DHFR stops growing at 1.00 M sorbitol (= 1.60 osmolality) in the presence of 100 ng tetracycline/ml. We can vary the tetracycline concentration so that more or less R67 DHFR is produced and monitor the effect on cell growth. We would predict that addition of a higher tetracycline concentration would allow growth at this osmolality.

A third issue considers whether osmotic stress is the variable that blocks cell growth. For example, sorbitol can be used as a carbon source by *E. coli* [97], thus we propose to additionally use NaCl as an osmotic stressor. Preliminary studies by Noelle Lebow, a summer REU student, indicate NaCl addition can block the growth of LH18 carrying pKTS-R67 DHFR on minimal media at osmolalities lower than the upper limit (i.e. where no free water remains). As NaCl contains 2 ions which contribute to the solution osmolality, cell growth stops at media containing 0.75 M NaCl. Further the measured osmolalities of the agar compare to those measured in sorbitol containing media. These preliminary experiments are consistent with osmotic stress induced by either sorbitol or NaCl resulting in intracellular titration of R67 DHFR activity such that *E. coli* growth is no longer supported.

4.1.2 Folypolyglutamate Synthase (FPGS)

E. coli: SF2 (*folC strA*) [50] has a leaky mutation at A309T that decreases the catalytic activity to 1-3% of wild-type FPGS levels and the total folate pool drops to 10 to 30 % of normal *in vivo* concentration. SF2 is auxotrophic for methionine. For this strain to grow in minimal media, methionine is required. Addition of glycine further stimulates growth. The K_Ms' of A309T, FolC are much higher compared to the wild type [98]. Because *in vivo* activity of the mutant is low, it seemed feasible to assess the effects of increasing osmolality directly on the chromosomal enzyme on supplemented media. In other words, the low turnover rate of the enzyme would allow *in vivo* selection [22]. If osmolytes weakly interact with dihydropteroate and/or tetrahydrofolate based substrates, this could further weaken their binding to FPGS and potentially titrate the activity of the mutant enzyme. Since loss of FPGS activity is lethal to the cell, this could block cell growth.

Variable cell growth patterns are one of the main challenges of assessing *in vivo* assays for several unknown factors. To increase our *in vivo* assay interpretation power, we plated SF2 and its parent strain MG1485 with and without a plasmid containing the wild type FolC clone. We assumed the SF2 carrying clone and the parent strain would have similar cell growth patterns. However, as seen in Figure 3-10: page 63, growth of SF2 and SF2 carrying a functional clone decreased on a 1.00 M sorbitol plate and stopped on a 1.25 M sorbitol plate. Moreover, the parent strain (wt) and parent strain carrying the pPM103-FPGS plasmid stopped growing in 1.50 M sorbitol, while the parent strain carrying pAC5 stopped in growing in 1.25 M sorbitol containing media. One possibility for the decreased growth of both the parent and SF2 strains containing plasmid could be the loss of the plasmid. In an attempt to retain the plasmid by increasing the metabolic selection pressure, the methionine concentration was decreased to a minimal level while the glycine concentration remained in excess. As shown in Figure 3-11-page-65, increasing the metabolic selection pressure did not resolve the problem.

1) Inability of FolC to rescue SF2 under high osmotic pressure - Because the presence of a plasmid carrying the wt FPGS gene did not rescue the SF2 cell under high osmolality conditions, we asked whether the A309T mutation could be dominant negative over the wt gene. When considering models of dominant negative action, a mutation can lead to an oligomer containing wild type and mutant polypeptides, which has greatly diminished activity [99]. This scenario

seems unlikely as FPGS is a monomer. Indeed, a truncated FPGS gene was found not to be dominant negative over wt FPGS in a human blood cell line [100].

2) The polyglutamylation state of folates in the cell can impact the function of folate mediated 1C metabolism enzymes. For example, with low γ-FPGS activity, most folates may be mono- to tri-glutamylated on the γ-carboxylate. After this, an α-FPGS adds glutamates at the α-carboxylate. With a higher γ-FPGS activity, longer γ-polyglutamylated folates may be made which could affect the sensitivity of the cell to osmotic stress.

3) In a more likely alternative, we speculate that the ethylmethane sulfonate (EMS) mutagenesis [49] procedure that was carried out on MG1655 to generate the FolC mutant could have created an additional mutation(s) that impacts cell growth under osmotic stress. For example, if SF2 contained additional mutations in stress response and/or osmotic stress response gene(s), the loss of this function could be manifested in our assay condition.

To pursue the effect of osmotic stress on FPGS in the future, we have several avenues. One is to continue using the *ΔfolC::kan* knockout of Pyne et al. [67], which is based on the SF2 strain Since Pyne et al[67] could only delete the chromosomal *FolC* gene when a plasmid *FolC* gene was present in trans, several FPGS mutants at residue A309 were used with progressively decreasing activities. For example, the A309V, A309I, A309G, A309V, A309R, A309E and L A309L mutants have progressively weaker activities[50] and require progressively more folate end products to be added to the media to allow growth. While we requested and received several of these strains, they did not grow up. The Bognar lab also had difficulty in retrieving them from their freezer stocks. We can try re-requesting them.

We also have the option of requesting the knockout strain constructed by Pyne et al. [67] that has the C600 *E. coli* background. This strain carries a pPMpac3a plasmid that can be segregated or cured once transformed with another plasmid carrying the *FolC* gene. We would clone either the wt or a mutant FPGS gene into pKTS and transform this *ΔfolC::kan* strain with it. We could cure the strain of the pPMpac3a plasmid by growth at 37-42°C. We could re-try the sorbitol titration.

4.1.3 5,10-Methylenetetrahydrofolate Reductase (MTHFR)

Our initial literature review indicated the K_M of MTHFR for its substrate, 5,10-methylene-THF_n , is ~30X [35] less than the *in vivo* concentration of this molecule [33] [51]. As shown in Table 1, the gene was cloned into pKTS and the tetracycline concentration to rescue a knockout cell from methionine auxotrophy was determined. The system was set up and Deepika Nambiar joined the lab and is continuing to assay the sensitivity of the *metF* system to osmotic stress. She finds blockage of growth of *ΔmetF::kan* cells carrying the *metF*-pKTS clone on minimal media containing lower concentration of sorbitol, while the *ΔmetF::kan* cells continue to grow in supplemented media containing higer concentration of sorbitol. These results suggest as the intracellular osmolality of the cell increases, the activity of MTHFR decreases and is no longer able to rescue the host cells from methionine auxotrophy. Considering our model showing the preferential interaction of osmolytes weaken DHF binding with the enzyme Figure 1-5 page 5, if the host cell generates betaine [17], and betaine preferentially interacts with 5,10-methylene-THF_n, the ability of MTHFR to provide the missing metabolite should decrease with increasing osmotic pressure. Overgrowing colonies occur in these titrations (but still stop growing at low concentrations of sorbitol), so additional experiments still need to be performed. However a similar trend was observed as with our osmotic pressure titration of Quad4 and R67 DHFR activities *in vivo*.

4.1.4 Serine Hydroxymethyl Transferase (SHMT)

As shown in Figure 3-20 page 80, the tetracycline dependent growth of for *E. coli* JW2535-1 (Δ*glyA::kan*) carrying the pKTS-*glyA* showed protein production-dependent cell growth that can be illustrated in Figure 1-7page 11. A study on the effects of increasing osmolality on the function of GlyA is in progress by Deepika Nambiar.

4.2 Conclusion

This thesis describes the *in vivo* genetic complementation assays that show an effect of increasing osmolality on the function of essential folate enzymes. This study is expanded from *in vitro* studies that showed preferential interaction of osmolytes with DHF/folate, which weakens binding and lowers the catalytic efficiencies of three structurally different dihydrofolate reductase

enzymes [2, 3, 23]. Our *in vivo* results for R67 DHFR and Quad4 established a proof of concept that our *in vivo* assay conditions mimic our *in vitro* results, as we can titrate the activity of targeted folate enzymes *in vivo*. DHFR activity could be titrated out by the addition of external osmolytes, frustrating the growth of the cell. Additionally, *in vivo* assays are in progress for three other folate enzymes: MTHFR, SHMT and DHPS. Collectively, the results of these assays, in conjunction with several *in vitro* studies, suggest the effects of preferential interaction between DHF/folate and osmolytes on the function of folate enzymes can be detrimental to the cell. Moreover, unintended consequences of the folate-osmolyte interactions on other folate cycle and/or cellular networks is in progress using a metabolomics approach.

4.3 Future experiments

Preferential interaction of DHF/folate with osmolytes is a unique event that is detected by the Howell lab. This environmental parameter can be measured with *in vitro* as well as *in vivo* experiments. Our *in vivo* studies are at an initial stage. While solid media is useful for broader assessments of the effects of osmolytes on cell growth, liquid media can provide an alternative to determine the growth rate, which can be correlated with *in vitro* enzyme parameters. For example, Caley et al. [17] showed adding 1 mM betaine in a growth media stimulated and determined the rate of production/accumulation and types of intracellular osmolytes. It will be interesting to assess the effects of different solute/osmolyte addition in the variations of internal osmolality and its effects on the activity of the folate enzyme *in vivo*.

If this approach with other wt enzymes does not work, one possibility is that the enzyme activity remains sufficiently high so that it is refractive to sorbitol titration. To decrease the total enzyme activity in the cell, we can mutagenize active site residues. For example, if we are unable to titrate DHPS activity, we can construct the N27A mutation, which decreases enzyme activity 77 fold [101].

We recognize that the cell is a complicated environment. Thus another reason for loss of growth in our in-cell osmotic stress assays would be a decrease in the DHFR concentration under high osmolality conditions. Future experiments will monitor the effect of osmotic pressure on the total DHFR concentration using an ELISA assay or a Western. However we note that in one

osmotic stress response study, most *E. coli* proteins were found to show similar expression levels (within a 2 fold window) [102].

A second complicating factor may be that other folate pathway enzymes could also be affected. For example, when EcDHFR activity is inhibited by TMP addition, Kwon et al. found the DHF concentration rises [35]. This in turn inhibits the activity of FPGS. Kwon et al. term this a "domino effect" in that several consecutive events can occur, which can amplify the initial effect. To consider this scenario, we propose to perform folate metabolomics with Shawn Campagna in the chemistry department to monitor the concentrations of many folate metabolites. This will allow us to identify any additional inhibitory effects by monitoring whether the metabolite concentrations fall or rise. Use of metabolomics will also allow us to monitor the concentrations of *E. coli* osmoprotectants.

An additional complication considers the preferential interaction coefficient (μ23/RT) predictions given in Table 1.1. page 9. Elongation of the polyglutamate tails of folate and its redox states allows retention of folates in eukaryotic cells by the presence of additional negative charges, which decreases ligand efflux out of the cell. In prokaryotic cells, polyglutamylation is proposed to be important for binding to certain enzymes, for example binding of methyleneTHF to the non-B12-dependent methionine synthase [49]. The calculated μ23/RT values in Table 1.1 predict the overall exclusion of osmolytes from the polyglutamylated folate species, thus one may predict tighter binding of the polyglutamylated folates in the presence of osmolytes. However, if the polyglutamylated tail is not used in binding and does not need to be desolvated, then removal of any osmolytes from the pterin and pABA rings could dominate and lead to weaker binding. We are addressing this issue for one specific case by performing ITC studies of PG5 (folate with 5 glutamates) binding to R67 DHFR. PG5 shows the same K_d as for folate [103], suggesting the additional 4 glutamates in the tail are not in contact with the enzyme binding pocket. If water and/or osmolytes do not need to be removed for the ligand to bind, then they will not contribute to the experimental μ23/RT value; thus the experimental and calculated μ23/RT values may differ depending on the extent of the ligand contact with the active site.

Reference

1. Chopra, S., et al., *A balancing act between net uptake of water during dihydrofolate binding and net release of water upon NADPH binding in R67 dihydrofolate reductase.* J Biol Chem, 2008. **283**(8): p. 4690-8.

2. Grubbs, J., et al., *Thermodynamics and Solvent Effects on Substrate and Cofactor Binding in Escherichia coli Chromosomal Dihydrofolate Reductase.* Biochemistry, 2011. **50**: p. 3673-3685.

3. Bhojane, P.P., et al., *Investigation of osmolyte effects on FolM: comparison with other dihydrofolate reductases.* Biochemistry, 2014. **53**(8): p. 1330-41.

4. Neuenschwander, M., et al., *A simple selection strategy for evolving highly efficient enzymes.* Nat Biotechnol, 2007. **25**(10): p. 1145-7.

5. Feng, J., et al., *Radical redesign of a tandem array of four R67 dihydrofolate reductase genes yields a functional, folded protein possessing 45 substitutions.* Biochemistry, 2010. **49**(34): p. 7384-92.

6. Bekaert1, S., et al., *Folate biofortification in food plants.* Trends Plant Sci, 2008. **13**(1): p. 28-35.

7. Michael R. Duff, J. and E.E. Howell, *"Thermodynamics and solvent linkage of macromolecule-ligand interactions".* submitted to Methods 2014.

8. Krahn, J.M., et al., *Crystal structure of a type II dihydrofolate reductase catalytic ternary complex.* Biochemistry, 2007. **46**(51): p. 14878-88.

9. Fratte, S.D., et al., *The function of arginine 363 as the substrate carboxyl-binding site in Escherichia coli serine hydroxymethyltransferase.* Eur J Biochem, 1994. **225**(1): p. 395-401.

10. Sepasi Tehrani, H., et al., *Effect of compatible and noncompatible osmolytes on the enzymatic activity and thermal stability of bovine liver catalase.* J Biomol Struct Dyn, 2013. **31**(12): p. 1440-54.

11. Khan, S.H., et al., *Naturally occurring organic osmolytes: from cell physiology to disease prevention.* IUBMB Life, 2010. **62**(12): p. 891-5.

12. Harries, D. and J.r. Ro¨sgen, *A Practical Guide on How Osmolytes Modulate Macromolecular Properties.* METHODS IN CELL BIOLOGY, 2008. **84**.

13. Parsegian, V.A., R.P. Rand, and D.C. Rau, *Osmotic stress, crowding, preferential hydration, and binding: A comparison of perspectives.* Proc Natl Acad Sci U S A, 2000. **97**(8): p. 3987-92.

14. Rosgen, J., *Molecular basis of osmolyte effects on protein and metabolites.* Methods Enzymol, 2007. **428**: p. 459-86.

15. M. Thomas Record, J., et al., *Biophysical compensation mechanisms buffering E. coli protein-nucleic acid interactions against changing environments.* Trends Biochem Sci, 1998. **23**(5): p. 190-4.

16. M. Thomas Record, J., et al., *Responses of E. coli to osmotic stress: large changes in amounts of cytoplasmic solutes and water.* Trends Biochem Sci, 1998. **23**(4): p. 143-8.

17. Cayley, S. and J. M. Thomas Record, *Roles of cytoplasmic osmolytes, water, and crowding in the response of Escherichia coli to osmotic stress: biophysical basis of osmoprotection by glycine betaine.* Biochemistry, 2003. **42**(43): p. 12596-609.

18. Stone, S.R. and J.F. Morrison, *Mechanism of inhibition of dihydrofolate reductases from bacterial and vertebrate sources by various classes of folate analogues.* Biochim Biophys Acta, 1986. **869**(3): p. 275-85.

19. Amyes, S.G.B. and J.T. Smith, *The purification and properties of the trimethoprim-resistant dihydrofolate reductase mediated by the R-factor, R388.* Eur J Biochem, 1976. **61**(2): p. 597-603.

20. Howell, E.E., *Searching sequence space: two different approaches to dihydrofolate reductase catalysis.* Chembiochem, 2005. **6**(4): p. 590-600.

21. Chopra, S., et al., *Effects of temperature and viscosity on R67 dihydrofolate reductase catalysis.* Biochemistry, 2006. **45**(21): p. 6596-605.

22. Butz, M., et al., *An N-terminal protein degradation tag enables robust selection of highly active enzymes.* Biochemistry, 2011. **50**(40): p. 8594-602.

23. Capp, M.W., et al., *Interactions of the osmolyte glycine betaine with molecular surfaces in water: thermodynamics, structural interpretation, and prediction of m-values.* Biochemistry, 2009. **48**(43): p. 10372-9.

24. Guinna, E.J., et al., *Quantifying why urea is a protein denaturant, whereas glycine betaine is a protein stabilizer.* Proc Natl Acad Sci U S A, 2011. **108**(41): p. 16932-7.

25. Diehl, R.C., et al., *Quantifying additive interactions of the osmolyte proline with individual functional groups of proteins: comparisons with urea and glycine betaine, interpretation of m-values.* Biochemistry, 2013. **52**(35): p. 5997-6010.

26. Baba, T., et al., *Construction of Escherichia coli K-12 in-frame, single-gene knockout mutants: the Keio collection.* Mol Syst Biol, 2006. **2**: p. 2006 0008.

27. Bertram, R. and W. Hillen, *The application of Tet repressor in prokaryotic gene regulation and expression.* Microb Biotechnol, 2008. **1**(1): p. 2-16.

28. Hillen, W. and C. Berens, *Mechanisms underlying expression of Tn10 encoded tetracycline resistance.* Annu Rev Microbiol, 1994. **48**: p. 345-69.

29. Skerra, A., *Use of the tetracycline promoter for the tightly regulated production of a murine antibody fragment in Escherichia coli.* Gene, 1994. **151**(1-2): p. 131-5.

30. *Molecular Operating Environment (MOE).* Chemical Computing Group Inc., 1010 Sherbooke St. West, Suite #910, Montreal, QC, Canada, H3A 2R7, 2012, MOE 2012.10.

31. R.Schmitzer, A., F.o. Le´pine, and J. N.Pelletier, *Combinatorial exploration of the catalytic site of a drug-resistant dihydrofolate reductase: creating alternative functional configurations.* Protein Eng Des Sel, 2004. **17**(11): p. 809-19.

32. Pejchal, R., R. Sargeant, and M.L. Ludwig, *Structures of NADH and CH3-H4folate complexes of Escherichia coli methylenetetrahydrofolate reductase reveal a spartan strategy for a ping-pong reaction.* Biochemistry, 2005. **44**(34): p. 11447-57.

33. Sheppard, C.A., E.E. Trimmer, and R.G. Matthews, *Purification and properties of NADH-dependent 5, 10-methylenetetrahydrofolate reductase (MetF) from Escherichia coli.* J Bacteriol, 1999. **181**(3): p. 718-25.

34. Mathieu, M., et al., *Escherichia coli FolC structure reveals an unexpected dihydrofolate binding site providing an attractive target for anti-microbial therapy.* J Biol Chem, 2005. **280**(19): p. 18916-22.

35. Kwon, Y.K., et al., *A domino effect in antifolate drug action in Escherichia coli.* Nat Chem Biol, 2008. **4**(10): p. 602-8.

36. J. Neel Scarsdale, et al., *Crystal structure at 2.4 A resolution of E. coli serine hydroxymethyltransferase in complex with glycine substrate and 5-formyl tetrahydrofolate.* J Mol Biol, 2000. **296**(1): p. 155-68.

37. DeBenedetti, S., et al., *Characterization of serine hydroxymethyltransferase GlyA as a potential source of D-alanine in Chlamydia pneumoniae.* Front Cell Infect Microbiol, 2014. **4**: p. 19.

38. Achari, A., et al., *Crystal structure of the anti-bacterial sulfonamide drug target dihydropteroate synthase.* Nat Struct Biol, 1997. **4**(6): p. 490-497.

39. Bergleza, J., et al., *Analysis in Escherichia coli of Plasmodium falciparum dihydropteroate synthase (DHPS) alleles implicated in resistance to sulfadoxine.* Int J Parasitol, 2004. **34**(1): p. 95-100.

40. Shaw, G.X., et al., *Structural enzymology and inhibition of the bi-functional folate pathway enzyme HPPK-DHPS from the biowarfare agent Francisella tularensis.* Febs j, 2014. **281**(18): p. 4123-37.

41. Li, Y., et al., *Catalytic roles of arginine residues 82 and 92 of Escherichia coli 6-hydroxymethyl-7,8-dihydropterin pyrophosphokinase: Site-directed mutagenesis and biochemical studies.* Biochemistry, 2003. **42**(6): p. 1581-1588.

42. Bennett, B.D., et al., *Absolute quantitation of intracellular metabolite concentrations by an isotope ratio-based approach.* Nat Protoc, 2008. **3**(8): p. 1299-311.

43. Bennett, B.D., et al., *Absolute quantitation of intracellular metabolite concentrations by an isotope ratio-based approach.* Nat Protoc, 2009. **3**(8): p. 1299-311.

44. Howella, E.E., et al., *One site fits both: a model for the ternary complex of folate + NADPH in R67 dihydrofolate reductase, a D2 symmetric enzyme.* J Comput Aided Mol Des, 2001. **15**(11): p. 1035-52.

45. Matthews, D.A., et al., *Crystal structure of a novel trimethoprim-resistant dihydrofolate reductase specified in Escherichia coli by R-plasmid R67.* Biochemistry, 1986. **25**(15): p. 4194-204.

46. Narayana1, N., et al., *A plasmid-encoded dihydrofolate reductase from trimethoprim-resistant bacteria has a novel D2-symmetric active site.* Nat Struct Biol, 1995. **2**(11): p. 1018-25.

47. Kimlova, L.J., et al., *Mutagenesis of the folC gene encoding folylpolyglutamate synthetase-dihydrofolate synthetase in Escherichia coli.* Arch Biochem Biophys, 1991. **284**(1): p. 9-16.

48. Spencer, H.T., J.E. Villafranca, and J.R. Appleman, *Kinetic scheme for thymidylate synthase from Escherichia coli: determination from measurements of ligand binding, primary and secondary isotope effects, and pre-steady-state catalysis.* Biochemistry, 1997. **36**(14): p. 4212-22.

49. Ferone, R., et al., *Isolation and characterization of an E. coli mutant affected in dihydrofolate- and folylpolyglutamate-synthetase.* Chemistry and biology of pteridines. de Gruyter, Berlin., 1983: p. 585-589.

50. Keshavjee, K., C. Pyne, and A.L. Bognar, *Characterization of a mutation affecting the function of Escherichia coli folylpolyglutamate synthetase-dihydrofolate synthetase and*

further mutations produced in vitro at the same locus. J Biol Chem, 1991. **266**(30): p. 19925-9.

51. Trimmer, E.E., et al., *Folate activation and catalysis in methylenetetrahydrofolate reductase from Escherichia coli: roles for aspartate 120 and glutamate 28.* Biochemistry, 2001. **40**(21): p. 6216-26.

52. Lee, M.N., et al., *Functional role for the conformationally mobile phenylalanine 223 in the reaction of methylenetetrahydrofolate reductase from Escherichia coli.* Biochemistry, 2009. **48**(32): p. 7673-85.

53. Trimmer, E.E., *Methylenetetrahydrofolate reductase: biochemical characterization and medical significance.* Curr Pharm Des, 2013. **19**(14): p. 2574-93.

54. Scarsdale, J.N., et al., *Crystal Structure at 2.4 AÊ Resolution of E. coli Serine Hydroxymethyltransferase in Complex with Glycine Substrate and 5-Formyl Tetrahydrofolate.* J. Mol. Biol., 2000. **296**: p. 155 - 168.

55. Schirch, V., et al., *Serine hydroxymethyltransferase from Escherichia coli: purification and properties.* J Bacteriol, 1985. **163**(1): p. 1-7.

56. Dallas, W.S., et al., *Cloning, sequencing, and enhanced expression of the dihydropteroate synthase gene of Escherichia coli MC4100.* J Bacteriol, 1992. **174**(18): p. 5961-70.

57. Xiao, B., et al., *Crystal structure of 6-hydroxymethyl-7,8-dihydropterin pyrophosphokinase, a potential target for the development of novel antimicrobial agents.* Structure with Folding & Design, 1999. **7**(5): p. 489-496.

58. McNeil, J.B., A.L. Bopart, and R.E. Pearlman, *In vivo analysis of folate coenzymes and their compartmentation in Saccharomyces cerevisiae.* Genetics, 1996. **142**(2): p. 371-81.

59. Perry, K.M., et al., *Structures of thymidylate synthase with a C-terminal deletion: role of the C-terminus in alignment of 2'-deoxyuridine 5'-monophosphate and 5,10-methylenetetrahydrofolate.* Biochemistry, 1993. **32**(28): p. 7116-25.

60. Invitrogen, *MAX Efficiency® DH5α™ Competent Cells.* http://tools.lifetechnologies.com/content/sfs/manuals/18258012.pdf. **Cat. No. 18258-012**.

61. Howell, E.E., P.G. Foster, and L.M. Foster, *Construction of a dihydrofolate reductase-deficient mutant of Escherichia coli by gene replacement.* J Bacteriol, 1988. **170**(7): p. 3040-5.

62. Bognar, A.L., C. Osborne, and B. ShaneS, *Folylpoly-gamma-glutamate synthetase-dihydrofolate synthetase. Cloning and high expression of the Escherichia coli folC gene and purification and properties of the gene product.* J Biol Chem, 1985. **260**(9): p. 5625-30.

63. Fermer, C. and G. Swedberg, *Adaptation to sulfonamide resistance in Neisseria meningitidis may have required compensatory changes to retain enzyme function: kinetic analysis of dihydropteroate synthases from N. meningitidis expressed in a knockout mutant of Escherichia coli.* J Bacteriol, 1997. **179**(3): p. 831-7.

64. Invitrogen, *One Shot ®TOP10F Competent Cells* http://tools.lifetechnologies.com/content/sfs/manuals/oneshottop10f_man.pdf.

65. EE Howell, et al., *Functional role of aspartic acid-27 in dihydrofolate reductase revealed by mutagenesis.* Science, 1986. **231**(4742): p. 1123-8.

66. Reece, L.J., et al., *Construction of a synthetic gene for an R-plasmid-encoded dihydrofolate reductase and studies on the role of the N-terminus in the protein.* Biochemistry, 1991. **30**(45): p. 10895-904.

67. Pyne, C. and A.L. Bognar, *Replacement of the folC gene, encoding folylpolyglutamate synthetase-dihydrofolate synthetase in Escherichia coli, with genes mutagenized in vitro.* J Bacteriol, 1992. **174**(6): p. 1750-9.

68. Buwembo, W., et al., *Point Mutations in the folP Gene Partly Explain Sulfonamide Resistance of Streptococcus mutans.* Int J Microbiol, 2013. **2013**: p. 367021.

69. Yan, H. and X. Ji, *Role of Protein Conformational Dynamics in the Catalysis by 6-Hydroxymethyl-7, 8-Dihydropterin Pyrophosphokinase.* Protein & Peptide Letters, 2011. **18**(4): p. 328-335.

70. Zhao, Y., et al., *Development of a pterin-based fluorescent probe for screening dihydropteroate synthase.* Bioconjug Chem, 2011. **22**(10): p. 2110-7.

71. Zhao, Y., et al., *Structure-based design of novel pyrimido[4,5-c]pyridazine derivatives as dihydropteroate synthase inhibitors with increased affinity.* ChemMedChem, 2012. **7**(5): p. 861-70.

72. Talarico, T.L., et al., *Cloning, sequence analysis, and overexpression of Escherichia coli folK, the gene coding for 7,8-dihydro-6-hydroxymethylpterin-pyrophosphokinase.* J Bacteriol, 1992. **174**(18): p. 5971-7.

73. Blaszczyk, J., et al., *Catalytic center assembly of HPPK as revealed by the crystal structure of a ternary complex at 1.25 A resolution.* Structure, 2000. **8**(10): p. 1049-58.

74. Xiao, B., et al., *Unusual conformational changes in 6-hydroxymethyl-7,8-dihydropterin pyrophosphokinase as revealed by X-ray crystallography and NMR.* Journal of Biological Chemistry, 2001. **276**(43): p. 40274-40281.

75. Iurescia, S., et al., *Site-directed mutagenesis techniques in the study of Escherichia coli serine hydroxymethyltransferase.* Protein Expr Purif, 1996. **7**(3): p. 323-8.

76. Florio, R., et al., *Structural stability of the cofactor binding site in Escherichia coli serine hydroxymethyltransferase--the role of evolutionarily conserved hydrophobic contacts.* FEBS J, 2009. **276**(24): p. 7319-28.

77. Florio, R., et al., *Serine hydroxymethyltransferase: a model enzyme for mechanistic, structural, and evolutionary studies.* Biochim Biophys Acta, 2011. **1814**(11): p. 1489-96.

78. Hong, B., F. Maley, and A. Kohen, *Role of Y94 in proton and hydride transfers catalyzed by thymidylate synthase.* Biochemistry, 2007. **46**(49): p. 14188-97.

79. Changchien, L.-M., et al., *High-level expression of Escherichia coli and Bacillus subtilis thymidylate synthases.* Protein Expr Purif, 2000. **19**(2): p. 265-70.

80. Blattner, F.R., et al., *The complete genome sequence of Escherichia coli K-12.* Science, 1997. **277**(5331): p. 1453-62.

81. Renzette, N., *Generation of Transformation Competent E. coli.* Current Protocols in Microbiology, 2011.

82. *MicroPulser™Electroporation Apparatus Operating Instructions and Applications Guide.* BIO-RED Manual **165-2100**.

83. Cawood, R., *Adding Restriction Sites using PCR : Method for Adding Restriction Sites to the Ends of DNA.* http://oxfordgenetics.com/cloning-resources/cloning-guides/adding-restriction-sites-by-pcr.

84. NEB, *Tm Calculator* https://www.neb.com/tools-and-resources/interactive-tools/tm-calculator.

85. Cayley, S., et al., *Characterization of the cytoplasm of Escherichia coli K-12 as a function of external osmolarity. Implications for protein-DNA interactions in vivo.* J Mol Biol, 1991. **222**(2): p. 281-300.

86. Cayley, D.S., H.J. Guttman, and J. M. Thomas Record, *Biophysical characterization of changes in amounts and activity of Escherichia coli cell and compartment water and turgor pressure in response to osmotic stress.* Biophysical Journal, 2000. **78**(4): p. 1748-64.

87. invitrogen, *TOPO® TA Cloning® Kit for Sequencing, Five-minute cloning of Taq polymerase-amplified PCR products for sequencing.* Manual:http://tools.lifetechnologies.com/content/sfs/manuals/topotaseq_man.pdf, (MAN0000109): p. 1-41.

88. Neuenschwander, M., et al., *Equipping in vivo Selection Systems with Tunable Stringency.* Protein Engineering Handbook, 2009.

89. Bloch, K.D. and B. Grossmann, *Digestion of DNA with restriction endonucleases.* Curr Protoc Mol Biol, 2001. **Chapter 3**: p. Unit3 1.

90. Swedberg, G., S. Ringertz, and O. Skold, *Sulfonamide resistance in Streptococcus pyogenes is associated with differences in the amino acid sequence of its chromosomal dihydropteroate synthase.* Antimicrob Agents Chemother, 1998. **42**(5): p. 1062-7.

91. Shaha, P. and M.A. Gilchrista, *Explaining complex codon usage patterns with selection for translational efficiency, mutation bias, and genetic drift.* Proc Natl Acad Sci U S A, 2011. **108**(25): p. 10231-6.

92. Agashe, D., et al., *Good codons, bad transcript: large reductions in gene expression and fitness arising from synonymous mutations in a key enzyme.* Mol Biol Evol, 2013. **30**(3): p. 549-60.

93. Sochacki, K.A., et al., *Protein diffusion in the periplasm of E. coli under osmotic stress.* Biophys J, 2011. **100**(1): p. 22-31.

94. Cayley, S. and M.T.R. Jr, *Large changes in cytoplasmic biopolymer concentration with osmolality indicate that macromolecular crowding may regulate protein-DNA interactions and growth rate in osmotically stressed Escherichia coli K-12.* J Mol Recognit, 2004. **17**(5): p. 488-96.

95. Freeman, B.C., et al., *Physiological and transcriptional responses to osmotic stress of two Pseudomonas syringae strains that differ in epiphytic fitness and osmotolerance.* J Bacteriol, 2013. **195**(20): p. 4742-52.

96. Cheung, C., et al., *The Effect of Ionic (NaCl) andNon-ionic (Sucrose) Osmotic Stresson the Expression ofβ-galactosidase in Wild Type E.coli BW25993 and in the Isogenic BW25993 ΔlacI Mutant* Journal of Experimental Microbiology and Immunology 2009. **13**: p. 1-6.

97. Bouvet, O.M.M., S. Pernoud, and P.A.D. Grimont, *Temperature-dependent fermentation of D-sorbitol in Escherichia coli O157:H7.* Appl Environ Microbiol, 1999. **65**(9): p. 4245-57.

98. Bognar, A.L., C. Osborne, and B. Shane, *Primary structure of the Escherichia coli folC gene and its folylpolyglutamate synthetase-dihydrofolate synthetase product and regulation of expression by an upstream gene.* J Biol Chem, 1987. **262**(25): p. 12337-43.

99. Veitia, R.A., *Exploring the molecular etiology of dominant-negative mutations.* Plant Cell, 2007. **19**(12): p. 3843-51.

100. Stark, M., et al., *Aberrant splicing of folylpolyglutamate synthetase as a novel mechanism of antifolate resistance in leukemia.* Blood, 2009. **113**(18): p. 4362-9.

101. Yun, M.-K., et al., *Catalysis and sulfa drug resistance in dihydropteroate synthase.* Science, 2012. **335**(6072): p. 1110-4.

102. Weber, A., S.A. Kogl, and K. Jung, *Time-dependent proteome alterations under osmotic stress during aerobic and anaerobic growth in Escherichia coli.* J Bacteriol, 2006. **188**(20): p. 7165-75.

103. Jackson, M., et al., *Calorimetric studies of ligand binding in R67 dihydrofolate reductase.* Biochemistry, 2005. **44**(37): p. 12420-33.